SINGLE CELL DIFFERENTIATION IN THE ACELLULAR SLIME MOLD, *Didymium iridis*

BY

THOMAS JEFFREY RAUB

A DISSERTATION PRESENTED TO THE GRADUATE COUNCIL OF
THE UNIVERSITY OF FLORIDA
IN PARTIAL FULFILLMENT OF THE REQUIREMENTS FOR THE
DEGREE OF DOCTOR OF PHILOSOPHY

UNIVERSITY OF FLORIDA

1982

ACKNOWLEDGEMENTS

I would like to express my appreciation to Dr. Henry C. Aldrich, chairman of the supervisory committee, for his friendship, confidence in my abilities, and efforts in maintaining financial assistance. I am especially grateful for the freedom he gave me in directing the course of my research.

Thanks are also extended to Drs. Arnold S. Bleiweis, James F. Preston, and R. Michael Roberts, members of the supervisory committee, for their advice and critical reading of the dissertation.

Special thanks go to Dr. Stephen G. Zam for his friendship and encouragement, willingness to share his laboratory, help in the immunological study, and reading of the dissertation. I am also indebted to Zelma Zam for the time she invested in producing polyclonal antibodies.

I thank Steve Hurst, Microbiologist, for his expertise in gas-liquid chromatography and amino acid analysis. Without him the biochemical analyses would have been impossible. Gratitude is expressed to Dr. Bleiweis for use of the equipment.

I am grateful for the friendship of Dr. Greg W. Erdos, who listened to my complaints and offered encouragement and critical suggestions throughout my graduate studies.

Most of all, I express sincere appreciation to my wife, Kathy, who showed unrelenting patience and encouragement. This accomplishment is as much hers as it is mine for the aggravations she endured.

TABLE OF CONTENTS

ACKNOWLEDGEMENTS....ii

LIST OF TABLES....vi

LIST OF FIGURES....vii

KEY TO ABBREVIATIONS....xi

ABSTRACT....xii

CHAPTER

1 ULTRASTRUCTURAL CHANGES AND KINETICS OF MICROCYST FORMATION....1

Introduction....1
Materials and Methods....3
Organism and Growth....3
Induction of Encystment....3
Preparation for Electron Microscopy....4
Results....5
Kinetics of Encystment....5
Ultrastructural Observations....7
Cell Surface Changes During Microcyst Wall Formation....15
Discussion....21

2 ULTRASTRUCTURE AND KINETICS OF MICROCYST GERMINATION....28

Introduction....28
Materials and Methods....30
Organism and Growth....30
Induction of Excystment....30
Sample Preparation....31
Results....31
Kinetics of Excystment....31
Morphology of Germination....36
Discussion....53

3 ISOLATION, FRACTIONATION, AND CHEMICAL ANALYSIS OF THE MICROCYST WALL....56

Introduction....56

Materials and Methods....58
Organism and Growth....58
Chemicals....58
Encystment Conditions....58
Preparation of Microcyst Walls....59
Preparation of Crude Slime....60
Chemical Fractionation of Clean Walls....60
General Analytical Methods....62
Acid Hydrolyses....62
Neutral Sugar Analyses....63
Amino Sugar and Protein Analyses....63
Paper and Thin-layer Chromatography....63
Gas-liquid Chromatography....64
Amino Acid Analyses....64
Column Chromatography....64
Gel Electrophoresis....64
Electron Microscopy....65
Selected Area Electron Diffraction....65
Results....66
Isolation of Microcyst Walls....66
Composition of Crude Slime....66
Gross Composition of the Microcyst Wall....69
Fraction 1....78
Fraction 2....78
Fraction 3....79
Fraction 4....79
Fraction 5....83
Discussion....83

4 AN IMMUNOCYTOCHEMICAL APPROACH TO MICROCYST WALL BIOGENESIS....88

Introduction....88
Materials and Methods....90
Organism: Growth and Encystment....90
Chemicals....90
Antibody Production....90
Antigen Identification....91
Immunofluorescence....92
Preparation of Gold-labeled Goat Anti-rabbit IgG....92
Immunoelectron Microscopy of Cell Suspensions....93
Immunoelectron Microscopy of Sectioned Material....93
Results....94
Discussion....108

5 RADIOLABEL INCORPORATION DURING MICROCYST WALL FORMATION....113

Introduction....113
Materials and Methods....116
Organism: Growth and Encystment....116
Radioactive Labeling....116
Chemical Fractionation of Labeled Cells....116

Preparation of Crude Slime from Encystment Buffer....117
Analytical Methods....118
Light Microscope Autoradiography....119
Electron Microscope Autoradiography....119
Results....120
Discussion....140

CONCLUDING REMARKS....146

LITERATURE CITED....149

BIOGRAPHICAL SKETCH....162

LIST OF TABLES

TABLE

3-1 Chemical composition of crude slime precipitated from encystment buffer at 48 h.....70

3-2 Neutral sugar composition of crude slime precipitated from encystment buffer at 48 h.....71

3-3 Amino acid analysis of proteins.....72

3-4 Chemical composition of the microcyst wall.....75

3-5 Neutral sugar composition of microcyst wall.....76

3-6 Chemical composition of microcyst wall fractions.....77

5-1 Changes in composition of the hot SDS/KOH-insoluble wall fraction during encystment.....123

5-2 Specific activity of radiolabel incorporated into the hot SDS/KOH-insoluble wall fraction after 36 h.....136

LIST OF FIGURES

FIGURE

1 Rate of encystment in 10 mM potassium phosphate buffer pH 6.....6

2 Myxamoeba 2 h after suspension in encystment buffer.....9

3 Cytochemical localization of acid phosphatase.....9

4 An encysting cell 4 h after induction of encystment.....11

5 Gross organization of a young microcyst at 8 h.....11

6 Cytochemical demonstration of glycogen using amylase digestion on sectioned material.....14

7 The mature microcyst after 24 h in suspension.....14

8 Scanning electron micrographs of stages of encystment.....17

9 Changes in the density of intramembrane particles during encystment.....18

10 Micrographs of both fracture faces during encystment.....20

11 Thin sections through the cell periphery at different times during encystment.....23

12 Thin-sectioned encysting cells (10 h) stained with PASH...23

13 Rate of excystment after suspension in 5 mM potassium phosphate buffer at pH 6.2.....32

14 Effects of various molar concentrations on microcyst germination.....34

15 Effects of cycloheximide and actinomycin D on microcyst germination.....34

16 Phase-contrast micrographs of haploid cells stained with Lugol's iodine.....38

17 Mature microcyst prior to germination.....40

18 Mature microcyst immediately after wetting.....43

19 Microcyst in the initiated stage 10 min after wetting.....43

20 Characteristics of the cell surface at 10 min of excystment.....43

21 Microcyst at the swollen stage after 35 min in excystment buffer.....45

22 Changes in the density of intramembrane particles during excystment.....47

23 Changes in the size of the nucleus and nucleolus during excystment.....47

24 Nuclear changes during excystment.....50

25 A pre-emergent microcyst 35 min after wetting.....52

26 Early protrusion of the microcyst cytoplasm through the ruptured inner wall layer.....52

27 A scanning electron micrograph of the emerging cytoplasmic bud.....52

28 Germinated swarm cell 40 min after suspension in excystment buffer.....52

29 A schematic of chemical fractionation of purified microcyst walls after lipid extraction.....61

30 Phase-contrast micrograph of cell wall fragments after breakage in a Braun homogenizer.....68

31 Electron micrographs of cell wall fragments after extensive washing.....68

32 Sodium dodecyl sulfate-PAGE (7.5%) of wall fraction 1 and the crude slime.....74

33 High magnification of wall fraction 2 that has been negatively stained with 1% uranyl acetate.....81

34 Selected area electron diffraction patterns of fraction 2, chitin, and cellulose.....81

35 Elution profile of the neutralized KOH-soluble wall components fractionated on a Bio-Gel P-2, 200-400 mesh, column.....82

36 Immunodiffusion gels of wall fraction 1 and rabbit anti-microcyst wall sera.....96

37 Identification of antigens in wall fraction 1 by Western blot onto nitrocellulose.....96

38 Immunofluorescence of unfixed microcysts showing specificity of the antiserum to microcyst cell wall.....98

39 Immunofluorescence of formaldehyde-fixed cells at different stages of encystment.....100

40 Immunocolloid gold labeling of unfixed microcyst suspensions.....103

41 Quantitative changes in the pattern of gold label on sectioned material.....105

42 Immunocolloid gold labeling of sectioned cells at 0 h of encystment.....107

43 Smooth-membraned vesicles (arrow) located near the cell surface.....110

44 The cisternae of rough endoplasmic reticulum.....110

45 Regions that consist almost entirely of smooth-membraned elements.....110

46 Label is distributed throughout the cell wall.....110

47 Thin section through a microcyst after treatment with boiling SDS and KOH.....122

48 Kinetics of microcyst wall formation during encystment.....124

49 Incorporation of ^{3}H-galactose into cell fractions during encystment in the presence of continuous label.....126

50 Light microscope autoradiogram of encysted cells (24 h) after continuous label with ^{3}H-galactose.....128

51 Paper chromatographic analysis of crude slime labeled with a 2 h pulse of ^{3}H-galactose.....129

52 Incorporation of ^{3}H-glucosamine HCl into cell fractions during encystment in the presence of continuous label.....130

53 Light microscope autoradiogram of encysted cells (24 h) after continuous label with ^{3}H-glucosamine HCl.....132

54 Light microscope autoradiogram of encysted cells (24 h) after continuous label with ^{14}C-galactosamine HCl.....132

55 Elution profile of SDS-soluble material fractionated on a Bio-Gel P-2, 200-400 mesh, column after 4 h continuous label with ^{3}H-galactose, ^{3}H-glucosamine HCl, and ^{14}C-galactosamine HCl.....133

56 Fate of radioactivity in cell fractions during encystment after 2 h pulse with ^{3}H-glucosamine HCl.....135

57 Electron microscope autoradiograms of encysting cells pulse labeled (2 h) with ^{3}H-glucosamine HCl.....138

58 Fate of radioactivity in cell fractions during encystment after a 1 h pulse with ^{3}H-galactose.....139

59 Electron microscope autoradiograms of encysting cells pulse labeled (1 h) with ^{3}H-galactose.....142

KEY TO ABBREVIATIONS

AV	autophagic vacuole
bb	basal body
C	centriole
CW	cell wall
Cc	cone complex
cc	condensed chromocenters
db	dense body
EF	ectoplasmic fracture
f	fibrous region
FITC	fluorescein isothiocyanate
G	Golgi apparatus
g	glycogen granule
IWL	inner wall layer
L	lipid inclusion
m	mitochondrion
mb	microbody
mt	microtubule
N	nucleus
Nu	nucleolus
ne	nuclear envelope
OWL	outer wall layer
PAS	periodic acid-Schiff
PASH	periodic acid-silver hexamine
PF	protoplasmic fracture
PM	plasma membrane
RER	rough endoplasmic reticulum
SDS-PAGE	sodium dodecyl sulfate-polyacrylamide gel electrophoresis
SMC	smooth-membraned cisternae
ss	slime sheath
V	food vacuole

Abstract of Dissertation presented to the Graduate Council of the University of Florida in Partial Fulfillment of the Requirements for the Degree of Doctor of Philosophy

SINGLE CELL DIFFERENTIATION IN THE ACELLULAR SLIME MOLD, Didymium iridis

By

Thomas Jeffrey Raub

December, 1982

Chairman: Henry C. Aldrich
Major Department: Microbiology and Cell Science

Amoebae of the myxomycete, Didymium iridis (Ditmar) Fries, differentiate into dormant structures called microcysts by forming a cell wall. Myxamoebae were removed from the bacterial food source and induced to encyst by transfer to 10 mM phosphate buffer. After 24 h in suspension approximately 90% of the myxamoebae had formed microcysts. Early stages of encystment were characterized by the appearance of autophagosomes and an extracellular slime sheath. Crude preparations of sheath material contained neutral sugar, mostly galactose, and protein.

The outer wall layer, consisting of dense fibrils, was unevenly deposited after 4 h. A second wall layer appeared between 5-10 h, followed by a third wall layer adjacent to the plasma membrane. Chemical analyses of purified walls identified neutral sugars, protein, and hexosamine as the major components. Wall polysaccharides were mostly composed of galactosamine with smaller amounts of glucose and

galactose. The protein component consisted of large quantities of threonine and aspartate/asparagine with trace amounts of the sulfur-containing amino acids. Most of the wall protein was soluble in alkaline urea. Sodium dodecyl sulfate-polyacrylamide gel electrophoresis (SDS-PAGE) was used to identify seven major bands, at least four of which were acidic glycoproteins. Immunodiffusion and SDS-PAGE overlay studies with antibodies raised against purified whole wall identified most of these bands as weak immunogens.

Most of the galactosamine was found in a urea/hot alkali-insoluble fraction that also contained a large quantity of glucose. This galactosaminoglucan was partially sulfated and acetylated. It consisted of microfibrils that displayed a weak crystalline structure and maintained cell shape.

Both cytochemical stain for polysaccharide and electron microscope autoradiography suggested that wall formation involved smooth-membraned vesicles of possible Golgi origin. Radiolabeled galactose and glucosamine were incorporated into cytoplasmic polymers that were transported extracellularly.

Microcysts were induced to excyst by transfer to 5 mM potassium phosphate buffer. After 1 h in suspension, 90% of the microcysts had germinated. A requirement for protein synthesis, but not RNA synthesis, exists during the first 20 minutes. Initially, the outer wall layers separated from the inner wall layer, which gradually expanded and loosened. The protoplast rehydrated and reverted to a vegetative morphology. Excysting populations were classified into four characteristic stages: mature, initiated, swollen, and pre-emergent microcysts.

CHAPTER 1
ULTRASTRUCTURAL CHANGES AND KINETICS OF MICROCYST FORMATION

Introduction

Didymium iridis Ditmar (Fries) is a plasmodium-forming organism of the class Myxomycetes that is commonly referred to as a true slime mold. The life cycle (Alexopoulos and Mims, 1979) involves the fusion of haploid amoebae to form the characteristic vegetative stage, a multinucleate, diploid plasmodium. During suitable conditions, this stage differentiates into fruiting bodies containing uninucleate spores, products of meiosis. These germinate to continue the cycle.

Amoebae have the ability to undergo reversible differentiation in response to environmental conditions unfavorable for continued phenotypic development. Microcyst formation or encystment occurs when a "naked" amoeba becomes encased in a protective cell wall. Excystment is the reverse process by which an activated amoeba emerges from the microcyst wall. Both of these events represent cellular differentiation processes where morphological and biochemical changes occur in response to environmental stimuli. As a model system, *D. iridis* has the advantage of differentiating without complex sexual events or continued cell division.

Several other organisms have been exploited in the study of encystment. The cellular slime mold, *Polyspondylium pallidum* (Taoma

and Raper, 1967; Hohl et al., 1970; Githens and Karnovsky, 1973; Lonski and Pesut, 1977), and the free-living soil amoeba, Acanthamoeba castellanii (Neff et al., 1964; Griffiths, 1970; Weisman, 1976), are induced to encyst by solutions of high osmolarity. Both appear to encyst similarly to the Myxomycetes. Studies have also been done with several ciliates (Matsusaka, 1976; Matsusaka, 1977) and zoospores of oomycetous fungi (Bartnicki-Garcia and Hemmes, 1976). The latter are quite unique from these other systems in that encystment is complete within two minutes. This difference is in response to a stimulus other than nutritional deprivation. As in the Myxomycetes, the other systems require a minimum of 12 h to complete encystment.

The Myxomycete microcyst is capable of withstanding prolonged desiccation and starvation. Microcysts form naturally in aging cultures over a period of several days. They may also be induced to form in Physarum flavicomum by starvation in basal salts medium (Henney and Chu, 1977a) and in Physarum polycephalum using 0.5 M mannitol or mannose (Turner and Johnson, 1975c; Haars et al., 1979).

The cytological events associated with encystment were first studied by Howard (1931) and later examined using the electron microscope (Koevenig, 1964; Schuster, 1965). More recent studies briefly describe the fine structure of D. iridis microcysts (Aldrich and Blackwell, 1976; Ling and Moore, 1979) and intermediate stages during encystment of axenic strains of P. polycephalum (Turner and Johnson, 1975a, c; Haars et al., 1979). Several comprehensive reviews on myxamoebal encystment are available (Aldrich and Blackwell, 1976; Collins, 1979; Gorman and Wilkins, 1980; Raub and Aldrich, 1982).

This chapter describes a method by which encystment is synchronously induced and quantified. The cytological events associated with differentiation are studied using transmission, scanning and freeze-fracture electron microscopy.

Materials and Methods

Organism and Growth

Didymium iridis strain C-4 (A_8) amoebae were grown with Escherichia coli on DS/2 agar (Shipley and Ross, 1978) (1 g dextrose, 0.5 g yeast extract, 0.1 g $MgSO_4.7H_2O$, 1.5 g K_2HPO_4, 1 g KH_2PO_4, and 20 g agar per liter) at 22 C. Amoebae used for encystment were grown in 9 X 11 inch baking pans.

Induction of Encystment

Mid-exponential phase myxamoebae were harvested in 10 mM potassium phosphate buffer at pH 6 and centrifuged at 176 x g for 15 min at 4 C. The cells were resuspended in 2 ml of 5% sucrose buffer at 10^8 cells/ml, layered over 20 ml of 15% sucrose buffer, and centrifuged at 78 x g for 25 min. This effectively removed most of the bacteria. The cells, washed twice with buffer, were resuspended in buffer to give 10^7 cells/ml. Up to 40 ml of cell suspension were placed in 125 ml Erlenmeyer flasks at 22 C and agitated at 160 rpm. Samples were removed at regular intervals, suspended in Lugol's iodine (Taylor and Kahn, 1969), and cell counts made using a Spencer Bright-line hemacytometer. At least 500 cells were counted at each time interval.

Inhibitor studies were performed by adding 250 μg/ml actinomycin D (Sigma) or 10 μg/ml cycloheximide (Sigma) to the encystment medium.

Preparation for Electron Microscopy

Transmission electron microscopy: Samples were taken at 1 h intervals for the first 12 h of induction and at 3 h intervals thereafter until 36 h. The cells were fixed in 2.5% glutaraldehyde, buffered with 0.05 M cacodylate to pH 7.2, for 1 h at room temperature. After post-fixation in similarly buffered 1% OsO_4 for 1 h at room temperature, samples were agar embedded, ethanol dehydrated, and embedded in low-viscosity resin (Spurr, 1969). Sections, poststained with 1% uranyl acetate and lead citrate (Reynolds, 1963), were examined and photographed with a Jeol JEM-100CX electron microscope operated at 60 kV.

Grey-silver sections mounted on nickel grids were treated with periodic acid-silver methenamine according to Rambourg (1967). Controls were processed by omitting periodate oxidation. The controls showed a low level of nonspecific staining.

Digestion of glycogen from sectioned material was accomplished using 5 mg/ml α-amylase (barley malt, Sigma) in 20 mM phosphate buffer at pH 7 for 2 h at 37 C preceded by osmium removal using 3% H_2O_2 for 60 min at room temperature (Lewis and Knight, 1977). Controls were obtained by heat inactivating the amylase.

Acid phosphatase was localized according to Kazama and Aldrich (1972). Controls were obtained by omitting the substrate, β-glycerophosphate (Sigma).

Scanning electron microscopy (SEM): Cells were collected on 0.6 μm Nuclepore filters (13 mm diam) and osmium (4%)-vapor fixed for 2 h. Specimens were dehydrated, critical point dried in liquid CO_2, gold

coated, and examined with a Hitachi S-450 operated at 20 kV or a Jeol JEM-100CX electron microscope operated in secondary electron-imaging mode at 20 kV.

Freeze-fracture electron microcscopy: Samples were gently centrifuged and frozen in a propane jet according to Muller et al. (1980) without prior fixation or cryoprotection. Specimens were fractured using a double replica holder in a Balzers BA 360 freeze-etch apparatus at -110 C and shadowed with platinum/carbon followed by carbon. The replicas were cleaned in 50% commercial bleach (Chlorox, 5.25% sodium hypochlorite) for 3 h followed by 40% chromic acid for 24-36 h. Micrographs were taken with a Jeol JEM-100CX electron microscope operated at 80 kV.

Intramembrane particles (IMP) were counted from micrographs overlaid by four, randomly placed squares that totalled 1 μm^2. Counts were made on no less than 8 micrographs per fracture face per sample and the results averaged. The nomenclature of Branton et al. (1975) was used.

Results

Kinetics of Encystment

Differentiation of myxamoebae to microcysts in a solution of low osmolarity can be quantified after staining with Lugol's iodine by observing the appearance of highly refractile, yellow microcysts. Figure 1 shows the rate of microcyst formation from the time myxamoebae were placed in the induction medium. A range in pH from 4-6 had no effect. More alkaline conditions caused cell lysis. Of the conditions tested, 10 mM phosphate buffer at pH 6 was found to be optimal.

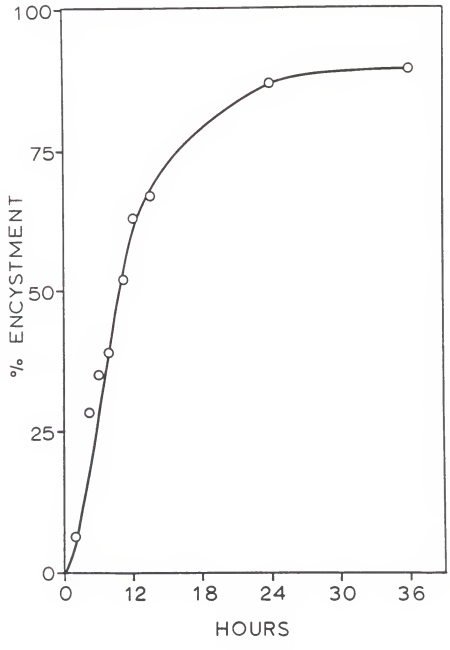

Figure 1. Rate of encystment in 10 mM potassium phosphate buffer pH 6. Mid-exponential phase myxamoebae were washed free of bacteria and suspended in 40 ml buffer at 10^7 cells/ml. Samples were removed at various times, mixed with Lugol's iodine and the percentage of encysted cells determined using phase-contrast optics.

Encystment was unaffected by cycloheximide or actinomycin D. The resulting microcysts were morphologically normal and capable of germinating. A requirement for divalent cations was indicated by the inhibition of encystment by 1 mM ethylenediaminetetraacetic acid (EDTA). In addition, induction did not appear to be a function of cell density as is found in the soil amoeba, A. castellanii (Akins and Byers, 1979), since the rate of formation was similar with cell concentrations from 5×10^5 to 5×10^7 cells/ml.

Ultrastructural Observations

Previous studies have been done using poorly synchronized populations. With the synchronous induction of microcysts in D. iridis, encystment could be followed cytologically. Most of the population had encysted within 18 h, yet some morphologically mature microcysts were observed as early as 8 h.

After 2 h of induction, the onset of differentiation was indicated by the appearance of autophagic vacuoles (Fig. 2). These continued to increase in number until 8-10 h. As expected, these vacuoles stained heavily for acid phosphatase (Fig. 3b) and activity was diminished in the single vacuole found in mature microcysts (Fig. 3c). At 2 h differentiation was also distinguished by the appearance of a diffuse extracellular material (Fig. 2, inset) that surrounds each individual cell. A well-defined Golgi apparatus that was associated with paired centrioles, also found in vegetative cells (Schuster, 1965; Wright et al., 1979), was observed at all stages of differentiation (Figs. 2, 5).

By 4-5 h the cells had become spherical and the cytoplasm was much more condensed (Fig. 4). Beneath the plasma membrane was a narrow

Figure 2. Myxamoeba 2 h after suspension in encystment buffer. The morphology was similar to the vegetative cell at 0 h showing mitochondria with tubular cristae, lipid inclusions, food vacuoles, and a pair of centrioles associated with the Golgi apparatus. Differentiation was observed by the appearance of autophagosomes and an extracellular slime sheath. Inset: High magnification of the cell periphery showing the extracellular "slime" sheath and glycogen granules.

Figure 3. Cytochemical localization of acid phosphatase. (a) Control amoeba where the substrate, β-glycerophosphate, was omitted. (b) Encysting cell at 2 h showing heavy lead deposit within the vacuole. (c) Mature microcyst (24 h) typically had low levels of enzyme (arrow).

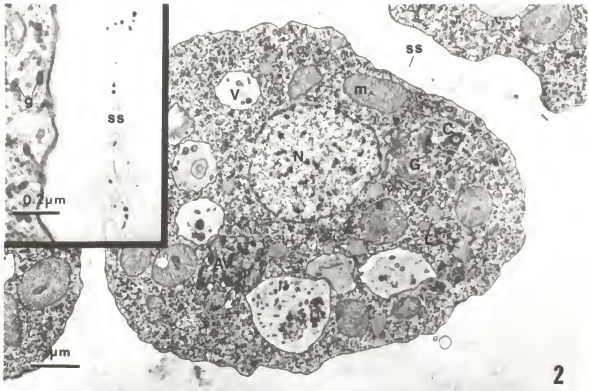

2

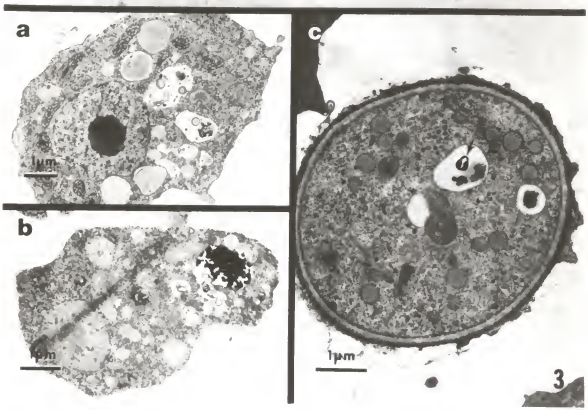

3

Figure 4. An encysting cell 4 h after induction of encystment showing a condensed cytoplasm containing rough endoplasmic reticulum and numerous autophagosomes. Cell wall deposition has begun with the appearance of clumps of electron-opaque, fibrous material (arrows) beneath the slime sheath. Inset: This stage in differentiation frequently has an inconspicuous cortical region beneath the plasma membrane (arrow).

Figure 5. Gross organization of a young microcyst at 8 h. An electron-lucent, second wall layer (arrow) has formed beneath the fibrous outer wall layer (also see Fig. 11b). The nucleus contains numerous condensed chromocenters typical of the mature microcyst.

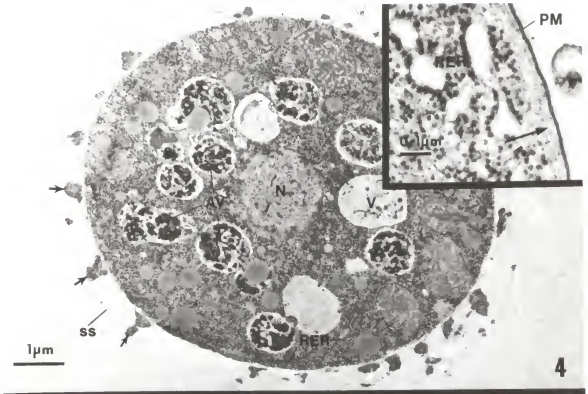

4

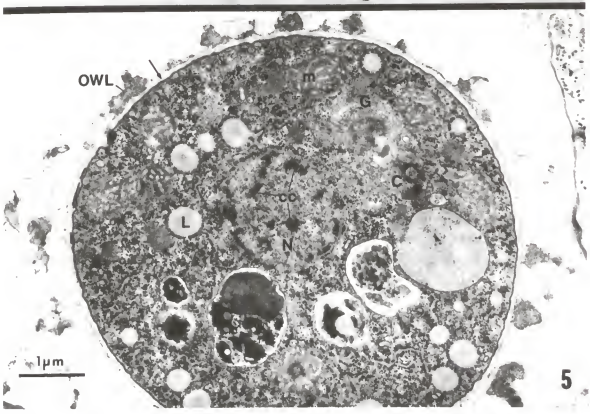

5

ectoplasmic region (Fig. 4, inset) that lacked organelles and ribosomes. More characteristic and interesting was the deposition of electron-opaque, fibrous material (Fig. 4) arranged in clumps on the cell surface. At the same time there was an abundance of rough endoplasmic reticulum and smooth-membraned vesicles.

The fibrous material eventually formed a confluent layer around the cell that became the outer wall layer. Within 5-10 h an amorphous, second wall layer of less electron opacity had formed (Figs. 5, 11b). Lipid droplets distributed throughout the cytoplasm were more abundant and were curiously surrounded by tightly packed ribosomes. Glycogen granules were numerous as they are in vegetative cells and were occasionally grouped (Figs. 6c, 11c).

The later events of microcyst maturation were less distinct. Rough ER was less abundant and glycogen granules had noticeably decreased as shown by amylase digestion of sectioned material (Fig. 6). Most notable was the continued elaboration of the cell wall. A third electron-opaque layer was deposited adjacent to the plasma membrane, completing the trilaminar structure characteristic of the mature microcyst wall (Fig. 7a, 11d). The mature cell wall was 0.2-0.4 μm thick. A fracture through the wall (Fig. 7b) revealed a loose network of fibrils approximately 8 nm in diam. Treatment of thin sections with periodic acid-silver methenamine (PASH) stain for polysaccharide gave a positive reaction in the outer wall layer but not in the innermost wall layers (Fig. 7c).

Figure 6. Cytochemical demonstration of glycogen using amylase digestion on sectioned material. Holes remain where material containing α-(1-4) glycosidic linkages is localized. (a) Amoebae at 0 h showing an even distribution of glycogen particles. (b) Microcyst at 24 h with very little glycogen at all. (c) A common phenomenon in the early stages of encystment is the arrangement of glycogen granules into large aggregates (arrows).

Figure 7. The mature microcyst after 24 h in suspension. (a) A whole microcyst showing the trilaminar wall: the irregular outer wall layer (1); lighter, middle wall layer (2); and densely packed, inner wall layer (3) (also see Fig. 11d). (b) Replica of a fracture through the cell wall exposing a network of fibrils. (c) A thin section through the cell wall stained with PASH. The outer wall layer shows a strongly positive reaction whereas the inner wall layers are indistinguishable.

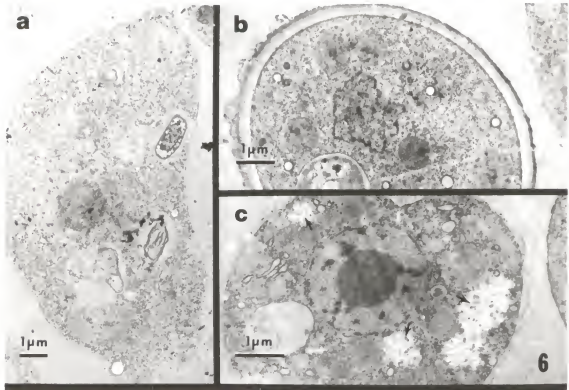
a
1µm
b
1µm
c
1µm
6

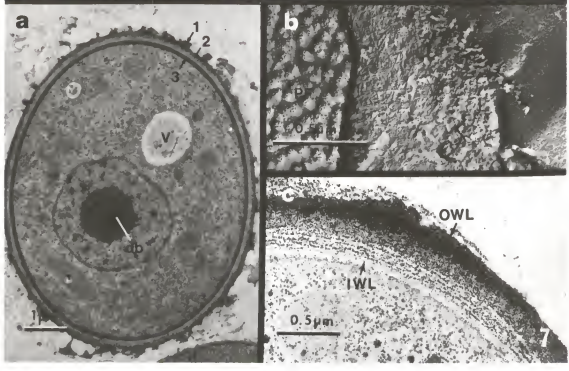
a
1
2
3
V
db
b
P
0.5µm
c
OWL
IWL
0.5µm
7

Cell Surface Changes During Microcyst Wall Formation

In other studies on myxamoebal encystment, little attention has been given to cell surface events during differentiation, so I performed a time-course study of encystment, using scanning and freeze-fracture electron microscopy.

With SEM, the first sign of microcyst formation was the transition from myxamoebae (Fig. 8a) that were rather flat in appearance to cells that were rounded (Fig. 8b). At 4-5 h, when cells were engaged in the deposition of fibrous material, projections were observed on the cell surface (Fig. 8b and 8c). These structures had a mean length of 0.32 μm as compared to 0.37 μm for the extracellular material seen in thin section. These are considered equivalent, particularly since they have similar distribution. Concomitant with the appearance of this material, the cells began to aggregate into clumps of 200-300 cells. By 24 h these cells were covered by a continuous coating (Fig. 8d). In thin section the cells at this stage were embedded in a fibrous matrix that was PASH positive (Fig. 8e).

Thin-section and freeze-fracture techniques were used to further investigate the progress of differentiation (Figs. 9-11). Peculiar to the PF face of the vegetative phase (Fig. 10a) were numerous tetrads of particles (arrows) dispersed among the single particles. These are also found in the vegetative plasmodium of D. iridis but not in P. polycephalum (Dougherty, 1976). As encystment proceeded, the density of IMP's in the PF face increased. The density in the EF face shows a decrease from 0-24 h (Fig. 9). The only exception to this was a 2-fold increase in EF particles at 2 h when extracellular material was first observed. Intramembrane particles were generally evenly distributed in both faces at 0 h (Figs. 10a, b).

Figures 8. Scanning electron micrographs of stages of encystment: (a) A confluent monolayer of myxamoebae at 0 h. One cell's border marked by arrows. (b) Encysting cells after 5 h in encystment buffer. Cells have become round and possess projections (arrow). (c) High magnification of the surface of encysting cells at 5 h. (d) Mature microcysts after 24 h in suspension. Cell clumps appear to be covered by a common material (arrow). (e) Thin section through a clump of mature microcysts (24 h) stained with PASH. Microcysts are embedded within a fibrous, PASH-positive material.

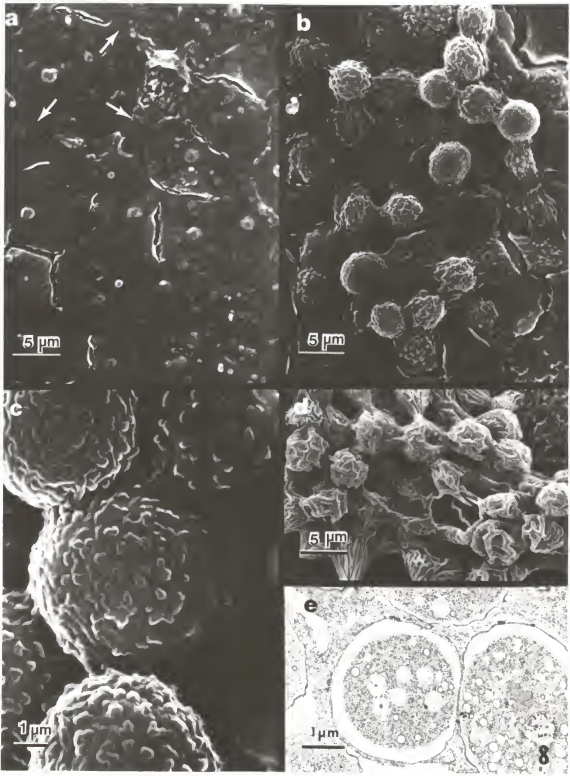
a
5 µm
b
5 µm
c
1µm
d
5 µm
e
1 µm
8

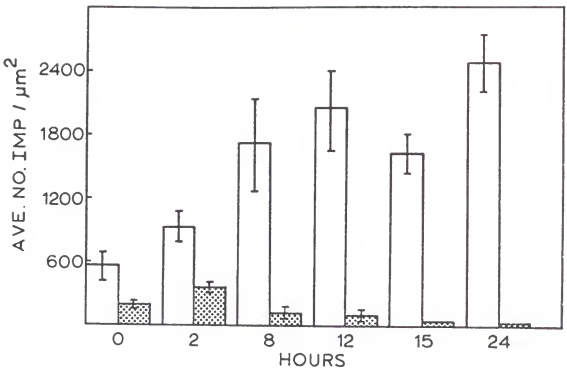

Figure 9. Changes in the density of intramembrane particles during encystment. Data are presented as the average number of particles per μm^2 of membrane. Standard deviations are shown. White: PF face; dotted: EF face.

Figure 10. Micrographs of both fracture faces during encystment (left: PF face; right: EF face). (a) and (b) Myxamoeba at 0 h. Note the tetrads of particles (arrows) on the PF face. (c) and (d) Encysting cell at 8 h. (e) and (f) Young microcyst at 12 h. (g) and (h) Mature microcyst at 24 h.

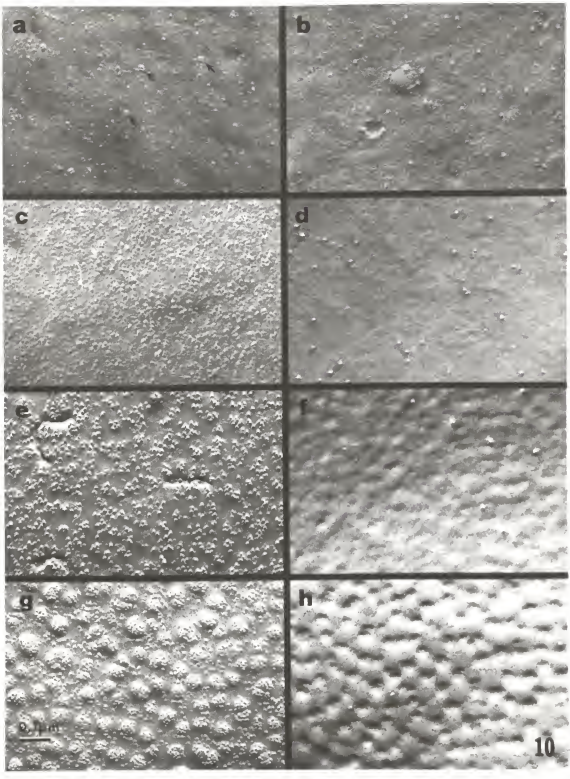
a
b
c
d
e
f
g
h
0.1 μm
10

The IMP's of the PF face showed signs of patterning by 15 h (Fig. 10e). This continued with the particles arranged into elevated clusters (Fig. 10g) 56 ± 6 nm in diameter. Conversely, the EF face (Fig. 10h) had gradually become covered with depressions which were thought to be complementary to the PF face clusters, based on their distribution and mean diameter of 52 ± 4 nm.

In thin section (Figs. 11a-d), the plasma membrane began to show invaginations. These appeared to parallel an increase in vesicular activity. In 4-5 h old cells, the isolated clumps of fibrous material were usually associated with membrane invaginations or cytoplasmic vesicles that were adjacent to the membrane (Figs. 4 and 11b). They were also often observed in later stages of encystment after all three wall layers were deposited. These vesicles contained electron-opaque material resembling that of the outer wall layer (Fig. 11c). The contents were also PASH positive (Fig. 12a) and similar vesicles had been observed budding from the Golgi apparatus (Fig. 12b).

Discussion

Didymium iridis encysts more rapidly and synchronously than P. flavicomum (Henney and Chu, 1977a) and P. polycephalum (Haars et al., 1979). We did not find the rate of encystment to be enhanced by increasing osmolarity as reported for D. iridis (Ling and Moore, 1979) and P. polycephalum (Gorman and Wilkins 1980). Encystment was not induced in basal salts solution (Henney and Chu, 1977a), Osterhout solution (Matsusaka, 1977), encystment media of Neff et al. (1964) and Bowers and Korn (1969), and 0.05 M mannitol (Turner and Johnson, 1975c;

Figure 11. Thin sections through the cell periphery at different times during encystment. (a) Myxamoeba at 0 h. (b) Encysting cell at 8 h. The two outer wall layers (1 and 2) have formed. (c) Young microcyst at 15 h showing smooth-membraned cytoplasmic vesicles (arrow) that contain fibrous material. (d) Mature microcyst at 24 h clearly showing the three wall layers (1,2 and 3). Note the densely packed, electron-opaque inner wall layer (3) and the crenulated plasma membrane.

Figure 12. Thin-sectioned encysting cells (10 h) stained with PASH. (a) Cytoplasmic smooth-membraned vesicles with PASH-positive contents. (b) Golgi apparatus with budding vesicle (arrow) containing PASH-positive material.

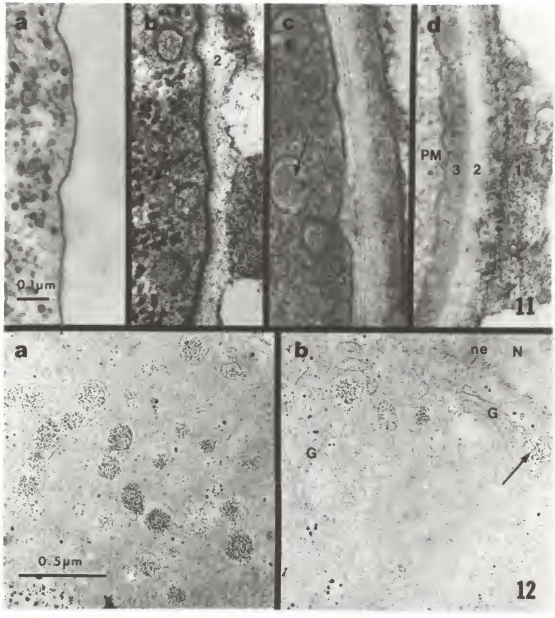
a
b
2
c
d
PM
3
2
1
0.1µm
11
a
0.5µm
b
ne
N
G
G
12

Haars et al., 1979). As noted by Aldrich and Blackwell (1976), inter- and intraspecific variabilities do exist. One must also bear in mind that the two strains of Physarum studied are axenic strains and possibly differ from wild-type strains due to genetic or nutritional differences. Regardless, the stimulus for the induction of encystment is starvation except in the case of mannitol-induced formation (Haars et al., 1979). Mannitol and a high osmolarity may mimic starvation by affecting the membrane (Gorman and Wilkins, 1980). This is also suggested by Lonski and Pesut (1977) for microcyst induction of P. pallidum by glycerol. In D. iridis, the synchrony of encystment appears to be dependent on the removal of the food source.

Encystment is inhibited by the availability of extracellular amino acids, particularly the aliphatic class, and in the absence of these amino acids, protein and carbohydrate pools are degraded (Henney and Chu, 1977a). This event is paralleled morphologically by the early appearance of autophagocytosis and gradual decrease in glycogen particles. It is established that encystment is a closed system since it is completed in buffer; therefore, all precursors required for dormancy are acquired from endogenous sources. This appears to be characteristic of most systems, with decreases in cellular levels of RNA, protein, and glycogen (Githens and Karnovsky, 1973; Weisman, 1976; Henney, 1982).

Since actinomycin D and cycloheximide did not have an effect, RNA and protein synthesis do not appear to be necessary for encystment. This is also the case in P. polycephalum (Haars et al., 1979). This is presumably true not only for morphological but also for physiological changes, since the microcysts formed in the presence of inhibitors were

still able to germinate even though the lag phase of excystment was prolonged (Chapter 2). EDTA is also reported to inhibit encystment of the soil amoeba, Hartmannella rhysodes (Band, 1963), and P. pallidum (Toama and Raper, 1967) where Mg^{2+} is required. We have shown this cation is important during excystment (Chapter 2); however, its precise function is unknown. It may not be involved directly since its addition to the medium did not enhance encystment. Griffiths (1970) comments on several possible functions for Mg^{2+} including its effect on membrane permeability.

The outer wall layer of D. iridis was initially deposited unevenly, much like spine formation in the spore (Aldrich, 1974; Aldrich and Blackwell, 1976). In fact, Aldrich (1974) reports similar PASH reactions in the spore wall and suggests that the inner wall layer does not react because it is either not a polysaccharide or it is not accessible to periodate oxidation. Several investigators have implicated Golgi-derived smooth-membraned vesicles in deposition of extracellular polysaccharide in the Myxomycetes (Mims, 1972; Aldrich, 1974; Zaar and Kleinig, 1974; Aldrich and Blackwell, 1976). Vesicles that contain polysaccharide or PASH-positive material were also observed to arise from dictyosome cisternae in this study. Turner and Johnson (1975a) suggest that the extracellular polysaccharide, stained with ruthenium red, is of vacuolar origin. However, this stain will not normally penetrate an undamaged cell membrane suggesting that the "vacuoles" were actually cross-sections through invaginations of the plasma membrane. Secretion of a polysaccharide that is presumably hydrated is thought to cause the condensation of the cytoplasm by dehydration (Zaar and Kleinig, 1974).

The microcyst wall consists of an intricate network of fibrils. The outer wall layer of D. iridis looks similar to the outer layer of spherule walls of P. polycephalum which is thought to consist of vegetative slime (Rhea, 1966; Patterson and Scheetz, 1977). The extracellular material observed at 2 h may be analogous to a slime sheath and may possibly function as a temporary protective coat or actually aid in wall deposition by entrapping the fibrous wall material as is suggested by Bartnicki-Garcia and Hemmes (1976) for the cyst coat in oomycete encystation. In fact, secretion of a pre-wall coat is a widespread phenomenon among fungi and likely serves as a protective layer during the early phase of encystment (Grove and Bracker, 1978).

There appeared to be a correlation between the increase in particle density in the EF face at 2 h and the appearance of extracellular material. The significance of this is not understood, particularly since particle density decreased during wall deposition. There did not appear to be a relationship between IMP patterns of lateral distribution and wall formation. The clustering of PF face particles was not an induced artifact since fixatives and cryoprotectants were not used and cells from earlier time intervals did not exhibit a similar phenomenon. Fracture faces of the spore were indistinguishable from those of the mature microcyst (data not shown). It is possible that this distribution is attributable to desiccation as is found in plant cells during plasmolysis (Wilkinson and Northcote, 1980).

These findings are generally unlike those found in P. pallidum (Erdos and Hohl, 1980); however, similar changes do occur in the IMP density of the EF face. These authors also show a greater proportion

of IMP's associated with the PF face and suggest this may reflect a "germination-ready" state. Preliminary results for D. iridis do not suggest a membrane-located site for wall assembly but rather assembly of prepackaged material delivered to the cell surface by exocytosis. A more extensive discussion on microcyst wall secretion will be presented in chapters 4 and 5.

CHAPTER 2
ULTRASTRUCTURAL CHANGES AND KINETICS OF EXCYSTMENT

Introduction

There remains a paucity of information in the literature concerning cyst germination. This is especially true for the Myxomycetes, although studies by Smart (1937) and Elliott (1949) examined the influence of external factors on spore germination. Solutions of organic compounds and wetting agents activate dormant spores. Braun (1971) reported a requirement for aeration in spores of Fuligo septica. In addition, Dahlberg and Franke (1977) showed evidence for a soluble, autocatalytic stimulatory factor present in spore suspensions of F. septica. Literature to the present is adequately reviewed by Gray and Alexopoulos (1968) and Raub and Aldrich (1982).

Excystment, as a paradigm to study differential gene expression of macromolecules, has best been studied using the cellular slime mold, Polysphondylium pallidum. Germination is complete within 3-4 h after transfer to a sterile, dilute buffer; therefore, exogenous nutrient sources are not required (O'Day, 1974). Amoeba emergence requires a discrete period of protein synthesis early in germination as determined by inhibition studies using cycloheximide (O'Day et al., 1976). RNA synthesis is not required. Amino acids are incorporated immediately

upon activation, and proteins are grouped into three classes according to their appearance and duration of synthesis. This suggests an interconnected network of regulators (Dowbewko and Ennis, 1982). Preliminary examination of excystment in Didymium iridis and Physarum polycephalum indicates similar events.

Germination of myxomycete microcysts is induced by transfer to fresh medium or to distilled water. Only an early light microscope study by Howard (1931) and a cursory ultrastructural examination (Aldrich and Blackwell, 1976) deal with morphological aspects of germination. Gorman et al. (1977) reported kinetics of excystment in P. polycephalum and obtained 98% germination within 5 h. Of the conditions examined, pH 6 and low molar concentrations at 26 C are optimal. A requirement for protein synthesis was also demonstrated by this group, but Haars et al. (1979) were unable to verify this. Recently, biochemical evidence shows that a burst of protein and RNA synthesis occurs early during germination (Larue et al., personal communication).

Most research on dormancy and reversion to the vegetative state has been conducted using the encysted diploid phase or spherule of P. polycephalum. Reviews are available by Gorman and Wilkins (1980) and Raub and Aldrich (1982). Spherules transferred to distilled water germinate within 12 h (Chet and Rusch, 1969). In only one hour, polysomes begin to form (Jeffery, 1979) during which time cycloheximide has no effect (Chet and Huttermann, 1970). After one hour, protein synthesis and emergence are inhibited. It appears that activation of macromolecular synthesis is similar to patterns found in P. pallidum.

Such changes may be ubiquitous to all amoeboid systems, since these results are not unlike those found in Acanthamoeba castellanii (Mattar and Byers, 1971).

This chapter describes a method for inducing rapid and synchronous microcyst germination, an assay for quantifying the process, the kinetics, and the ultrastructural events. These results are intended to define a system applicable to detailed biochemical studies as described above.

Materials and Methods

Organism and Growth

Using Enterobacter aerogenes as a food source, Didymium iridis strain C-4 (A_8) myxamoebae were grown on DS/5 agar at pH 6.2 (Shipley and Ross, 1978). Microcysts were formed by continuous incubation in dark at 22 C for 10 days. Maximal encystment occurred within 3-5 days after plating.

Induction of Excystment

Microcysts were harvested either in experimental solutions described below or in cold 5mM potassium phosphate buffer at pH 6.2 and centrifuged at 700 x g for 2 min at 4 C. Cells were washed and resuspended to give 1 x 10^7 microcysts/ml. Three milliliters of cell suspension were placed in 25 ml Erlenmeyer flasks at 23 C and agitated periodically. Samples were withdrawn at 20 min intervals beginning 10 min after wetting, suspended in Lugol's iodine (Chapter 1), and percent germination determined using a Spencer Bright-line hemacytometer. At

least 500 cells were counted for each time point. Buffer was adjusted with KOH or HCl for pH studies. Actinomycin D and cycloheximide were obtained from Sigma.

Sample Preparation

Transmission electron microscopy: At 5 min intervals for 45 min after wetting, germinating microcysts were prepared and examined as described in Chapter 1.

Scanning electron microscopy: Excysting cells were collected from suspension onto 0.6 μm nuclepore polycarbonate filters and prepared as described in Chapter 1. The filters were mounted on stubs with double-stick tape, sputter-coated with gold, and examined in secondary electron-imaging mode on a Jeol JEM-100CX operated at 20 kV.

Freeze-fracture electron microscopy: Suspensions of germinating cells were prepared and the distribution of intramembrane particles (IMP) analyzed as described in Chapter 1.

Results

Kinetics of Excystment

Five millimoles potassium phosphate buffer at pH 6.2 induces 90% microcyst germination at room temperature within 1 h (Fig. 13). A lag phase of 30-35 min is followed by 75% germination during the 30-50 min period. The optimal pH is from 6-7. More acidic pH is inhibitory, with only 20% germination at pH 5. However, microcysts formed at pH 4 and then germinated in pH 6.2 buffer germinate normally.

Optimal osmolarity of the germination medium is 5 mM or less. Comparable germination occurs in distilled water, although the pH is

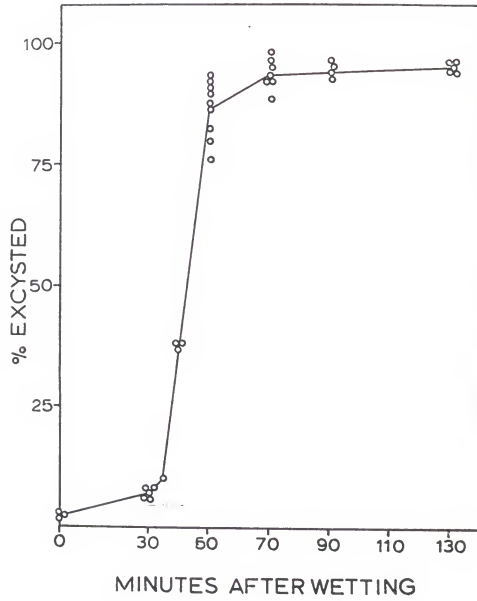

Figure 13. Rate of excystment after suspension in 5 mM potassium phosphate buffer at pH 6.2. Microcysts were prepared as described for the assay in Materials and Methods and the percentage of excysted cells determined using Lugol's iodine and phase-contrast optics.

Figure 14. Effects of various molar concentrations on microcyst germination. (○) 5 mM potassium phosphate buffer (KPO_4), (●) 10 mM KCl, (□) 10 mM KPO_4, (■) 20 mM KPO_4, (△) 40 mM KPO_4, (▲) 10 mM citric acid-KOH buffer. All solutions are pH 6.2.

Figure 15. Effects of cycloheximide and actinomycin D on microcyst germination. Solutions were buffered with 5 mM potassium phosphate pH 6.2. (○) buffer control, (●) 10 µg/ml cycloheximide at the time of wetting, i.e. 0 min, (□) 10 µg/ml cycloheximide 20 min after wetting. (■) 300 µg/ml actinomycin D at 10 min. Higher concentrations were tested with no additional effect.

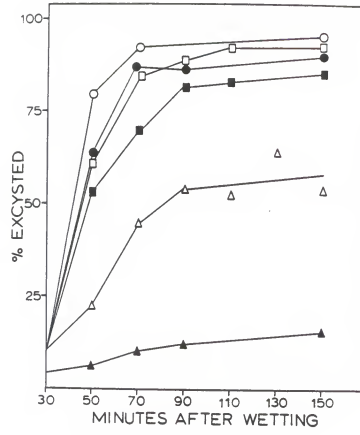
100
75
50
25
% EXCYSTED
30
50
70
90
110
130
150
MINUTES AFTER WETTING

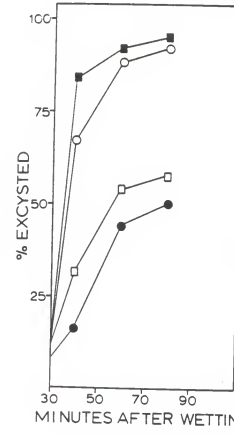
100
75
50
25
% EXCYSTED
30
50
70
90
MINUTES AFTER WETTING

not maintained. Germination in increasing molarities of potassium phosphate and KCl solutions follows similar kinetics, with increasing inhibition of germination above 10 mM (Fig. 14). Increasing concentrations of citric acid-KOH buffer reduce germination even more radically, with 10 mM concentration inhibitory by 85% (Fig. 14). Germination is also reduced if microcysts are formed on medium buffered with citric acid-KOH.

To see whether this inhibition by citrate was due to a chelating effect, the effect of EDTA on germination was tested. Two mM EDTA inhibited germination by 70%. Magnesium in excess of 1 mM reversed this effect, while calcium ions did not. Inhibition was also observed in the presence of 1 mM sodium azide.

Addition of peptone, yeast extract, and casein hydrolysate at 0.01 to 0.5% concentrations failed to enhance activation. Concentrations of ethanol from 0.1 to 1.0% had no effect unlike the stimulatory effect it had on P. pallidum (Ennis et al., 1978). The age of microcysts did not affect excystment since 10, 15, 20, and 30 day old microcysts produced similar kinetics.

Since Chet and Huttermann (1977) had reported a germination inhibitor molecule in spherules of P. polycephalum, such a phenomenon in D. iridis microcysts was investigated. Microcyst germination was assayed at microcyst concentrations from 5×10^5 to 5×10^7 cells/ml, but only the slightest decrease in germination percentage occurred at even the highest cell concentrations. This effect is attributed to reduced oxygen availability. To insure that our washing procedure was not diluting this hypothetical inhibitor, we tried using the initial harvest supernatant as the germination medium. We found only a slight

decrease in the final extent of germination, with no change in rate. These data suggest the absence of a germination inhibitor in D. iridis microcysts.

Dependence of the germination process upon RNA and protein synthesis was assessed. Addition of 10-40 μg/ml cycloheximide to the germination medium decreased both rate and extent of germination by 40% (Fig. 15). Inhibition by cycloheximide is more pronounced if it is added at 0 min than at 20 min, but in both cases the 30 min lag period persists. Actinomycin D at a concentration of 300 μg/ml had no effect (Fig. 15). Formation of microcysts in the presence of 50 μg/ml cycloheximide slowed the rate of excystment. Encystment in the presence of 400 μg/ml actinomycin D delayed the lag phase 20 min.

Morphology of Germination

Observing germinating cultures stained with Lugol's iodine under phase contrast, we can readily distinguish mature microcysts, swollen or activated microcysts, and myxamoebae. Mature microcysts (Fig. 16a) are refractile and stain yellow-brown. Activated microcysts (Fig. 16b) have lost refractility, stain reddish-brown, and have increased in diameter. This activated form is easily visible 10 min after germination induction. Empty wall casings are unstained. 35-40 min after induction, many activated cells have a cytoplasmic bud protruding through the microcyst wall (Fig. 16c). I classified these cells as "emergent," since the protoplast is no longer protected by a cell wall. A free myxamoeba is shown in Figure 16d.

Events of "activation" are best viewed ultrastructurally. Activation may be subdivided into initiation, swelling, and preemergent

Figure 16. Phase-contrast micrographs of haploid cells stained with Lugol's iodine showing stages of excystment in 5 mM potassium phosphate buffer pH 6.2. (a) Mature microcyst at 0 min. The microcyst at lower right is losing its outer wall layer (arrow). (b) Swollen microcysts 20 min after wetting. (c) Excysting microcyst after 35 min in the excystment buffer with a cytoplasmic bud penetrating the cell wall. (d) Germinated swarm cell after 40 min.

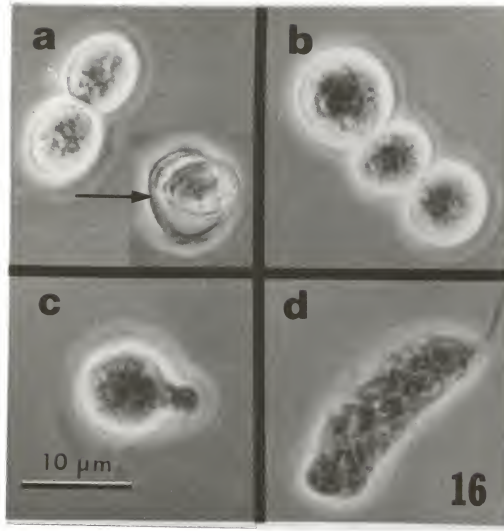
a
b
c
d
10 µm
16

Figure 17. Mature microcyst prior to germination. (a) Gross organization of microcyst showing rounded, condensed mitochondria accumulated around the nucleus. Numerous lipid bodies, surrounded by ribosomes, are seen scattered throughout the cytoplasm that is densely packed with unattached ribosomes. Note the uneven distribution of the fibrous, outer wall layer. (b) High magnification of the cell wall. The dense material (arrow) underneath the crenulated plasma membrane is an artifact resulting from the plane of the section and its thickness since it was absent in ultrathin sections (30 nm). (c) Freeze fracture of the plasma membrane, PF face. (d) High magnification of the PF face intramembrane particles.

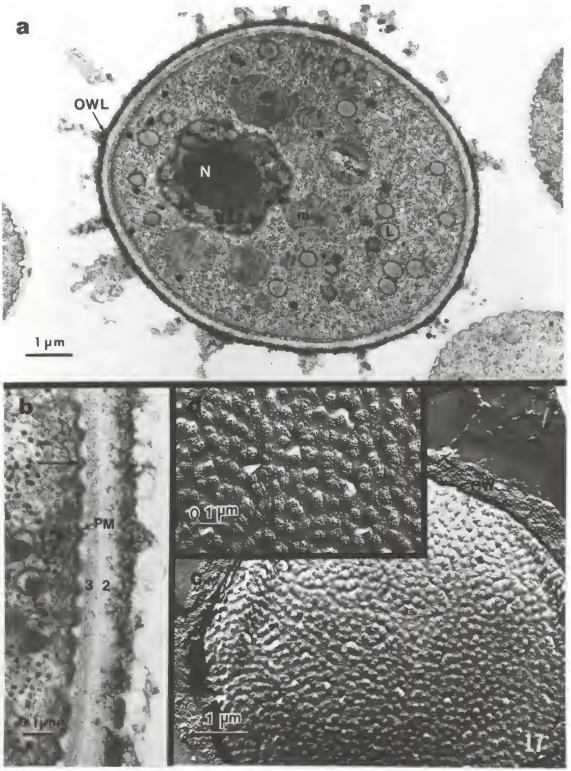
a
OWL
N
m
1 µm
b
PM
3
2
0.1µm
0.1µm
1 µm
1µm

stages. The mature microcyst is surrounded by a tri-layered wall (Figs. 17a, b). The outermost wall layer is a fibrillar network of high electron density, with the interior regions staining darkest, intergrading with the middle wall layer of light density. The innermost layer is of moderate electron density. The PF face (Figs. 17c, d) of the plasma membrane consists of clusters of particles that are elevated above a particle-free surface. In thin section, these would be located at the tip of the arrow in Figure 17b.

Mature microcysts transferred to germination buffer soon slough their outer wall layer (Fig. 18), separating through the median layer. The protoplast retains the inner wall layer, and parts of the middle layer usually adhere to either or both adjacent layers after separation (Figs. 19 and 20a). Within 10 min after loss of the outer layer, cytoplasmic vesicles increase and rough endoplasmic reticulum, absent in microcysts, reappears. The plasma membrane (Fig. 20a) has lost its crenulated appearance (compare with Fig. 17b) and retreats somewhat from the cell wall, with flat membrane sheets often evident between the plasma membrane and the wall. On the PF face (Figs. 20b, c), the clusters are lost and replaced by rows of particles that are still raised above a particle-free surface. The deep clefts are thought to represent fractures through sites of vesicle-plasma membrane fusions. These events define "initiation" of germination.

The "swollen" microcyst is evident 30-35 min after wetting (Fig. 21). The inner wall layer is less electron dense, probably due to its stretching as the protoplast expands or to actual dissolution (Figs. 21a, b). The plasma membrane is smoother and the cytoplasm less dense. The PF face is now similar to that of the vegetative cell (Figs. 21c,

Figure 18. Mature microcyst immediately after wetting. The outer wall layer is separating from the the middle wall layer after vigorous shaking.

Figure 19. Microcyst in the initiated stage 10 min after wetting. The outer wall layer is gone except for scattered fragments. Two wall layers are distinguishable. Much vesicular activity is evident with some rough endoplasmic reticulum. Microbody-like organelles have appeared (inset) that contain a fibrous inner core (arrow).

Figure 20. Characteristics of the cell surface at 10 min of excystment. (a) Thin section through the cell periphery showing wall layer 2 separating from layer 3. Part of the outer wall layer remains attached. The plasma membrane is no longer crenulated but irregular in profile. Membranous debris (arrow) appears to be released by the protoplast. (b) Freeze fracture of the PF face. (c) High magnification of the intramembrane particles and deep invaginations (arrow).

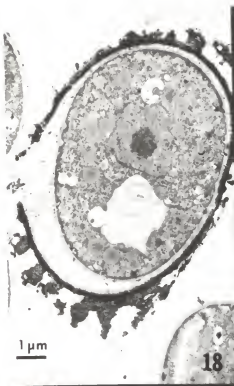
1 µm
18

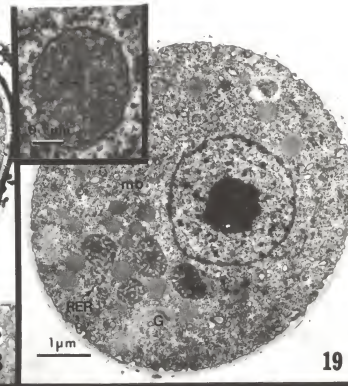
mo
RER
G
1 µm
19

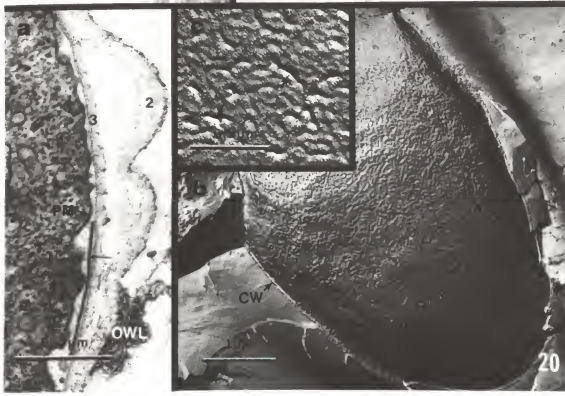
a
1
2
3
m
OWL
CW
20

d) having a smooth appearance with randomly distributed particles. The EF face has exhibited a gradual increase in particle number. These changes reflect a gradual reversion to the vegetative phase. Quantitative changes in IMP density are presented in Figure 22.

A contractile vacuole appears, while a single large food vacuole remains from the mature microcyst (Fig. 21a). Rough ER is abundant, and tubular cisternae and small vesicles occur at the periphery of the cytoplasm. Mitochondria become pleomorphic and show inflated cristae. Quantitative data (Fig. 23) shows a significant (Student t test=>99%) increase in nuclear size during germination and decrease during encystment. In contrast, the nucleolus shows a significant (Student t test=>90%) decrease in size after 45 min of excystment followed by an increase. The nucleolus retains a dense inclusion that was evident in mature microcysts (Figs. 24a, b). Chromatin is less condensed than in mature microcysts, and the nuclear envelope and adjacent cytoplasm often contain whorls of smooth membranes (Fig. 24c). Paired centrioles often associate with Golgi cisternae and microtubular arrays, forming the centrosome assembly characteristic of myxamoebae (Wright et al., 1979).

Finally, the "pre-emergent" stage, 35-40 min after wetting, a region of actin-like fibrils appears near the plasma membrane (Fig. 25). This fibrillar region bulges, rupturing the inner wall layer (Fig. 26). Scanning microscopy reveals a cytoplasmic bud protruding through a pore in the cell wall (Fig. 27). Finally, the pore enlarges and the myxamoeba emerges (Fig. 28).

Figure 21. Microcyst at the swollen stage after 35 min in excystment buffer. (a) Gross organization of a typical cell. A contractile vacuole has reappeared along with an organized cone complex and basal body. The mitochondria are less dense with inflated cristae. Fewer unattached ribosomes and more rough endoplasmic reticulum are observed. Only a single wall layer is visible. Inset: Portion of a swollen microcyst showing ringed-cisternal elements. (b) Thin section through the remaining inner wall layer that appears diffuse. The plasma membrane is noticeably smoother in profile. (c) Freeze fracture of the PF face. The round structure (arrow) is thought to result from vesicle-plasma membrane fusion. (d) High magnification of the intramembrane particles. Their distribution is like that of the vegetative cell.

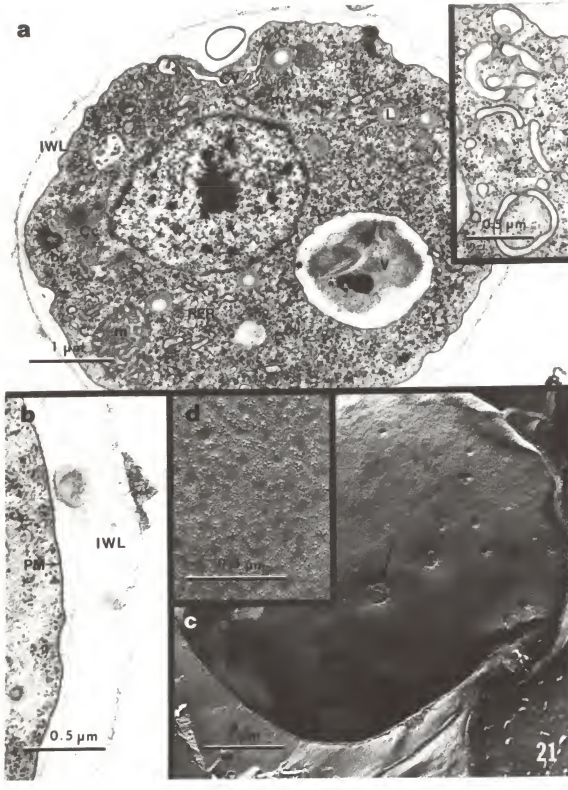
a
IWL
CV
L
V
RER
m
1 µm
0.5 µm
b
IWL
PM
0.5 µm
d
c
21

Figure 22. Changes in the density of intramembrane particles during excystment. Data are expressed as the average number of particles per μm^2 of membrane with standard deviation. White: PF face; dotted: EF face.

Figure 23. Changes in the size of the nucleus and nucleolus during excystment. Data are shown as an average diameter (with standard deviation) measured from at least 10 micrographs at constant magnification. Median sections were chosen based on the clarity of the nuclear envelope at opposing sides. Data was analyzed using the Student t test.

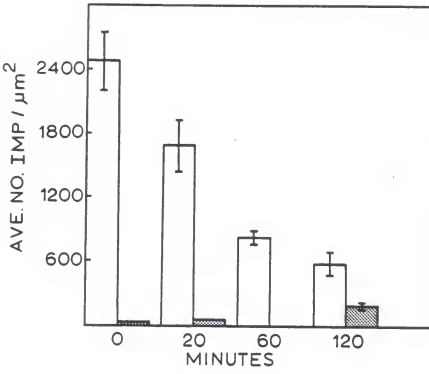
AVE. NO. IMP / μm²
2400
1800
1200
600
0
20
60
120
MINUTES

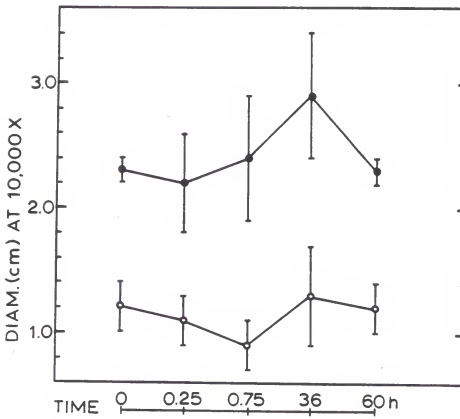
DIAM. (cm) AT 10,000 X
3.0
2.0
1.0
TIME
0
0.25
0.75
36
60 h

Figure 24. Nuclear changes during excystment. (a) Nucleus of a mature microcyst at 0 min. The large centric, nucleolus contains a dense body and is surrounded by numerous condensed chromocenters. (b) Nucleus of a swollen microcyst at 35 min with fewer chromocenters. The nucleolus appears slightly smaller in proportion and still contains the inclusion. (c) A portion of the nuclear envelope of a swollen microcyst at 35 min showing concentric, ER-like cisternae that are blebbing into the cytoplasm. Directly above (arrow), similar cisternae are seen.

a
N
cc
B
Nu
db
c
N
ne

Figure 25. A pre-emergent microcyst 35 min after wetting that contains a dense, fibrous zone adjacent to the site of emergence. The protoplast is beginning to bulge, stretching the inner wall layer (arrow).

Figure 26. Early protrusion of the microcyst cytoplasm through the ruptured inner wall layer (arrow).

Figure 27. A scanning electron micrograph of the emerging cytoplasmic bud. A pore is formed within the inner wall layer.

Figure 28. Germinated swarm cell 40 min after suspension in excystment buffer, showing basal bodies and the "beaked" nucleus.

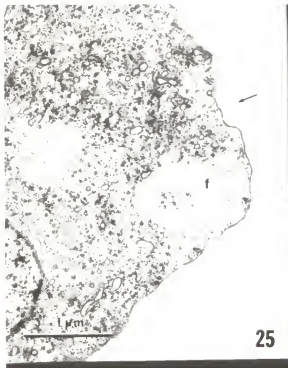

25

26

27

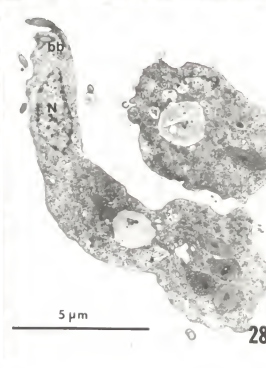

28

Discussion

Germination of D. iridis microcysts occurs in less than 1 h, with no requirement for activators or wetting agents. Gorman et al.(1977) reported similar optima for microcyst germination in P. polycephalum, although the germination rate in that system is considerably slower. This rate difference may be due to genetic variation, nutritional conditions during microcyst formation, or handling of microcysts for the assay. Consistent use of a Vortex mixer to resuspend microcysts for washing may have shortened the germination period by mechanically breaking the outer wall layer. Indeed, microcysts usually lacked an outer wall layer after the first wash.

Zaar et al. (1979) proposed that the fibrillar wall component of P. polycephalum spherules is hydrophobic, which discourages excessive dehydration or, possibly, premature rehydration. The D. iridis microcyst outer wall layer is in fact similar to the P. polycephalum spherule wall ultrastructurally, so the same reasoning could apply here. Loss of the outer microcyst wall layer would then be a prerequisite for rehydration and germination.

Enzymatic or osmotic lysis of the outer wall layer during spore germination has been suggested in Physarella oblonga (Farley et al., 1975) and Arcyria cinerea (Mims, 1971). Observation that high osmolarity inhibits germination of microcysts supports the hypothesis of osmotic involvement. Mims (1971) points out that hydrolysis of cytoplasmic storage polysaccharides could contribute to this increase in interior osmotic pressure, but it has not been demonstrated.

Demonstration of a magnesium requirement for microcyst germination appears to be without parallel in the Myxomycetes. Optimal levels are

extremely low since excystment proceeds in distilled water. This may reflect its importance for polysome formation and oxidative respiration.

The partial inhibition of germination by cycloheximide, coupled with appearance of rough ER during activation, suggests early protein synthesis during the germination sequence. This is consistent with the demonstration by Gwynne and O'Day (1978) that protein synthesis in P. pallidum occurs 15 min after induction. Lack of germination inhibition by actinomycin D suggests that a stable messenger is synthesized during encystment to prepare for rapid emergence when conditions are favorable, and such a finding was reported in P. pallidum (O'Day et al., 1976) and P. polycephalum spherules (Jeffery, 1979). This may be partially true in D. iridis since formation in the presence of RNA synthesis inhibitor delayed excystment. The observation that the nucleolus decreases in size during germination also argues against early RNA synthesis.

An increase in nuclear volume is consistent with metabolic activation during spore germination of fungi in general (Smith, 1976). The decrease in size observed when amoebae encyst is consistent with other data suggesting that mitosis is a prerequisite for differentiation (Mohberg and Rusch, 1971). Microcysts contain one-half the DNA content of vegetative cells and are presumed arrested in G_1 phase. Henney and Tavana (1982) have shown that inhibitors which block cell division block microcyst formation. Germinating microcysts would then be in the S phase of cell division and the appearance of pleomorphic mitochondrial shapes supports this. Elongate mitochondria indicate that mitochondrial division is occurring, which has been shown to initiate in early S phase (Kuroiwa, 1982).

Within the nuclear envelope, the whorls of tubular cisternae may contribute to the initial abundance of ER as has been suggested by Robb (1972) during teliospore germination in Ustilago. In fact, cytoplasmic elements are produced by nuclear envelope proliferation in certain oocytes during periods of high protein synthesis (Wischnitzer, 1973).

The need for additional detailed observations on the processes of spore and microcyst germination in Myxomycetes is clear, if we are to understand the "on-off" mechanism and regulation of haploid dormancy. Specifically, we need to know what signals initiate reversion to the vegetative state and, once induced, what the characteristic metabolic patterns are. It is also important to know the composition of the microcyst wall and the pattern of enzyme activities during encystment and germination. The present study establishes a base from which these additional studies can be pursued.

CHAPTER 3
ISOLATION, FRACTIONATION, AND CHEMICAL ANALYSES OF THE MICROCYST WALL

Introduction

The differentiation of haploid amoebae into microcysts was described in detail in Chapter 1. In summary, it is a morphological and biochemical process culminating in the formation of a cell wall from endogenously derived precursors. The cell wall of all Myxomycete resistant structures, inclusive of spores, microcysts and spherules, has not received a great deal of attention (reviewed by Henney, 1982). It is known that these cell walls are composed of a polygalactosamine polymer that is unique to the fungi. Galactosamine polymers are known to occur in nature (Distler and Roseman, 1960; Mahadevan and Tatum, 1965; Applegarth, 1967; Buck et al., 1969; Bardalaye and Nordin, 1976; Ruperez and Leal, 1981) but are most often found as minor components in the cell wall. The most similar composition is found in the walls of the trichomycete, Amoebidium parasiticum (Trotter and Whisler, 1965).

The spherule wall of Physarum polycephalum has been found to contain 88% galactosamine (McCormick et al., 1970b; Farr et al., 1977). Farr et al. (1977) further characterized it as an α-D-(1-4)-linked polymer that is partially acetylated (0.5%). In contrast to these findings, Zaar et al. (1979) reported that the wall contains 21% neutral sugars, 20% galactosamine, and 59% protein. They described the

wall as consisting of a fibrillar proteoglycan embedded in a glycoprotein matrix. Another study by Henney and Chu (1977b) using spherules of Physarum flavicomum revealed that its wall consists of 55% galactosamine, 4% neutral sugars, 16% lipid, and 15% protein.

Henney and Chu (1977b) also studied microcysts of P. flavicomum; their study represents the only example of microcyst wall composition in the Myxomycetes. The wall was found to contain 32% galactosamine, 10% neutral sugars, 22% lipid, and 21% protein. The amino acid component was similar to that of the spherule suggesting a conserved metabolic pathway between haploid and diploid differentiation.

The observation of an extracellular material prior to microcyst wall formation in Didymium iridis is the first of its kind in the Myxomycetes (Chapter 1). It is suspected of being a slime like that associated with the vegetative diploid phase (plasmodium). The slime of P. polycephalum has been the subject of several studies (McCormick et al., 1970a; Simon and Henney, 1970; Farr et al., 1972). These workers all agree that it is a highly branched, β-D-galactan that is partially sulfated. In contrast, Simon and Henney (1970) and Henney and Chu (1977b) have reported that the slime of P. polycephalum, P. flavicomum, and Physarum rigidum is a glycoprotein consisting of 68-72% galactose and 28-32% protein.

Many functions for slime have been proposed. It has been established that it is not a wall precursor nor is it metabolized (McCormick et al., 1970a). In analogy to the extacellular polysaccharide gels of many microbial cells (Geesey, 1982), it may reduce diffusion of substances to and from the cell, provide a suitable matrix for extracellular enzymes, provide a cation exchanger, protect, or prevent desiccation.

This chapter is devoted to describing the chemical composition of microcyst walls from D. iridis. Since it is the only study of its kind using Didymium, it is the first time two different families of the same order, Physarales, can be compared.

Materials and Methods

Organism and Growth

Didymium iridis clone C-4 (A_8) was maintained as described in Chapter 1.

Chemicals

The following reagents are identified by the place of purchase. All are reagent grade unless otherwise indicated.

Acetic anhydride, Mallinckrodt; aniline, Fisher; butanol, Mallinckrodt; benzene, Mallinckrodt; chloroform, Fisher; p-dimethylaminobenzaldehyde, Mallinckrodt; diphenylamine, Fisher; D(+)galactosamine HCl, Sigma; D(+)glucose, Sigma; lactic acid, Fisher; methanol, Fisher; methylene chloride, Fisher; phenol, Fisher; polyacrylamide, Bio-Rad; potassium sulfate, Mallinckrodt; 2-propanol (spectroanalyzed), Fisher; pyridine, Eastman; sodium borohydride, Eastman; sodium dodecyl sulfate (electrophoresis grade), Polysciences; Triton X-100 (scintillation grade), Eastman.

Encystment Conditions

Myxamoebae were induced to encyst as described in Chapter 1. A total of 30-40 pans were harvested for each wall preparation yielding 2-3 X 10^{10} cells. These were induced in 3-400 ml encystment buffer at

a concentration of 2 X 10^7 cells/ml by shaking 1,000-ml Erlenmeyer flasks at 140 rpm for 48 h. Microcysts were collected by centrifugation, washed 5X in 50 mM potassium phosphate buffer, pH 6.0, at 4 C, frozen in liquid nitrogen and stored at -40 C.

Preparation of Microcyst Walls

Microcysts were broken in a Braun homogenizer operated at 4,000 rpm for 2 min. A 25 ml suspension of 7-8 X 10^9 microcysts was placed in a Braun bottle one-third full of 0.12-0.15 mm acid-cleaned glass beads and 5 drops of tributyl phosphate added as an anti-foam agent.

Glass beads were removed by decanting. Crude walls were washed 50X with a repeating sequence of glass distilled water, 1% Triton X-100 and 1 M NaCl. Each sequence called for three washings in water followed by one wash with detergent that included three-30 sec treatments using a Sonic Dismembrator (Fisher Scientific, Model 150) operated at 40%. After repeating this cycle four or five times, NaCl was alternated with the detergent. Suspensions were immersed in an ethanol/ice bath at -5 C. Wall fragments were centrifuged at 1,250 x g for 15 min during the first 20 washes and increased to 1,950 x g for the remaining washes. This procedure was interrupted after 20 washes by treating crude wall fragments overnight in detergent with stirring.

Walls were suspended in 5 ml methanol (CH_3OH) with sonication for 30 sec, 10 ml chloroform ($CHCl_3$) were added and the mixture stirred for 3 h at room temperature. Fragments were centrifuged, washed once with methanol, washed 5X with water and excess reagent evaporated under a stream of dry N_2. Clean walls were lyophilized to determine dry weight yield and stored over desiccant before chemical fractionation.

Purity of the preparations was monitored by the absorbance of washes at 280 and 260 nm and by appearance using phase-contrast optics after staining with methylene blue. The final criterion was the absence of cytoplasmic debris in samples examined with electron microscopy.

All procedures were performed at 4 C unless otherwise noted. All glassware was acid-cleaned and solutions were prepared with glass distilled, deionized water filtered through a 0.45 μm Nuclepore polycarbonate filter.

Preparation of Crude Slime

Encystment buffer from 4 and 48 h old suspensions was concentrated by lyophilization. After resuspension in water, supernatant from a 15 min 2,000 x g centrifugation was treated overnight using 2 vol. 95% ethanol. After three repeated precipitations, the crude slime was dialyzed (Spectrapor/2, Fisher Scientific) overnight against water at 0 C, lyophilized, and stored over desiccant.

Chemical Fractionation of Clean Walls

Wall fragments were subjected to a series of extractions, modified from Zaar et al. (1979), outlined in Figure 29. Between each step, the residue was washed 5X with water by centrifugation at 4,990 x g for 15 min. Extraction with alkaline urea was performed according to Horst et al. (1980) except Nonidet P-40 and dithiothreitol were omitted. The soluble fraction was dialyzed for 3 days. All extractions were performed under stirring. The five fractions were lyophilized and stored over desiccant until further analysis.

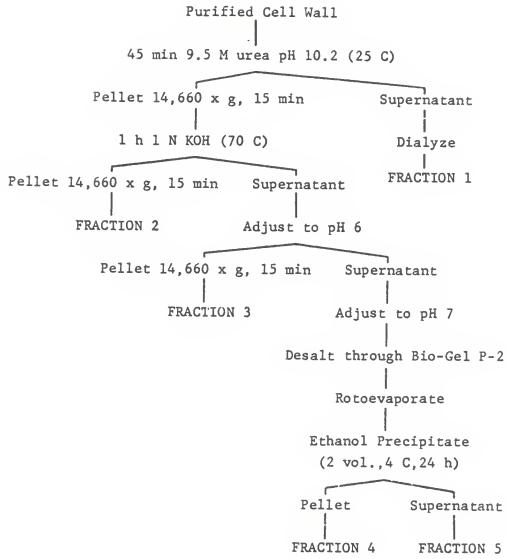

Figure 29. A schematic of chemical fractionation of purified microcyst walls after lipid extraction.

General Analytical Methods

Total protein was determined according to Lowry et al. (1951) and neutral sugars using the phenol-sulfuric acid method of Dubois et al. (1956). Hexosamines were determined according to Johnson (1971) after hydrolysis in 6 N HCl for 6 h at 100 C under N_2. Phosphate content was assayed according to Chen et al. (1956) and sulfate by the method of Dodgson and Price (1962). Reducing sugars were quantitated by a modified Park and Johnson method (Thompson and Shockman, 1968) and the presence of uronic acids assayed according to Dische (1946).

For the determination of acetyl groups, the method of Farr et al. (1977) was used. Sample (6.3 mg/ml) was hydrolyzed in 2 N HCl for 2 h at 100 C under N_2, neutralized, rotoevaporated, resuspended in 2% H_3PO_4, and analyzed for acetate using gas chromatography (Ottenstein and Bartley, 1971).

Acid Hydrolyses

To determine the optimal conditions for maximum liberation and minimum destruction, hydrolysis was carried out at 6 h intervals up to 48 h. All hydrolyses, using 1 mg/ml sample concentrations, were done in sealed ampoules under N_2 at 100 C. Proteins were hydrolyzed in 6 N HCl for 18 h, amino sugars in 4 N HCl for 12 h, and neutral sugars in 1 N HCl for 8 h. Hydrolysates were rotoevaporated and subjected to direct analysis.

Neutral Sugar Analysis

Paper and thin-layer chromatography were used to identify neutral sugars present in purified microcyst walls and extracted fractions. Further characterization and quantitation were performed using gas-liquid chromatography.

Amino Sugar and Protein Analysis

Hexosamine was identified using paper and thin-layer chromatography. Further characterization and quantitation were accomplished using the short acidic column of an amino acid analyzer. In each case unknowns were compared to D-galactosamine HCl as a standard.

Protein analysis was performed on an amino acid analyzer.

Paper and Thin-layer Chromatography

Samples were spotted onto Grade 1 Whatman paper and developed, descendingly, for 40 h using n-butanol-pyridine-water (6:4:3, by volume). Spots were visualized with alkaline silver nitrate (Churms, 1982). Hexosamines were also identified using Elson-Morgan reagents as described by Churms (1982).

Thin-layer chromatography was performed on precoated silica gel 60 plates (Merck; 20 X 20 cm; 0.25 mm thick) by ascending development with 2-propanol-acetone-1 M lactic acid (4:4:2, by volume) according to Hansen (1975). Spots were visualized after spraying with diphenylamine-aniline-phosphoric acid (Churms, 1982) and heating for 30 min at 105 C. Neutral sugars were blue and hexosamines were a light brown.

Gas-liquid Chromatography

Neutral sugars were prepared as their alditol acetate derivatives (Oades, 1967) and separated on a 6 ft X 2 mm column packed with 10% SP-2340 on a 100-120 Gas Chrom Q support in a Tracor 560 chromatograph equipped with a flame ionization detector. The column oven temperature was programmed from 180 to 240 C with a rate of 2 C/min. The temperature was held at 180 C for 5 min and at 240 C for 10 min. An internal standard of myo-inositol was added after hydrolysis but before rotoevaporation.

Amino Acid Analysis

Hydrolysates were reconstituted in 0.01 N HCl and injected into a Jeol Co. Model JLC-64H Analyzer equipped with an integrator. Unknowns were quantitated against Amino Acid Standard H (Pierce Chemical Co.).

Column Chromatography

A 4-5 ml volume of the neutralized supernatant was desalted on a 2.5 X 38 cm Bio-Gel P-2, 200-400 mesh, (Bio-Rad) column equilibrated with water. Separation was achieved with a flow rate of 3 cm/h. The eluate was monitored by absorbance at 280 nm. The column was calibrated with a mixture of hemoglobin and phenylalanine.

Gel Electrophoresis

Sodium dodecyl sulfate (SDS) polyacrylamide slab gel electrophoresis (PAGE) was performed according to Laemmli (1970) using a 3% stacking gel and a 7.5 or 10% separating gel. Samples containing approximately 100 ug protein were dissolved in a sample buffer

containing 4 M urea, 2% SDS, 5% 2-mercaptoethanol and 10% glycerol in 62.5 mM Tris-HCl buffer at pH 6.8 (Whitaker, 1982). Gels were fixed in 40% ethanol, 7% acetic acid and stained in 0.125% Coomassie Brilliant Blue R. The following were used as molecular weight markers: trypsinogen (24,000), actin (42,000), bovine serum albumin (66,000), phosphorylase A (94,000), β-galactosidase (134,000).

Alternatively, gels were fixed in 30% methanol, 12% trichloroacetic acid, 3.5% sulfosalicylic acid, and glycoproteins were stained with periodic acid-Schiff reagent according to Zacharius et al. (1969) and with Alcian blue according to Wardi and Michos (1972). Ovalbumin was used as a standard.

Electron Microscpopy

Purified wall fragments were fixed and embedded as described for cells in Chapter 1. A suspension of wall fraction 2 was negative stained with 1% aqueous uranyl acetate on Formvar-coated grids and examined using a Jeol JEM-100CX.

Selected Area Electron Diffraction (SAED)

Dilute solutions of samples and standards were dried onto carbon-stabilized, Formvar-coated copper grids (200 mesh). Standards included α -cellulose (Avicel, FMC Corp., Phila., Pa.) and chitin from crab shells (Sigma). Corresponding reciprocal lattices were obtained with a Jeol JEM-100CX in SA diffraction mode operating at 80 kV and photographed with a camera length of 76 cm and an exposure of 20 sec.

Results

Isolation of Microcyst Walls

Several different homogenization procedures were tested to obtain maximum breakage without a high degree of fragmentation. The multiple passes required for breakage using the French press resulted in small wall fragments. Microcysts would not rupture from nitrogen cavitation using a Parr bomb at 2,000 PSI and a 30 min equilibration period. Use of the Braun homogenizer resulted mostly in microcyst wall casings (Fig. 30). Larger glass bead diameters up to 1.23 mm were tested but resulted in smaller fragments.

Microcyst walls were fluffy white in appearance and had a tendency to flocculate; therefore, the use of sonic oscillation during the washes (Taylor and Cameron, 1973) was necessary. Satisfactory purification required at least 40 to 50 washes, after which absorbance at 280 and 260 nm was less than 0.02. Electron micrographs of purified walls (Fig. 31) failed to show cytoplasmic contamination although an occasional unbroken microcyst was observed. This was estimated to be well below one percent. In addition, corrections were not made for moisture content since weight loss at 80 C for 30 min was less than 0.015%. Total recovery of purified wall material after chemical fractionation averaged about 70% by dry weight.

Composition of Crude Slime

The appearance of a slime-like material during the early stages of microcyst formation (Fig. 2, Chapter 1) initiated the need to determine if this material was microcyst cell wall or a different extracellular polymer. After precipitation and dialysis, 1,000 ml of encystment

Figure 30. Phase-contrast micrograph of cell wall fragments after breakage in a Braun homogenizer

Figure 31. Electron micrograph of cell wall fragments after extensive washing. (a) Fragments retain cell shape and appear to be free of cytoplasmic debris. The fibrous outer wall layer is easily removed and is seen scattered throughout. (b) High magnification of the cell wall showing that at least two layers remain intact (1 and 2).

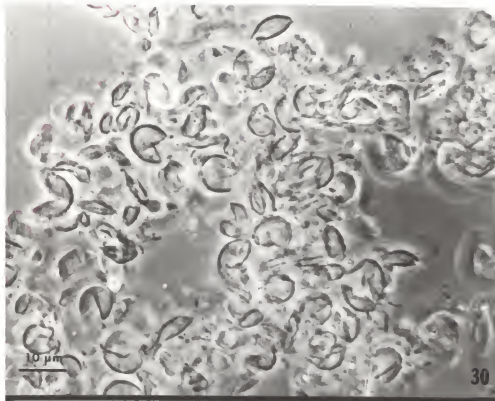
10 µm
30

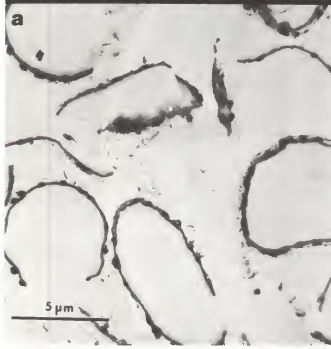
a
5 µm

b
0.1 µm
31

buffer yielded 7.0 mg of crude slime. Slime from 48 h old suspensions consisted of 45% neutral sugars, 11% hexosamine, and 30% protein (Table 3-1). The only hexosamine present was galactosamine and it was not detected in 4 h old suspensions. Gas chromatographic analysis of the sugars (Table 3-2) showed that the major monosaccharide constituent is galactose. At 4 h, the galactose content was 87% of the neutral sugars with the remaining 13% accounted for as glucose. Amino acid analysis of the protein component (Table 3-3) revealed an unusually large quantity of tyrosine (17.7 mol%). At least two bands with molecular weights of approximately 45,000 and 32,000 are separated by 7.5% SDS-PAGE (Fig. 32, lane d).

Gross Composition of the Microcyst Wall

Direct chemical analysis of pure microcyst wall (Table 3-4) shows it to consist of neutral sugars, hexosamine, protein and sulfate ion. Uronic acids were absent. The major polysaccharide component is galactosamine (35% by weight). Gas chromatographic analysis (Table 3-5) shows that the neutral sugars are almost entirely composed of galactose and glucose. Amino acid analysis (Table 3-3) reveals large quantities of threonine and aspartate/asparagine with low amounts of cystine/cysteine and methionine.

Chemical fractionation of the microcyst wall resulted in five fractions. The general composition of each fraction is given in Table 3-6 with particular attention given to the alkali-insoluble polymer, fraction 2. Most of the protein is extracted with alkaline urea,

Table 3-1. Chemical composition of crude slime precipitated from encystment buffer at 48 h.

Component	% Dry Weight[a]
Neutral sugars	45
Hexosamine	11
Protein	30
Sulfate ion	13
Total components identified	99

[a]Calculated as described under Materials and Methods using galactose, galactosamine HCl, bovine serum albumin, and potassium sulfate as the respective standards.

Table 3-2. Neutral sugar composition of crude slime precipitated from encystment buffer at 48 h.

Monosaccharide	Relative %[a]
Deoxyribose	1.9
Rhamnose	10.4
Ribose	3.6
Mannose	6.3
Galactose	58.1
Glucose	19.8

[a]Calculated from gas-liquid chromatograms using total peak area equal to 100%.

Table 3-3. Amino acid analysis of proteins.[a]

Amino Acid	Slime	Whole Wall	Wall Fractions 1	3	5
Lysine	2.9	3.4	4.4	5.2	2.8
Histidine	1.2	1.2	1.4	0	0.8
Arginine	1.9	3.4	3.9	0	2.0
Aspartate (NH_2)	10.1	10.3	10.8	24.2	12.9
Threonine	9.9	12.2	10.6	5.0	7.2
Serine	9.8	7.4	7.8	6.1	4.1
Glutamate (NH_2)	5.9	7.3	8.1	14.7	9.8
Proline	5.2	9.1	7.7	0	9.4
Glycine	7.9	9.2	9.1	16.2	11.6
Alanine	7.6	8.0	7.9	12.4	9.1
Cystine/Cysteine	1.6	2.0	tr	0	0
Valine	6.3	8.3	5.2	7.1	9.0
Methionine	0	tr	tr	0	0.8
Isoleucine	3.3	5.0	4.8	0	7.1
Leucine	5.4	5.5	6.8	4.6	5.7
Tyrosine	17.7	4.6	4.9	4.5	5.4
Phenylalanine	3.2	3.1	3.6	0	3.6

[a]Data expressed as mol %.
tr, trace amount.

Figure 32. Sodium dodecyl sulfate-PAGE (7.5%) of wall fraction 1 and crude slime. (a) Molecular weight markers with their relative molecular weights. (b) Fraction 1 stained with Coomassie blue. (c) Another preparation of fraction 1. (d) Crude slime stained with Coomassie blue. (e) Fraction 1 stained for glycoproteins with PAS. (f) Fraction 1 stained for negatively charged groups with Alcian blue.

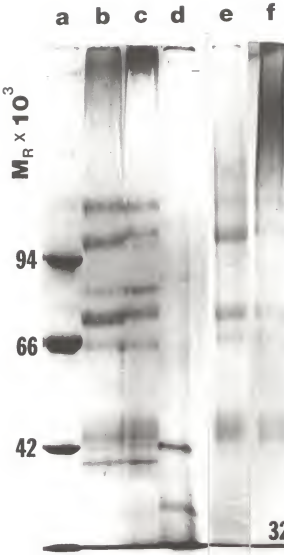
a
b
c
d
e
f
$M_R \times 10^3$
94
66
42
32

Table 3-4. Chemical composition of the microcyst wall.

Component	% Dry Weight
Neutral sugar	28
Hexosamine	35
Protein	29
Sulfate ion	7
Total components identified	99

Table 3-5. Neutral sugar composition of microcyst wall.[a]

Monosaccharide	Whole Wall	Wall Fractions 1	2	3	4	5
Deoxyribose	5.7	3.5	2.0	35.9	24.1	30.6
Rhamnose	9.9	15.7	0	0	0	23.2
Ribose	6.6	19.2	0	0	0	0
Mannose	0	2.6	0	0	0	0
Galactose	34.5	59.0	0	64.1	38.4	46.3
Glucose	43.3	0	98.0	0	37.6	0

[a]Calculated from gas-liquid chromatograms using the total peak area equal to 100%.

Table 3-6. Chemical composition of microcyst wall fractions.

Component	% Dry Weight				
	1 (22%)[a]	2 (21%)	3 (10%)	4 (34%)	5 (12%)
Neutral sugar	17	59	4	3	6
Hexosamine	10	31	48	31	0
Protein	56	0	5	0	72
Sulfate ion	nd	7	nd	nd	nd
Phosphate ion	3	0	0	11	6
Acetate	nd	3	nd	nd	nd

[a]Percentage of wall material recovered in each fraction.

nd, not determined.

identifying it as a noncovalently bound component. A majority of the galactosamine is found in fraction 2 and the alkali-soluble, ethanol-precipitable fraction 4.

Fraction 1

This fraction is obtained by treating pure microcyst walls with 9.5 M urea at pH 10.2 and represents 22% of total material (Table 3-6). A second treatment showed that greater than 95% had been removed during the first extraction. This fraction consists mostly of protein with small amounts of galactosamine (10%) and neutral sugars. The predominant monosaccharide is galactose (Table 3-5). It appears that most of the ribose is removed with this fraction.

Amino acid analysis (Table 3-3) showed that aspartate/asparagine, threonine and glycine are present in the greatest quantities with only trace amounts of cystine/cysteine and methionine. SDS-PAGE (Fig. 32, lanes b, c) revealed at least seven major bands of the following calculated molecular weights (M_R): 170,000; 120,000; 83,000; 77,000; 62,500; 44,300; 39,000. Five of these were periodic acid-Schiff reagent-positive (Fig. 32, lane e) and four were stainable with Alcian blue (Fig. 32, lane f). In Chapter 4, this fraction is also shown to represent the antigenic determinant.

Fraction 2

Further extraction of the alkaline urea residue with strong alkali fractionated the wall into soluble (fractions 3-5) and insoluble (fraction 2) components. This insoluble residue represents the structural backbone of the microcyst wall shown by maintenance of cell

shape (Chapter 5, Fig. 47). It is comprised entirely of 31% galactosamine (Table 3-6) and 59% neutral sugar, 98% of which is glucose (Table 3-5). This galactosaminoglucan appears to be partially acetylated (2.6%) and sulfated (7%). Use of the Thompson and Shockman (1968) method for determining reducing sugars of insoluble material gave 1.3% by weight suggesting that fraction 2 is not highly branched.

Although protein was absent from this preparation (Table 3-6), nine amino acids could be detected in trace amounts if the extraction was mild, such as 1 N NaOH at room temperature for 24 h.

Negatively stained preparations reveal a random network of microfibrils (Fig. 33). Analysis of fraction 2 with SAED (Fig. 34a) resulted in a hexagonal reciprocal lattice ($\gamma = 61.4 \pm 2.4$). Lattices of chitin and cellulose are also shown for comparison (Figs. 34b, c).

Fraction 3

It was observed that a precipitate formed in the alkali-soluble supernatant when the pH was adjusted to 6.0 but remained soluble at neutral pH. Analysis of this precipitate showed that it is mostly comprised of galactosamine (Table 3-6). The 5% protein component is composed of the acidic amino acids, aspartate/asparagine and glutamate/glutamine, as well as glycine and alanine (Table 3-3).

Fraction 4

After readjusting the supernatant to pH 7.0, it was concentrated and desalted on Bio-Gel P-2. The elution profile is shown in Figure 35. The two peaks eluted before the salts were combined and treated with ethanol giving two fractions. Fraction 4, precipitated by

Figure 33. High magnification of wall fraction 2 that has been negatively stained with 1% aqueous uranyl acetate.

Figure 34. Selected area electron diffraction patterns of (a) fraction 2, (b) crab shell chitin, and (c) $^{\alpha}$-cellulose.

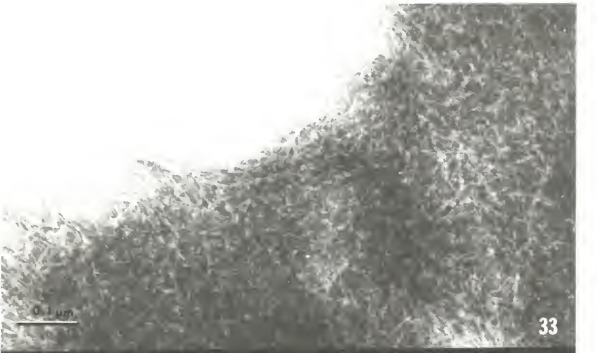
0.1 μm
33

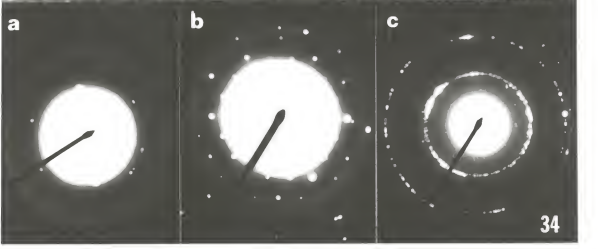
a
b
c
34

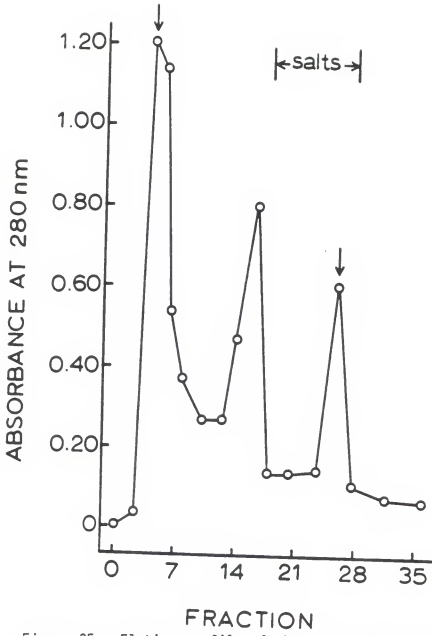

Figure 35. Elution profile of the neutralized KOH-soluble wall components fractionated on a Bio-Gel P-2, 200-400 mesh, column. The arrows denote the positions of hemoglobin and phenylalanine, respectively, that were used for calibration. The two peaks to the left of the salt fractions were pooled and subjected to further treatment.

ethanol, appears similar in composition to fraction 3. It is also mostly comprised of galactosamine (Table 3-6); however, there is no associated protein. This fraction was found to contain a high quantity of phosphate (Table 3-6).

Fraction 5

Fraction 5 was not precipitated by ethanol. It is mainly comprised of protein (Table 3-6) that is most likely composed of small polypeptides with molecular weights greater than 1,500 (excluded on Bio-Gel P-2) but lower than 14,000 since bands were not detected on 10% SDS-PAGE. This would be expected due to the harsh extraction procedure and failure to precipitate with ethanol. Amino acid analysis (Table 3-3) revealed high quantities of aspartate/asparagine and glycine. It is also interesting that the small amount of neutral sugars present includes a high percentage of galactose (Table 3-5). This fraction also contained a large quantity of phosphate (Table 3-6).

Discussion

Previous studies on myxomycete cell wall chemistry (McCormick et al., 1970b; Farr et al., 1977) included several washes with 0.1% sodium lauryl sulfate and resulted in cell wall fragments containing very little protein. Zaar et al. (1979) showed that treatment with 0.1% SDS at 60 C for 24 h removed 54% of the total material. To avoid this, microcyst walls were washed with distilled water, 1 M NaCl, and the nonionic detergent Triton X-100. It is possible that the detergent may have removed some components, and they are known to form complexes with the protein moiety (Taylor and Cameron, 1973); however, this treatment

was necessary to remove cytoplasmic constituents. Salt washes are also reported to remove galactosamine-containing compounds (Edson and Brody, 1976) although this loss does not appear to be substantial.

Initial hydrolyses were done using 0.25 N HCl in the presence of ion exchange resin (Porter, 1975), but the technique was discontinued when the hexosamines could not be eluted quantitatively. Zaar et al. (1979) report that only 37% of the original amino sugar concentration was recovered and a correction factor was introduced. In this study hydrolyses of galactosamine standards revealed that 20% were destroyed. In fact this is probably an underestimate for in situ hydrolysis, since the presence of amino acids and neutral sugars are not accounted for. These standards also explained the source of a large peak eluted after phenylalanine as a degradative product. Hydrolysis will also deaminate asparagine and glutamine and destroy the sulfur amino acids (Taylor and Cameron, 1973).

Gross composition of the microcyst wall of D. iridis is similar to P. flavicomum microcysts (Henney and Chu, 1977b) where both contain approximately the same amount of galactosamine. The protein contents may also be similar if this study had included lipid composition. In fact, the amino acid compositions were alike except for the large quantity of lysine found in P. flavicomum walls. Didymium iridis walls also appear to contain small quantities of the sulfur amino acids as do P. polycephalum (McCormick et al., 1970b) and P. flavicomum (Henney and Chu, 1977b). This appears to be typical of the fungi (Taylor and Cameron, 1973); however, they are easily destroyed during hydrolysis.

In contrast to the recovery of 22% of total material in fraction 1 of this study, Zaar et al. (1979) recovered 8% and found only two

periodic acid-Schiff reagent positive bands using SDS-PAGE. McCormick et al. (1970b) solubilized a single PAS-positive band from spherule walls that migrated similarly to the 55,000 molecular weight band from spore walls (Jockusch et al., 1970). The spore wall also contained a 70-75,000 molecular weight band. In no instance did the wall of D. iridis contain unusually large quantities of phenylalanine as reported by Zaar et al. (1979). Fraction 1 is most likely associated with other wall components via hydrogen bonding and may represent the bulk of the matrix polymers. It contains a 1:3 molar ratio of galactose to serine/threonine suggesting that O-glycosidic linkages, commonly found in plant cell wall glycoproteins (Sharon, 1975), are present.

Fraction 2 appears to be a polymer unique to the Myxomycetes since it consists mostly of glucose in association with galactosamine. It is the structural component of the microcyst wall and appears to be resistant to alkali, as are chitin and cellulose. Selected area electron diffraction shows that this extracted polymer possesses a weak crystalline structure although it is not known whether this is true in the native state. The bright spots are due to inorganic impurities (Gemperle et al., 1982). The alkali-resistant polymer of P. polycephalum spherules also appears to be crystalline (Zaar et al., 1979). Fraction 2 is found to be partially acetylated, most likely at C2 of galactosamine, as was shown by Farr et al. (1977). It is also associated with sulfate and lacks phosphate groups, unlike similar fractions studied previously. The results of mild alkali extraction suggest that this polymer is covalently associated with protein, since trace amounts of nine common amino acids were detected after extensive washing.

The alkali-soluble fractions account for most of the galactosamine, as is the case for P. polycephalum (Zaar et al., 1979). Fraction 3 is particularly interesting since it is associated with protein even after harsh alkali extraction. This may indicate the presence of a resistant glycosidic linkage, such as between galactosamine (or the acetylated form) and aspartate or asparagine. Such a linkage would be analogous to the N-glycosidic bond between N-acetylglucosamine and asparagine found in many glycoproteins (Sharon, 1975). Regardless, acidic amino acids in this fraction appear to be responsible for its precipitability at pH 6.5.

Fraction 4 has no protein although its galactosamine content is similar to fraction 3. It may represent smaller fragments of the same polymer but amino acids have been cleaved by β-elimination. Fraction 4 and especially fraction 5 are similar to fraction 2 from spherule walls (Zaar et al., 1979) in that they contain a large quantity of amino acids (most likely small polypeptides) cleaved during alkali extraction. These fractions contain large quantities of aspartate/asparagine, glutamate/glutamine, and glycine typical of fungi in general (Taylor and Cameron, 1973).

In several of the wall fractions, 100% of total material could not be accounted for. The reason for this is unclear. It is obvious that the wall preparation was contaminated with cytoplasm since the nucleic acid pentoses were present. High concentrations of phosphate in some of the fractions may also indicate contamination from inert materials. There was some concern about contamination from the bacteria used as a food source to grow the vegetative amoebae; however, amino acids common to the cell wall of Escherichia coli were never observed.

Purification of a polymer believed to be analogous to slime was difficult. Quantities of galactosamine and glucose from the microcyst wall and cyotoplasmic constituents (deoxyribose, ribose, rhamnose, and mannose) were usually present. These contaminants were absent in preparations from 4 h-old suspensions and it is suspected that much of it arises from cell leakage or lysis during differentiation.

Crude slime from D. iridis does appear to contain protein, as has been reported in P. polycephalum, P. flavicomum, and P. rigidum (Simon and Henney, 1970; Henney and Chu, 1977b). A comparison between amino acid profiles shows many similarities except that the abundance of lysine in Physarum is replaced by tyrosine in Didymium. Crude slime is separated into two bands using SDS-PAGE with the higher molecular weight species migrating similar to a faint band in wall fraction 1 (Fig. 32). Simon and Henney (1970) also reported two bands but one of these is thought to be a contaminating glycoprotein of unknown origin (McCormick et al., 1970a). Comparison is difficult since molecular weights were not provided. While these data alone do not suggest that a different polymer forms prior to microcyst wall formation, ^{3}H-galactose was incorporated into an extracellular galactose polymer precipitated from the encystment buffer (Chapter 5).

Chapters 4 and 5 will discuss the secretion of these extracellular polymers during encystment.

CHAPTER 4
AN IMMUNOCYTOCHEMICAL APPROACH TO MICROCYST WALL BIOGENESIS

Introduction

Secretion of macromolecules is a basic cellular process of all cell types (Palade, 1975). Essentially two models are proposed for the transport of secretory product to the cell exterior: (1) reverse pinocytosis preceded by processing within the endomembrane system; (2) free "diffusion" across the plasma membrane. By far, the majority of the systems studied fall into the first category. In the past few years a great deal of attention has been devoted to understanding the cellular processes during secretion in mammalian systems, particularly the involvement of the Golgi apparatus (see reviews by Morre and Ovtracht, 1977; Whaley and Dauwalder, 1977; Morre et al., 1979; Farquhar and Palade, 1981; Rothman, 1981; Rothman et al., 1982).

Cellular sites of secretion products in the fungi are less defined. This is especially true for polysaccharide synthesis, it remains unclear whether synthesis occurs only at the plasma membrane or is initiated at an intracellular site enroute to the cell surface. In contrast, the secretion of fungal glycoproteins is well known to involve vesicle transport (Farkas, 1979; Gooday and Trinci, 1980). The synthesis of yeast mannans is the best characterized process with respect to its secretory pathway. Protein-mannans are found to be processed much like mammalian and plant cell wall glycoproteins (Cabib

and Roberts, 1982). Synthesis begins within the rough endoplasmic reticulum followed by glycosylation and other modifications as the product is transported through the Golgi apparatus and transported to the plasma membrane by vesicles. Synthesis in the yeasts has recently been studied using genetic mutants interrupted at successive cellular sites of invertase secretion (Novick, 1981).

To date there has not been an attempt to identify cellular sites of cell wall synthesis in the Myxomycetes. Very little is known, in any system, about the degree of prefabrication of a polymer prior to secretion. Most information arises from ultrastructural observations during differentiation occasionally in combination with cytochemical stains. Both Goodman and Rusch (1970) and Zaar and Kleinig (1975) suggest that the Golgi apparatus is involved in the synthesis of plasmodial slime. In contrast, a vacuolar origin is suggested based on observations after staining with ruthenium red (Cheung et al., 1974; Turner and Johnson, 1975a). However, since this compound can not penetrate the plasma membrane, these results are questionable (Patterson and Scheetz, 1977). Vesicles whose contents stain for polysaccharide are observed budding from the dictyosome in encysting cells (Chapter 1).

This chapter describes the use of antibodies raised against purified microcyst wall to study its pathway of secretion. This was approached using colloidal gold-labeled secondary antibodies as electron dense markers for transmission electron microscopy. The technique was first described by Faulk and Taylor (1971) and later improved by Horisberger and Rosset (1977) and Geoghegan and Ackerman (1977) for use on fungal and mammalian tissue. A gold sol containing

particles of uniform diameter can be prepared due to a net negative charge that stabilizes the colloid by electrostatic repulsion. These particles can then be electrostatically coated using proteins in their Zwitterion form. In the past five years, this technique has been exploited extensively.

Materials and Methods

Organism: Growth and Encystment

Didymium iridis strain C-4 (A_8) was grown and encysted as previously described (Chapter 1). Encystment was allowed to continue for 36 h or samples were removed at selected times during differentiation and used for immunocytochemical localization of antigens.

Chemicals

Bovine serum albumin (Fraction IV), Sigma; o-dianisidine dihydrochloride (Sigma); FITC-conjugated goat anti-rabbit IgG (Whole serum), Sigma; goat anti-rabbit IgG (IgG fraction), Sigma; gold trichloride acid, Polysciences; HRP-conjugated goat anti-rabbit IgG (IgG fraction), Sigma; sodium citrate, Fisher; sodium metaperiodate, Fisher.

Antibody Production

One milligram of purified microcyst walls (see Chapter 3) was suspended in 0.5 ml distilled water containing 50 µg/ml Penicillin G sodium and Streptomycin sulfate and emulsified in an equal volume of complete Freund's adjuvant for the first injection. Incomplete

Freund's adjuvant was used thereafter. New Zealand white rabbits were injected intramuscularly (hind legs) once a week for two weeks, subcutaneously for the next two weeks, and once more intramuscularly. One and two weeks later the rabbits were bled, the sera tested by immunodiffusion, pooled and stored at -40 C. Prior to injection, the sera was pooled for a preimmune control.

Antigen Identification

Sera were tested against wall fraction 1 (see Chapter 3) by immunodiffusion (Ouchterlony, 1949) in 1% agarose, 0.15 M Tris buffered normal saline, pH 7.2, that was prepared using immunodiffusion tablets (Bio-Rad). After 48 h, the agarose gels were dried, stained in 0.125% Coomassie Blue R, 40% ethanol, 7% acetic acid for 1 h, and destained in 10% ethanol, 7% acetic acid.

The antigen was further characterized by the Western blot technique of Towbin et al (1979). Fraction 1 was electrophoresed in a 10% sodium dodecyl sulfate-polyacrylamide gel (SDS-PAGE) (Chapter 3). After equilibrating for 15 min in 25 mM TRIS/192 mM/20% methanol, pH 8.3, the gel was electrophoretically transfered onto 0.45 μm nitrocellulose (Millipore) for 1.5 h at 300 mA (6V/cm). The blot was treated with 3% BSA in buffered saline, washed, and reacted with a 1:20 dilution of immune serum overnight. The blot was washed and reacted with a 1:1000 dilution of peroxidase (HRP) conjugated goat anti-rabbit IgG for 2 h. The o-dianisidine/H_2O_2 color reaction was used to identify the sites of bound antibody.

Immunofluorescence

Encysting cells were collected and fixed in 1.5% formaldehyde at 4 C. The 36 h-old microcysts were unfixed. All treatments were performed in 1.5 ml microfuge tubes (Fisher Sci. Products) at 4 C. Cells were washed 3X in PBS by centrifugation at 500 Xg for 30 sec. After soaking in PBS containing 1% bovine serum albumin (BSA) for 10 min, cells were resuspended in 500 μl of a 1:10 serum dilution for 1 h. Cells were washed 3X in PBS and reacted with a 1:50 dilution of FITC-conjugated goat anti-rabbit IgG for 1 h. After several washes, cells were counterstained in 1% Evans blue (Nichols and McComb, 1962) for 30 min and washed several more times before preparing wet mounts. Cells were photographed with Kodak Tri-X Pan 35 mm film using a Nikon Labophot microscope equipped with epifluorescence.

Preparation of Gold-labeled Goat Anti-rabbit IgG

Colloidal gold was prepared according to the method of Frens (1973) with modifications by Whitaker (1982). This produced particles approximately 15 nm in diameter. Goat anti-rabbit IgG was then used to label the gold particles (Geoghegan and Ackerman, 1977). The pH of the colloid was adjusted to 7.6 with 0.1 M K_2CO_3 and the optimal amount of protein required to stabilize the gold particles was determined using the assay of Horisberger et al. (1975) with modifications by Roth and Binder (1978).

All glassware was meticulously cleaned and well rinsed. All solutions were prepared using glass distilled, deionized water that was passed through a 0.45 μm Millipore filter.

Immunoelectron Microscopy of Cell Suspensions

Microcysts, 36 h old, were handled as described for immunofluorescence. After treatment with gold-labeled goat anti-rabbit IgG, 1:2 dilution, the cells were washed several times in PBS and processed for transmission electron microscopy (Chapter 1). Controls included microcysts treated with preimmune serum and colloidal gold-labeled IgG alone.

Immunoelectron Microscopy of Sectioned Material

Encysting cells, selected from 0 to 24 h during differentiation, were fixed in 1% glutaraldehyde buffered with 0.05 M cacodylate buffer at pH 7.4 for 1 h at 4 C. After several washes in buffer, embedding in 2.5% agar, and dehydration through a graded ethanol series, cells were embedded in Epon 812 (Luft, 1961). Light gold sections were picked up on 300 mesh nickel grids and dried.

The following labeling protocol was modified from the technique of Bendayan and Zollinger (1982). All treatments were done at room temperature using solutions that were filtered prior to use. Grids were floated on drops of saturated sodium metaperiodate (aqueous) for 1 h, rinsed in water 3X for 5 min each, and floated on a drop of 2.5% BSA in PBS, pH 7.2, for 30 min. After treating sections with a 1:100 dilution of rabbit serum (diluted with 1% BSA in PBS), grids were washed 3X for 5 min each in PBS, and transferred to a drop of colloidal gold-labeled IgG (1:5 dilution) for 1 h. Grids were rinsed as before followed by post-staining in 1% uranyl acetate for 15 min and lead citrate (Reynolds, 1963) for 10 min. Sections were examined as previously described (Chapter 1).

Labeling density was estimated by combining the number of gold particles and the area of certain cytoplasmic features. Gold particles were counted from micrographs at constant magnification (25,400X) of at least five cells per time period of differentiation that were chosen from different regions of the grid. Area and distance were calculated using a Hi-Pad digitizer (Houston Instruments) and a TRS-80 Model I microcomputer.

Results

Ouchterlony diffusion of sera against wall fraction 1 revealed at least two precipitin bands (Fig. 36a-c). Preimmune serum (Fig. 36d) did not react. There did appear to be differences between the sera from the two rabbits. One serum produced two distinct bands whereas bands from the other serum were less pronounced. Western blots of fraction 1 after SDS-PAGE (Fig. 37) revealed that this extract contains a complex mixture of antigens.

Immunofluorescence of 36 h-old unfixed microcysts showed strong fluorescence at the cell periphery (Fig. 38a). Controls using preimmune serum (Fig. 38b) and FITC-conjugated goat anti-rabbit IgG alone (Fig. 38c) did not fluoresce. It was necessary to counterstain with Evans blue to reduce autofluorescence produced by the microcyst wall. Labeling of encysting cells during differentiation (Fig. 39) revealed little. Fluorescence was not observed at the cell periphery until 3 to 4 h (Figs. 39c, d) after which time it steadily increased with time. Earlier stages appear to fluoresce intensely; however, black and white photography fails to show that this is caused by the bright red fluorescence of the counterstain.

Immunocolloid gold labeling of microcysts prior to fixation and embedding showed label at the outer surface of the cell wall. This was

Figure 36. Immunodiffusion gels of wall fraction 1 and rabbit anti-microcyst wall sera. (a) Center well contains undiluted serum from one rabbit. Outer wells contain serial dilutions of fraction 1: Clockwise, undiluted to 1:5. (b) Center well contains undiluted serum from the second rabbit. Outer wells are the same as in (a). (c) Center well contains undiluted fraction 1. The outer wells contain dilutions (left to right, undiluted to 1:2) of serum from one rabbit (1) and another rabbit (2). (d) Center well contains undiluted fraction 1. The outer wells contain serial dilutions of preimmune serum. Gels were stained with Coomassie blue.

Figure 37. Identification of antigens in wall fraction 1 by Western blot onto nitrocellulose. Primary labeling was detected by a color reaction of HRP-conjugated goat anti-rabbit IgG. (a) 10% SDS-PAGE of molecular weight standards. (b) Fraction 1 profile on a 10% SDS-PAGE stained with Coomassie blue. This is a lane adjacent to those that were bloted. (c) A blot of fraction 1 (2 adjacent lanes) from a 10% SDS-PAGE. The numbers on the right mark the seven major bands identified by Coomassie staining. The control blot, pretreated with preimmune serum, was blank.

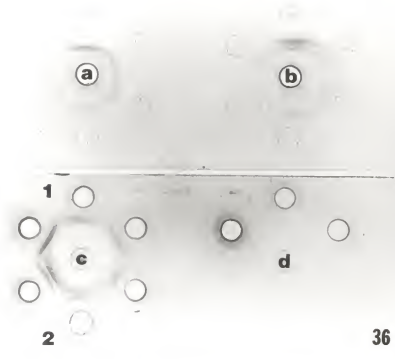
a
b
1
c
d
2
36

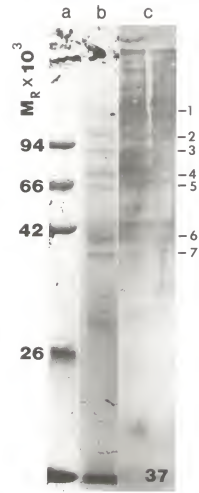
a
b
c
$M_R \times 10^3$
94
66
42
26
1
2
3
4
5
6
7
37

Figure 38. Immunofluorescence of unfixed microcysts showing specificity of the antiserum for microcyst cell wall. (a) 1:10 dilution of antiserum. (b) 1:10 dilution of preimmune serum. (c) FITC-conjugated goat anti-rabbit IgG alone. Cells were counterstained with Evan's blue.

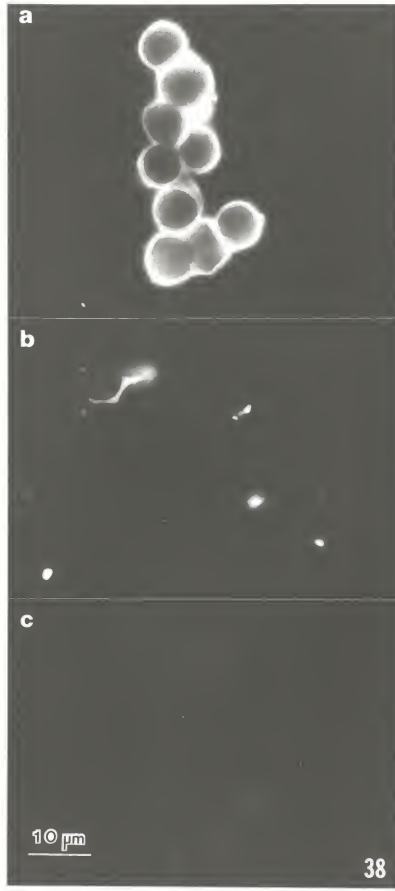
a
b
c
10 µm
38

Figure 39. Immunofluorescence of formaldehyde-fixed cells at different stages of encystment. (a) 0 h. (b) 2 h. Cytoplasmic staining is due to the bright red fluorescence of Evan's blue. (c) 3 h. (d) 4 h. A faint fluorescence is observed at the cell periphery (arrow). (e) 6 h. (f) 12 h. The latter stages do not take up the counterstain due to the presence of the cell wall.

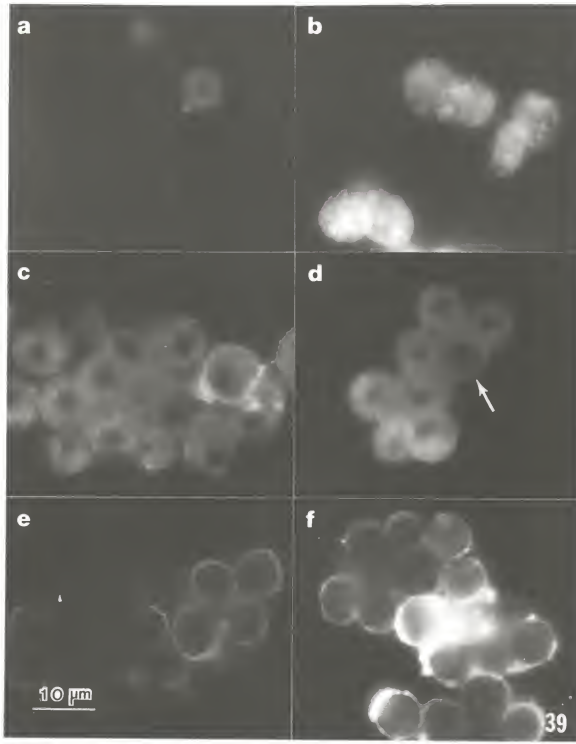
a
b
c
d
e
f
10 µm
39

more pronounced with microcysts that were in an early stage of wall formation (Fig. 40a). Gold particles were frequently associated with wall material resembling spines and rarely located within the slime material (Fig. 40b). The gold particles were unable to penetrate through the cell wall towards the plasma membrane. Cells treated with preimmune serum (Fig. 40c) and gold-labeled IgG alone (Fig. 40d) contained low levels of background binding that was usually localized within microcyst clumps.

Sectioned material was treated with antibody and colloidal gold to localize intracellular sites of antigen. The cytoplasmic details of glutaraldehyde fixed cells were difficult to distinguish. This was particularly true for the Golgi apparatus which apperared to be "washed out." Frequently, regions of cytoplasm appeared leached and membranes damaged. Fixation also caused the shrinkage of plasma membrane away from the cell wall. Gold label was already significantly greater than controls at 0 h of differentiation. Figure 41 summarizes the changes in gold particle density from 0 to 8 h of encystment. Nuclear and mitochondrial labeling are consistent with background labeling and therefore represent an "internal" control.

At 0 h (Fig. 41a) there was a significant pattern of label over vacuoles (Fig. 42a) and the plasma membrane (Fig. 42b), particularly the vacuole membrane. Both increased by 3 h of encystment by as much as a 7-fold difference over control (Fig. 41b). Within 8 h, label over the plasma membrane had decreased, apparently at a rate faster than that associated with the vacuole membrane (Fig. 41c). In contrast, label within the vacuoles had steadily increased with time as did label associated with cytosol.

Figure 40. Immunocolloid gold labeling of unfixed microcyst suspensions. (a) A young microcyst in the early stages of wall formation treated with antiserum followed by gold-labeled goat anti-rabbit IgG. (b) High magnification of the microcyst periphery showing gold particles associated with the fibrous wall material. Note the absence of label within the slime sheath. (c) Control microcysts treated with preimmune serum. (d) Control microcysts treated with gold-labeled goat anti-rabbit IgG alone.

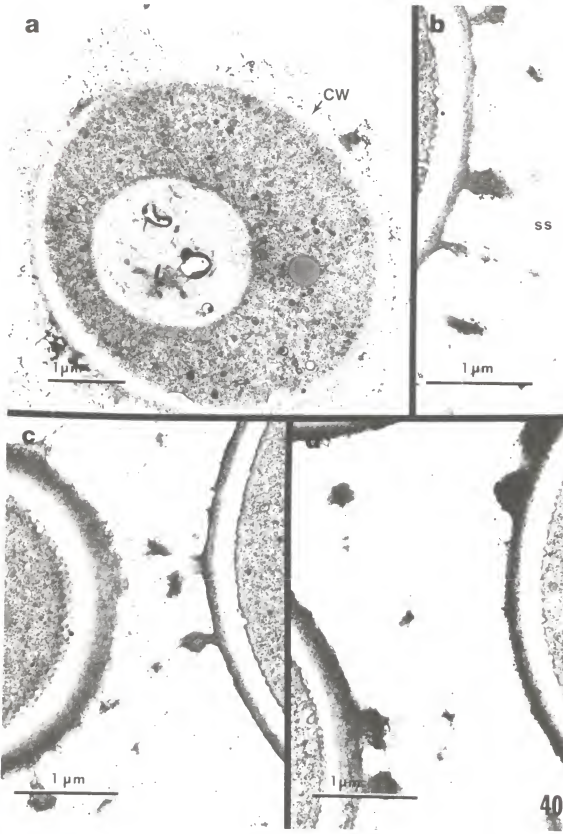
a
CW
1 µm
b
ss
1 µm
c
1 µm
1 µm
40

Figure 41. Quantitative changes in the pattern of gold label on sectioned material. Thin sections of cells from (a) 0, (b) 3 h, and (c) 8 h of encystment were treated with antiserum followed by gold-labeled goat anti-rabbit IgG and the distribution of gold particles analyzed using morphometry. The values for membrane label are reported as number of gold particles/cm. White: control cells treated with preimmune serum; dotted: cells treated with antiserum.

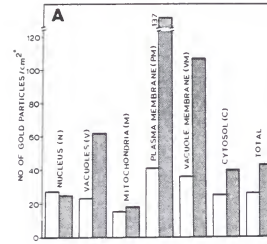
A
NO OF GOLD PARTICLES/(nm)²
NUCLEUS (N)
VACUOLES (V)
MITOCHONDRIA (M)
PLASMA MEMBRANE (PM)
VACUOLE MEMBRANE (VM)
CYTOSOL (C)
TOTAL
117

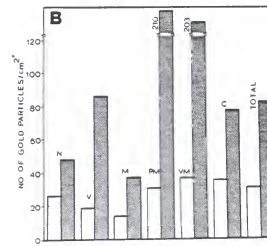
B
NO OF GOLD PARTICLES/(nm)²
TOTAL
292
203

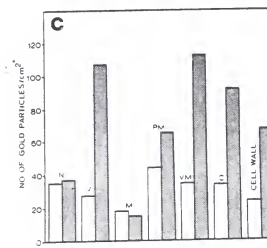
C
NO OF GOLD PARTICLES/(nm)²
CELL WALL
TOTAL

Figure 42. Immunocolloid gold labeling of sectioned cells at 0 h of encystment. (a) Amoeba treated with antiserum showing specificity of label over vacuoles. (b) High magnification of cell periphery showing gold particles associated with the plasma membrane at regions that have blebbed due to fixation damage. (c) Control cell treated with preimmune serum.

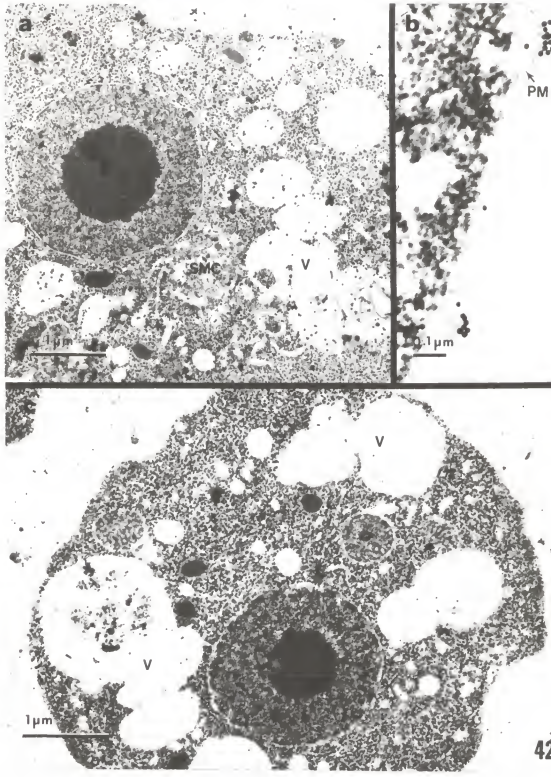

42

Cytosol includes all cytoplasmic constituents such as endoplasmic reticulum, Golgi apparatus, smooth-membraned vesicles, etc. Label specific to any one of these components was difficult to assess. Gold particles were occasionally located over vesicles (Fig. 43), within rough endoplasmic reticulum cisternae (Fig. 44), and regions of smooth-membraned cisternae (Fig. 45a).

By 8 h of encystment, label was located over the cell wall (Fig. 46a). This was accompanied by an increase in label within the space between the cell wall and plasma membrane. Label over wall material was observed as early as 4 h and no qualitative differences were observed in labeling of the slime-like material.

Discussion

By using microcyst wall fragments for immunization, antibodies were generated against wall components that are solubilized by alkaline urea. The antigen is presumably a group of acidic glycoproteins that contain approximately 10% galactose (Chapter 3). The serum titer appears to be low, since there is a loss of fluorescence at dilutions greater than 1:50. These wall components are either poor immunogens or they are not accessible *in situ*. Such conclusions may explain my failure to generate polyclonal antibodies from the fusion of mouse spleen cells (immunized with whole microcysts) and Sp 2/0 myeloma cells (see Yelton and Sharff (1981) for a current review). Using ascites fluid, wall surface antigens were detected with a radioimmune assay but fluorescence was too low to be useful (data not shown).

Gold labeling showed that the antigen is distributed throughout the cell wall. It was first detected at 3 to 4 h of encystment using

Figures 43-46. Micrographs of cytoplasmic constituents that are occasionally labeled with gold particles.

Figure 43. Smooth-membraned vesicles (arrow) located near the cell surface.

Figure 44. The cisternae of rough endoplasmic reticulum.

Figure 45. (a) Regions that consist almost entirely of smooth-membraned elements. Label appears to be localized over cisternal contents. (b) An identical area from a control cell treated with preimmune serum.

Figure 46. (a) Label is distributed throughout the cell wall. Note that label is not associated with the slime sheath. (b) Cell wall from control cells treated with preimmune serum.

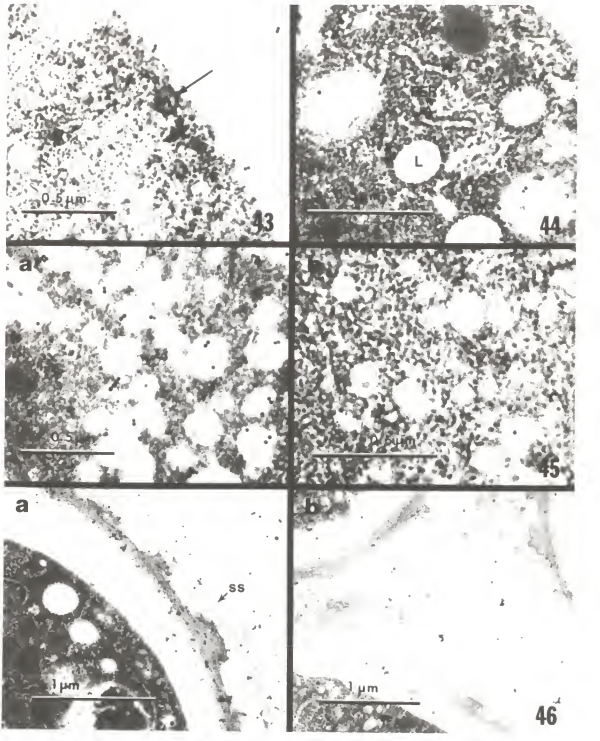
0·5 µm
43
L
44
a
0·5 µm
45
a
ss
1 µm
b
1 µm
46

fluorescence. This agrees with ultrastructural observations (Chapter 1) and radiolabel incorporation kinetics (Chapter 5) of microcyst wall formation. Generally, the matrix of fungal cell walls consists of glycoproteins (Farkas, 1979). Zaar et al. (1979) have proposed that glycoproteins comprise the spherule wall matrix of Physarum polycephalum. It is not understood whether these components are structural or enzymatic, although both are found in fungal (Gander, 1974; Farkas, 1979) and plant (Newcomb, 1980) cell walls.

Specific labeling of the plasma membrane and vacuolar membrane was unexpected. This may be related to the increase of intramembrane particles observed at 2 h of encystment (Chapter 1). Although several speculations are possible, it remains unexplainable without further study. One must bear in mind that the "antigen" is actually a mixture of different immunogens, a few of which may be found elsewhere in the cell. One possibility is that these molecules actually share the same antigenic determinants. Dow et al. (1981) recently describe similarities between a membrane-associated and filtrate glycoprotein from the fungus, Mucor rouxii. Similar results are found in the single-celled alga, Chlamydomonas (Lang, 1982). He suggests that membrane-associated glycoproteins may be precursors to cell wall glycoproteins. However, these studies do not distinguish membrane type and most likely do not include the plasma membrane. A secreted glycoprotein, invertase, is also found in the vacuoles of yeast (Meyer and Matile, 1975) although no functional role is provided.

Since gold particles were not consistently located over endomembrane elements commonly involved in glycoprotein secretion, the antigen may have a soluble mode of secretion much like amylase

secretion in barley aleurone cells (Jones, 1972). Label density associated with cytosol does increase with time; however, the absence of label may be due to the inability of antibodies to identify antigen if it were present in a pre-secreted form.

Another explanation may be that the antigen is extruded with autolysosomal contents and becomes entrapped in the forming cell wall during encystment. Lysosomal discharge is a ubiquitous phenomenon during encystment (Weisman, 1976). For example, glycogen particles are commonly found within the exocyst of Acanthamoeba castellanii (Griffiths, 1970). This explanation may be related to the following observation.

Statistically, the gold particle densities of the vacuolar and plasma membrane are at maximum at 3 h but the vacuolar membrane density decreases slightly through 8 h while the plasma membrane density is only slightly greater than control. This suggests antigen turnover via membrane cycling. For example, bidirectional flow between secondary lysosomes and plasma membrane occurs in macrophages (Muller et al., 1980). The vacuolar system may serve as an intermediate in plasma membrane removal and synthesis; therefore, a decrease in plasma membrane label at 8 h suggests that either the rate of removal is faster than replacement or cycling back to the plasma membrane has slowed. If the lifetime of a vacuolar membrane protein is related to the length of time it is exposed to the lysosome environment, then antigen common to both membranes would be found within the vacuole and outside the cell.

Extended studies on the biochemical profiles of the membranes are required to understand these events any further. While this study has

not shown that wall associated antigens are secreted via an endomembrane pathway, it has suggested the importance of membrane turnover. This turnover enables the cell to maintain a continuous balance between intracellular and plasma membranes during differentiation when a high degree of autophagocytosis and reverse pinocytosis are occurring (Chapter 1). Microcyst wall formation will be examined in Chapter 5 using incorporation of radiolabeled monosaccharides.

CHAPTER 5
RADIOLABEL INCORPORATION DURING MICROCYST WALL FORMATION

Introduction

Many of the opening remarks in Chapter 4 could be repeated here. In that study, immunocytochemistry was used to examine the secretion of cell wall immunogens during encystment. This chapter is concerned with the secretion of cell wall polysaccharides. Encysting cells were labeled with radioactive monosaccharides and examined using liquid scintillation and autoradiography.

It is generally accepted that the structural polysaccharides chitin, cellulose, and glucan are synthesized at the inner leaflet of the plasma membrane (Philippi and Parish, 1981; Cabib and Roberts, 1982). Until recently this was thought to involve the direct transfer of hexose to acceptor through the nucleotide sugar, but some evidence now implicates a lipid intermediate (Boer, 1979). In contrast, synthesis of yeast protein-mannans is a complex process occurring within the endomembrane system (Farkas, 1979; Cabib and Roberts, 1982). Secretion of all these polymers requires vesicles, whether they transport the polymer itself or precursors and enzymes involved in synthesis. For example, a ubiquitous cytoplasmic component, the chitosome, delivers chitin synthetase to the fungal cell surface (Bartnicki-Garcia et al., 1978).

A large number of polysaccharides are synthesized within the Golgi apparatus and delivered to the cell surface in vesicles (Morre and Ovtracht, 1977; Northcote, 1979). Of the many techniques available, electron microscope autoradiography has been used successfully to demonstrate the secretory pathway in a variety of systems. Some classic examples include studies on plant cell walls (Northcote and Pickett-Heaps, 1966; Pickett-Heaps, 1967), algae (Callow and Evans, 1974), mammalian cell protein secretion (Jamieson and Palade, 1967), and fungal cell walls (Gooday, 1971; Kosinova et al., 1974; Craig et al., 1979; Gooday, 1979; Fevre and Rougier, 1982).

Very little is known about the synthesis and secretion of extracellular polysaccharides in the slime molds. McCormick et al. (1970a) and Zaar (1978) followed the kinetics of slime synthesis in plasmodia of Physarum polycephalum using labeled glucose and sulfate. Zaar (1978) also studied the kinetics of spherule wall formation by following glucose incorporation into an alkali-insoluble component. Using P. polycephalum myxamoebae, Turner and Johnson (1975b) reported the enhanced incorporation of galactose into encysting cells and suggest that a galactose compound is a component of the cell wall. Lastly, Henney and Chu (1977a) studied metabolic patterns during encystment of Physarum flavicomum through the incorporation of amino acids. Leucine-labeled proteins produced by encysting cells were degraded less than those labeled with other amino acids. They showed that the availability of certain amino acids controlled differentiation, possibly by inhibiting proteolysis. In retrospect, the precursors used for polysaccharide synthesis arise from protein degradation via gluconeogenesis (Huttermann, 1973; Huttermann, 1982).

This chapter presents the results of studies of cell wall polysaccharide synthesis in encysting cells of Didymium iridis. An autoradiographic approach was used to determine if materials are transported by Golgi-derived vesicles (Chapters 1 and 4); however, the results were not particularly informative. Some interesting data did surface from analyses of the labeling kinetics of cell fractions.

Materials and Methods

Organism: Growth and Encystment

Didymium iridis strain C-4 (A_8) was maintained and induced to encyst as described in Chapter 1.

Radioactive Labeling

The following monosaccharides were used: D-[^{3}H(G)]galactose, specific activity of 3.7 Ci/mmol (New England Nuclear); D-[1-^{14}C]galactosamine hydrochloride, 60 mCi/mmol (Amersham); D-[1,6-^{3}H(N)]glucosamine hydrochloride, 30-60 Ci/mmol (New England Nuclear). For continuous labeling experiments, amoebae were induced to encyst in the presence of 0.1 μCi of label per ml of encystment buffer. In pulse labeling experiments, cells were exposed to 2 μCi/ml for 1 h at the onset of induction, centrifuged, washed 2X with buffer, and resuspended in fresh encystment buffer at a concentration of 1-2 X 10^7 cells/ml. Label was not chased.

Chemical Fractionation of Labeled Cells

During the course of encystment, 1 ml aliquots were withdrawn from duplicate flasks and centrifuged at 230 x g for 1 min in 15-ml conical

glass tubes. If samples were from a pulse labeling experiment, the supernatant was carefully removed and assayed for radioactivity. To estimate the soluble cytoplasmic radioactivity, duplicate pulse-labeled aliquots were extracted with 80% ethanol. The cell pellet was rinsed once with distilled water at 4 C and treated with 1 ml 10% sodium dodecyl sulfate (SDS) at 100 C for 15 min. After centrifugation at 1,000 x g for 5 min, the supernatant was removed for analysis. The residue was rinsed 2X with distilled water, treated with 1 ml 1 N KOH at 100 C for 30 min, centrifuged and the soluble fraction removed. The alkali-insoluble fraction that remained was rinsed 3X with distilled water and the radioactivity counted.

At selected times, an entire flask, approximately 1 X 10^9 cells, was extracted using 3 ml SDS and KOH. Fractions were analyzed for monosaccharide composition and specific activity using paper chromatography.

All chemicals were reagent grade.

Preparation of Crude Slime from Encystment Buffer

Encystment buffer from pulse labeled suspensions was decanted after centrifugation at 2,000 x g for 15 min and treated with 2 vol. 95% ethanol at 0 C overnight. The precipitate was collected by centrifugation, resuspended in glass distilled water, and dialyzed against water at 0 C overnight. The dialysate was lyophilized, hydrolyzed in 1 N HCl at 100 C for 12 h under N_2, and analyzed by paper chromatography.

Analytical Methods

Total carbohydrate was assayed using the anthrone method (Dische, 1962), neutral sugars by the phenol-sulfuric acid method of Dubois et al. (1956), and hexosamines according to Johnson (1971).

Incorporation of radioactivity into fractions was counted by liquid scintillation in a Beckman LS-230. Soluble fractions (100 ul) were counted in 5 ml Aquasol (New England Nuclear) after storing overnight in the dark. The alkali-insoluble fraction was filtered onto glass microfibre filters (Whatman 934-AH), dried, and counted in 5 ml toluene/PPO/POPOP (4.1 g PPO, 0.26 g POPOP, 1,000 ml toluene). Counting efficiency was determined by external standardization using ^{3}H-labeled toluene and respective extracts as quenching agents.

Paper chromatography of fractions was performed as described in Chapter 3. Samples were hydrolyzed in 1 N HCl at 100 C for 8 h under N_2. Spots were detected using alkaline silver nitrate (Churms, 1982). To determine which components were labeled, chromatograms were cut into 1.5-cm segments and eluted with 1-2 ml distilled water by squeezing through a syringe. The eluate was lyophilized, reconstituted in 100 μl, and 50 μl counted in 5 ml Aquasol. The remaining 50 μl was assayed for neutral sugars or hexosamine to calculate specific activity.

Sodium dodecyl sulfate extracts from batch suspensions were fractionated on a 1.5 X 47 cm column packed with Bio-Gel P-2, 200-400 mesh, (Bio-Rad) that was equilibrated with water and calibrated using hemoglobin and ^{14}C-glucose. Four milliliter fractions were assayed for radioactivity and absorbance at 280 nm. The void peak fractions were combined, concentrated by rotoevaporation, treated with ethanol, hydrolyzed, and analyzed by paper chromatography.

Light Microscope Autoradiography

After 36 h, microcysts from continuous label experiments were processed for transmission electron microscopy as described in Chapter 1. Sections (0.5 μm) were dried onto gelatin-chrome alum subbed glass slides (Williams, 1977), dipped in Ilford K5 emulsion, and exposed at 0 C for up to 5 weeks in slide boxes containing silica gel. Slides were developed in Kodak Dektol (diluted 1:2 with water) for 3 min at 20 C, rinsed, and fixed in 25% sodium thiosulfate. After drying, sections were stained at 45 C with Mallory's Azure II-methylene blue for 4 min followed by 1% toluidine blue O in 0.15 M phosphate buffer at pH 7 (Stevens, 1966) for 2 min.

Autoradiograms were photographed with Kodak Technical Pan film 2415 that was developed using Delagi #8 developer (25 g sodium sulfite anhydrous, 1.4 g Phenidone (Ilford), 0.8 g Kodalk (sodium metaborate, Kodak), 15 ml 0.2% benzotriazole, 1,000 ml water at 38 C) for 15 min at 20 C.

Electron Microscope Autoradiography

Pulse labeled, encysting cells were fixed and embedded (Chapter 1) at 2, 4, 8, 12, and 24 h during encystment. Light-gold sections were picked up on Formvar-coated nickel grids (50 mesh) and Ilford L4 emulsion applied using the loop technique described by Williams (1977). After exposure at 0 C for up to 12 weeks, grids were developed in freshly prepared Microdol-X for 4 min at 20 C according to Stevens (1966). Pretreatment with 100% ethanol was omitted since it appeared to retard gelatin removal. Autoradiograms were post stained with 1% uranyl acetate and lead citrate (Reynolds, 1963) for 10 min and examined with a Jeol JEM 100-CX operated at 80 kV.

Results

Extraction of whole microcysts with boiling SDS and KOH creates a cell wall "ghost" (Fig. 47) that is virtually free of cytoplasmic constituents. Paper chromatographic analysis of hydrolysates of this insoluble fraction revealed glucose, galactose and galactosamine as the major components. Expression of these monosaccharides appears to be regulated during encystment (Table 5-1). Detectable amounts of galactosamine appeared initially at 2 h followed by glucose at 4 h and then galactose.

The kinetics of wall formation were followed by the rate of incorporation of ^{3}H-galactose into the hot SDS/KOH-insoluble fraction (Fig. 48). Label was incorporated rapidly from 0 to 10 h of differentiation after which radioactivity remained constant. This was in direct proportion to the amount of carbohydrate detected (Fig. 48). These kinetics were not changed by the addition of a 10-fold increase in the amount of label; therefore, the cessation of incorporation is not due to a depletion of precursor. It was also found that the presence of a cell wall did not prevent uptake since label added at 4 or 8 h was incorporated with a 35 and 45% decrease, respectively, of incorporation at 0 h. Label added at 24 h was not incorporated and the insoluble fraction was not contaminated with label acquired by absorption.

^{3}H-galactose incorporation into each cell fraction is shown in Figure 49. A change in rate generally occurred between 8 and 10 h. After 12 h, the insoluble fraction remained constant but the SDS-soluble fraction decreased with time. This fraction contained membrane-associated and soluble label as well as SDS-soluble wall

Figure 47. Thin section through a microcyst after treatment with boiling SDS and KOH. The cytoplasm has been removed leaving behind insoluble wall material. Cytoplasmic debris remains after treatment with SDS only.

0.5 µm
47

Table 5-1. Changes in composition of the hot SDS/KOH-insoluble wall fraction during encystment.

Monosaccharide	Relative intensity of detected spot[a] at 2 h	at 4 h	at 36 h[b]
Galactosamine	+	++	+++
Galactose	-	-	+++
Glucose	-	++	++++

[a]Standard volumes of hydrolysate were spotted and chromatographed as described under Materials and Methods. Amounts were arbitrarily assessed by the visual intensity of spots using alkaline silver nitrate.

[b]This sample also produced an Elson-Morgan reagent-positive spot at 8.2 cm that is thought to be a disaccharide of galactosamine.

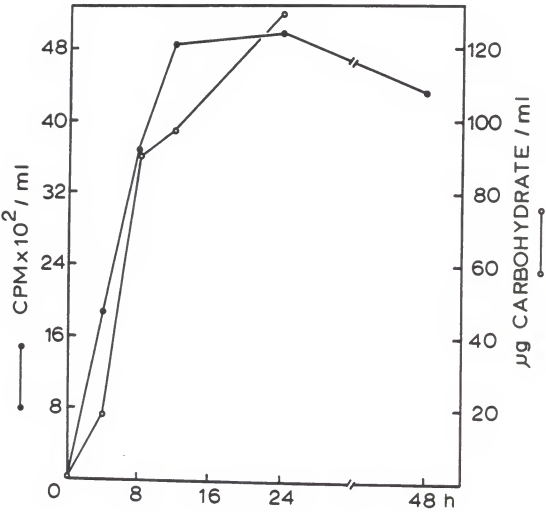

Figure 48. Kinetics of microcyst wall formation during encystment. Encysting cells were continuously labeled with ^{3}H-galactose, aliquots removed at selected times, and the SDS/KOH-insoluble wall fraction assayed. Polysaccharide synthesis was followed by the amount of total carbohydrate present and by the rate of incorporation. Total carbohydrate was determined by the Anthrone method using glucose as the standard.

components and consists mostly of glucose and galactosamine. The rate of incorporation into the insoluble fraction was slightly slower (Fig. 49). Light microscope autoradiograms (Fig. 50) showed fewer grains than were found in ^{3}H-glucosamine HCl labeled cells despite the higher number of counts.

To investigate the possibility that the slime observed prior to wall formation (see Chapters 1 and 3) is a galactose polymer, encystment buffer was treated with ethanol after a 2 h pulse with ^{3}H-galactose. Radioactivity was associated only with galactose (Fig. 51) after dialysis.

^{3}H-glucosamine HCl and ^{14}C-galactosamine HCl were also incorporated into encysting cells. In all continuous labeling experiments, the amount of radioactivity in the encystment buffer remained constant after 2 h; therefore, uptake must have been completed by this time; however, secretion of labeled material occurrs during this time. ^{3}H-glucosamine uptake (Fig. 52) into cell fractions was considerably lower than that observed for ^{3}H-galactose. The major difference was the lag period shown for incorporation into the SDS-soluble fraction. Light microscope autoradiograms (Fig. 53) showed many grains over microcysts, particularly located at or near the cell periphery.

Uptake of ^{14}C-galactosamine HCl was much less than that observed for the other two labels and is illustrated by fewer grains in autoradiograms (Fig. 54). Label had not been incorporated into the SDS-soluble fraction by 4 h, in comparison with ^{3}H-galactose and ^{3}H-glucosamine HCl, where radioactivity was associated with the void fraction of a Bio-Gel P-2 column (Fig. 55). Although radioactivity was

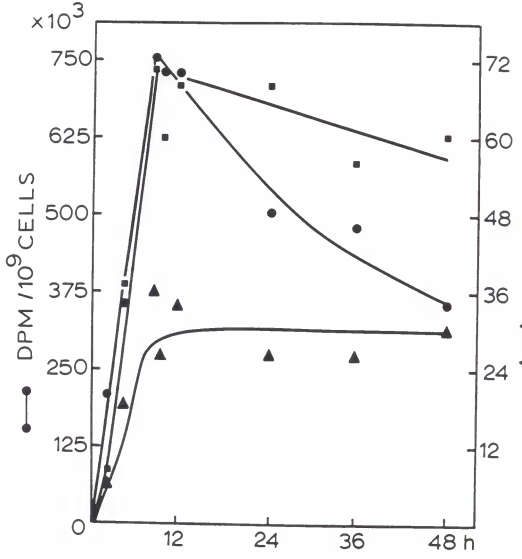

Figure 49. Incorporation of ^{3}H-galactose into cell fractions during encystment in the presence of continuous label. Aliquots were removed at selected times, treated sequentially with boiling 10% SDS and 1 N KOH, and the fractions assayed for radioactivity. (●) SDS-soluble material. (■) KOH-soluble material. (▲) Insoluble material.

Figure 50. Light microscope autoradiogram of encysted cells (24 h) after continuous label with ^{3}H-galactose. Cells were processed for electron microscopy by alcohol dehydration and embedding in plastic resin. Thick sections were coated with emulsion and exposed for 3-4 weeks. Most silver grains (arrows) are located over cell wall.

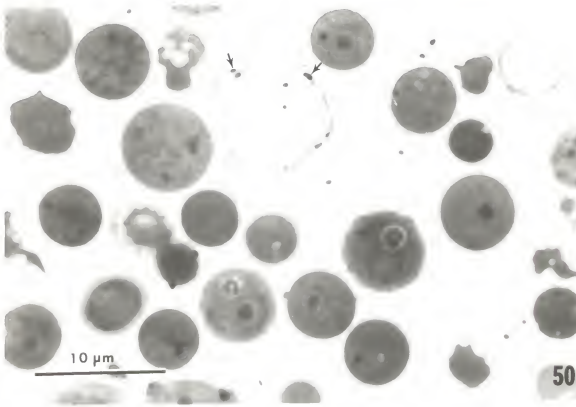
10 µm
50

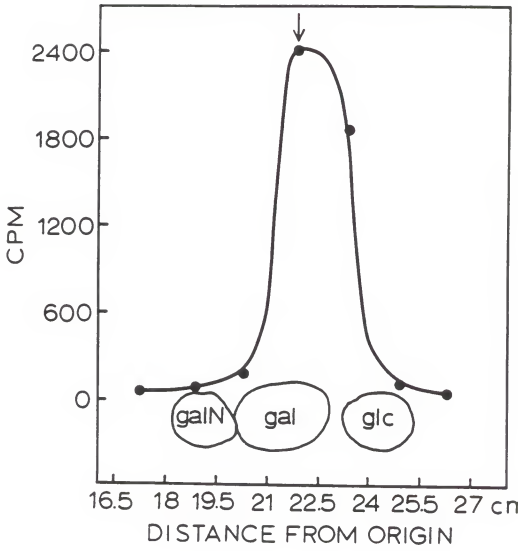

Figure 51. Paper chromatographic analysis of crude slime labeled with a 2 h pulse of ^{3}H-galactose. Slime was precipitated by ethanol from encystment buffer at 36 h, hydrolyzed, and the chromatograms assayed for radioactivity. The arrow marks the peak activity of a ^{3}H-galactose standard chromatographed in a lane adjacent to the unknown. GalN: galactosamine; gal: galactose; glc: glucose.

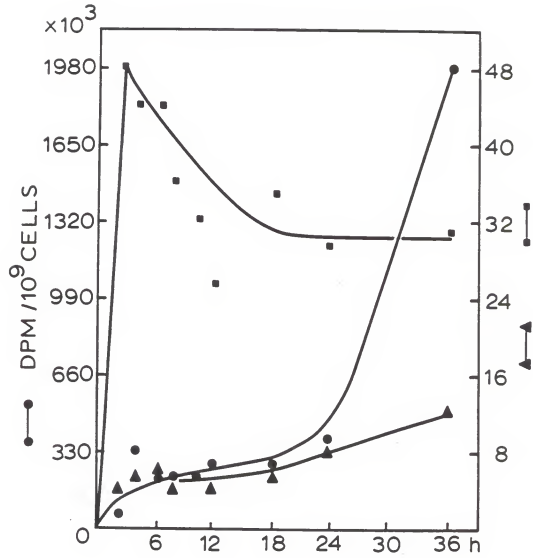

Figure 52. Incorporation of ^{3}H-glucosamine HCl into cell fractions during encystment in the presence of continuous label. Methods are briefly outlined in Figure 49 legend. (●) SDS-soluble material. (■) KOH-soluble material. (▲) Insoluble material.

Figure 53. Light microscope autoradiogram of encysted cells (24 h) after continuous label with ^{3}H-glucosamine HCl. Methods are briefly outlined in Figure 50 legend. Most of the silver grains appear to be at the cell surface.

Figure 54. Light microscope autoradiogram of encysted cells (24 h) after continuous label with ^{14}C-galactosamine HCl.

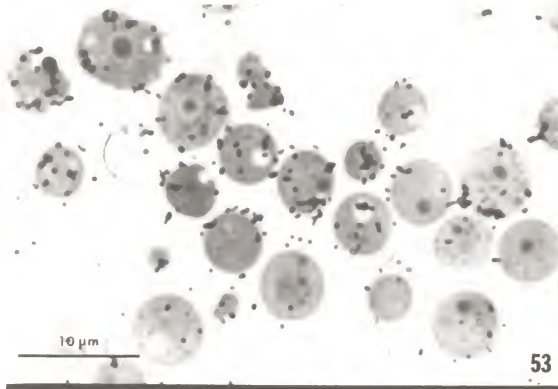

53

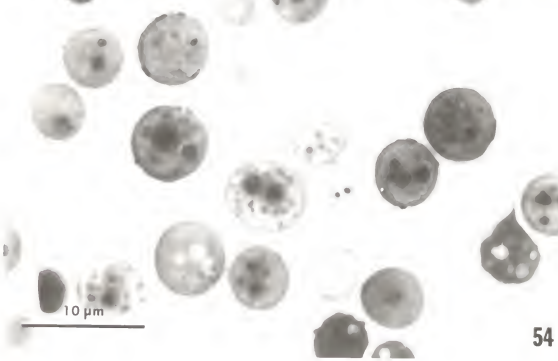

54

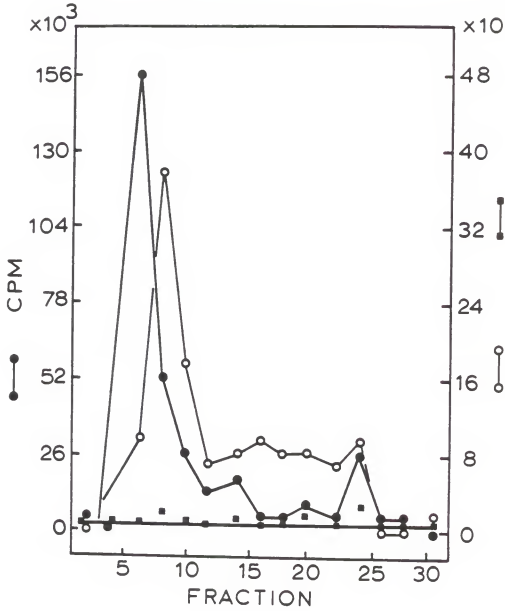

Figure 55. Elution profile of SDS-soluble material fractionated on a Bio-Gel P-2, 200-400 mesh, column after 4 h continuous label with (●) ^{3}H-galactose, (○) ^{3}H-glucosamine HCl, and (■) ^{14}C-galactosamine HCl. Approximately 10^{9} cells were treated with boiling 10% SDS and the supernatant applied to the column. Fractions were assayed for CPM by removing 100 µl. The major peak is void volume and the last peak on the right is monomer determined by calibration.

only 2-fold above background in ^{14}C-galactosamine HCl labeled cells, label appeared to be fixed as galactosamine in the insoluble fraction.

Wall formation was studied more closely using pulse labeling experiments and high resolution autoradiography. Radioactivity in cell fractions was followed after a 2 h pulse with ^{3}H-glucosamine HCl (Fig. 56). Radioactivity in the SDS-soluble fraction decreased from 70 to 57% of the total disintegrations per minute (dpm) while the supernatant increased from 17 to 36%. The insoluble fraction increased slightly to less than 10% of the total dpm. ^{3}H-glucosamine HCl was mostly incorporated into the insoluble fraction as galactosamine (Table 5-2).

To observe changes in intracellular soluble label, cells were extracted with ethanol. This fraction decreased rapidly until 8 to 10 h (Fig. 56). Label was incorporated into polymer within 2 h since most of the radioactivity was associated with the void peak from a Bio-Gel P-2 column. Paper chromatographic analysis of this material at 36 h revealed that label was incorporated as galactosamine. Some radioactivity was associated with an Elson-Morgan reagent-positive spot (purple) that migrated to the position of glucosamine.

At 2 h grains were found almost exclusively over vacuoles (Fig. 57a). The fate of label after uptake was not clearly established. Particular organelles were not observed to be specifically labeled except for occasional grains located over smooth-membraned cisternae or vesicles (Fig. 57b). Identification was difficult due to the large size of the grain relative to that of the cytoplasmic structure. In addition to grains located over wall material (Fig. 57c), label appeared to be associated with the plasma membrane.

In continuous labeling experiments, ^{3}H-galactose proved to be the best label in terms of uptake. Figure 58 shows the changes in

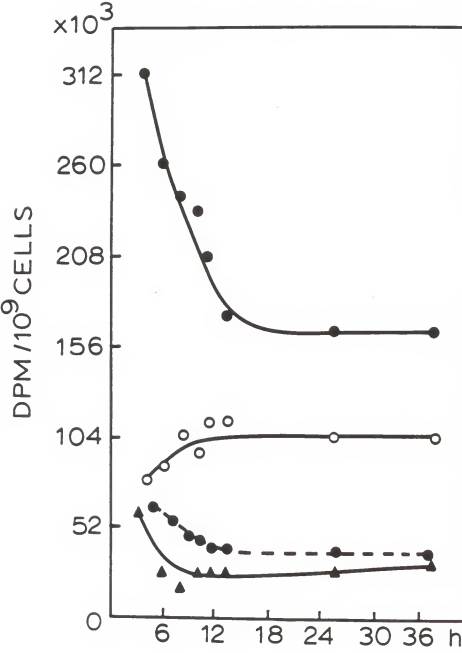

Figure 56. Fate of radioactivity in cell fractions during encystment after a 2 h pulse with ^{3}H-glucosamine HCl. Cells were pulsed, washed several times, and resuspended in fresh buffer. At selected time intervals cells were extracted as described under Materials and Methods after removing the supernatant. A parallel culture was treated with 80% ethanol and the soluble material counted. (○) Encystment buffer supernatant. (●) SDS-soluble material. (●---●) Ethanol-soluble material. (▲) Insoluble material.

Table 5-2. Specific activity of radiolabel incorporated into the hot SDS/KOH-insoluble wall fraction after 36 h.

Monosaccharide	dpm/ug neutral sugar or hexosamine[a]	
	^{3}H-glucosamine HCl	^{3}H-galactose
Galactosamine	58	4,986
Galactose	15	6,997
Glucose	0	3,432

[a]Determined as described under Materials and Methods where eluates from paper chromatograms were assayed.

Figure 57. Electron microscope autoradiograms of encysting cells pulse labeled (2 h) with ^{3}H-glucosamine HCl. At selected times cells were processed for electron microscopy as described in Materials and Methods. Thin sections were coated with emulsion using the Loop technique and allowed to expose for up to 12 weeks. (a) After 2 h, label was consistently associated with food vacuoles. (b) During the early stages of wall formation, silver grains were occasionally located over smooth-membraned cisternae, possibly vesicles (arrow). (c) At the completion of encystment (24 h), label was found within the cell wall.

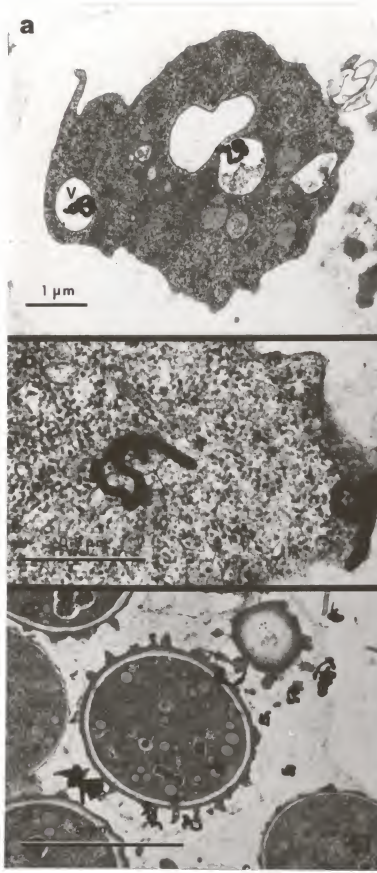
a
V
1 µm

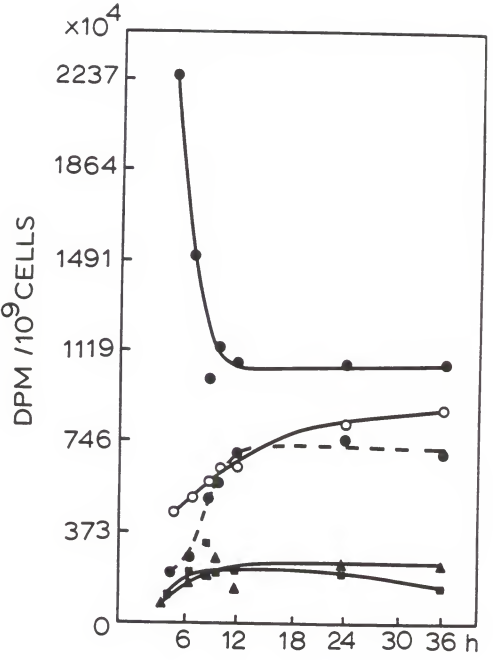

Figure 58. Fate of radioactivity in cell fractions during encystment after a 1 h pulse with ^{3}H-galactose. Methods are briefly outlined in Figure 56 legend. (○) Encystment buffer supernatant. (●) SDS-soluble material. (●---●) Ethanol-soluble material. (■) KOH-soluble material. (▲) Insoluble material.

radioactivity of cell fractions after a 1 h pulse. Calculations from the amount of label not incorporated showed that 61% did enter the cells. Results were similar to those observed for the ^{3}H-glucosamine HCl pulse labeling. The SDS-soluble fraction decreased from 85 to 53% of the total dpm and the supernatant increased from 14 to 42% with both becoming constant after 10 h. ^{3}H-galactose was incorporated into the insoluble fraction mostly as galactose (Table 5-2) but with comparable specific activities of glucose and galactosamine. These values are much greater than those observed for ^{3}H-glucosamine HCl (Table 5-2).

In contrast to ^{3}H-glucosamine HCl uptake, the ethanol-soluble pool increased 7-fold rather than decreasing (Fig. 58). This increase in soluble label was also accompanied by a loss of radioactivity in the Bio-Gel P-2 void fraction and an increase in a fractionated species at 36 h that contained little material absorbing at 280 nm.

Ultrastructurally, autoradiographs did not reveal a pathway for wall biogenesis. Early during encystment at 4 h, grains were located over the slime layer and vesicles containing fibrous material (Fig. 59a). Grains were mostly limited to the fibrous wall component although plasma membrane also appeared to be labeled (Fig. 59b).

Discussion

The initial event of wall formation involves the deposition of a fibrous material onto the cell surface (Chapter 1). These fibrils are composed of glucose and galactosamine (Chapter 3) in the mature microcyst wall. It appears from this study that these two monomers are deposited at different times; therefore, they are probably arranged into two homopolymers rather than intermixed as one polymer. This

Figure 59. Electron microscope autoradiograms of encysting cells pulse labeled (1 h) with ^{3}H-galactose. Methods are briefly outlined in Figure 57 legend. (a) Silver grains are localized over vesicles containing fibrous material and the extracellular material observed prior to wall deposition. (b) Upon completion of encystment, label is associated with cell wall but also plasma membrane (arrow).

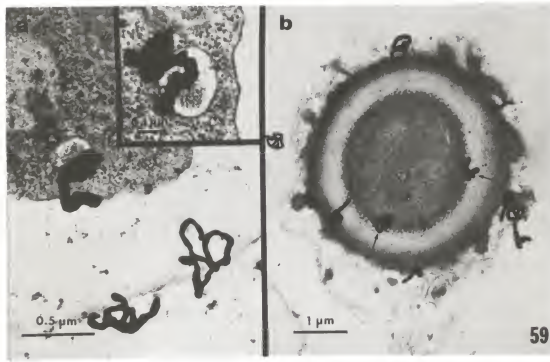
a
0.5 µm
b
1 µm
59

would be analogous to fungi in general where chitin-glucan and cellulose-glucan complexes are typical (Bartnicki-Garcia, 1968). Unfortunately, analysis of this polymer by thin-layer chromatography after mild hydrolysis failed to identify common glucose disaccharides (data not shown).

The kinetics of wall formation followed by radiolabel incorporation is consistent with ultrastructural observations and population kinetics (Chapter 1). A majority of the cell population possesses a visually mature cell wall by 10 to 12 h. Since the cessation of uptake is not caused by a depletion of label, it may reflect changes in membrane permeability and metabolic changes during encystment. Henney and Chu (1977a) reported a decrease in the rate of incorporation of labeled amino acids at 9 h of encystment in P. flavicomum.

Continuous labeling studies and light microscope autoradiography indicate that label is moved from cytoplasm to extracellular polymers. The SDS-soluble fraction, thought to include an endogenous pool, decreases in radioactivity and the insoluble wall material increases. Movement into this fraction is also suggested, since rate of incorporation lags slightly behind the "cytoplasmic" fraction. These events are better shown by following a pulsed label through differentiation. The SDS-soluble fraction decreases with concurrent increases in wall material and supernatant radioactivity. The latter appears to include cell wall material and a slime that is composed of galactose (see Chapter 3).

These extracellular polysaccharides are transported to the cell surface in vesicles but their point of origin remains unknown.

Interpretation of autoradiographs is difficult since turnover within the endomembrane system is rapid, particularly through the Golgi apparatus (Chrispeels, 1976). In the Myxomycetes, it becomes more challenging with one dictyosome per cell that consists of two to four cisternae. Confusion may also arise if the secretory product is not concentrated but transported via fluid-filled vesicles (Farquhar and Palade, 1981). These problems are enhanced by the low resolution characteristic of tritium label using Ilford L4 emulsion. It has a calculated resolution of 0.1 μm (Caro and Schnos, 1965), much greater than many cytoplasmic structures. It is now clear that further experiments are needed where label is pulsed for a shorter period immediately prior to wall formation, such as a 15 min pulse at 4 h of encystment.

An increase in soluble label following ^{3}H-galactose pulse labeling suggests that labeled polymers are turning over. This would explain the relatively low number of grains in light microscope autoradiographs despite the observed high levels of radioactivity since soluble components are removed during sample processing for electron microscopy (Pickett-Heaps, 1967). The same phenomenon was not observed for ^{3}H-glucosamine HCl labeled polymers although the efficiency of uptake appeared to be much lower. Nonspecific labeling is thought to be minimal when considering that these cells are metabolically "geared" to the synthesis of extracellular materials (Pickett-Heaps, 1967).

Labeling of the insoluble fraction by assimilation of ^{3}H-galactose and -glucosamine HCl into galactosamine suggests that hexosamine synthesis occurs by the epimerization of uridine diphosphate (UDP)-glucosamine. This is also indicated by the detection of the

purple spot in the SDS-soluble fraction that migrated similarly to glucosamine. A fixed purple color is indicative of the N-acetyl derivative (Churms, 1982). These results are inconsistent with the results of Nishi et al. (1981) using labeled galactosamine. They suggested that ^{14}C-galactosamine is directly incorporated into polymer via galactokinase and uridyltransferase activity rather than through epimerase activity commonly found in bacteria (Glaser, 1956), mammals (Maley and Maley, 1959; Davidson, 1966), and the fungus, Neurospora (Edson and Brody, 1976). In this study, direct incorporation of ^{14}C-galactosamine HCl was observed but at much lower levels than the other precursors.

CONCLUDING REMARKS

This study has demonstrated the usefulness and amenability of Didymium iridis as a paradigm for cytodifferentiation. The processes of encystment and excystment were induced to occur and quantitated using a simply designed assay. Once synchronous populations were established, these processes were characterized by the ultrastructural details of developmental changes. Chapter 2 is the first study to examine microcyst germination in the Myxomycetes and is intended to aid subsequent studies on biochemical events.

Encystment of Didymium iridis was similar to other organisms, the cellular slime molds and free-living soil amoebae, which have been thoroughly studied. If compared to other studies using the Myxomycetes, Physarum polycephalum and P. flavicomum, D. iridis had more rapid and synchronous kinetics. It also has the advantage of being a wild-type organism unlike the axenic strains of Physarum used above. Several of these strains appear to encyst, but do not produce a cell wall. This is the first opportunity to compare similar processes between different genera. Noted differences were the ultrastructure and chemical composition of the microcyst wall in D. iridis. Preceding wall formation, a slime sheath of a composition different from the cell wall, was deposited around the cell. It has not been described in the haploid phase and is presumed to be analogous to the slime layer found on the plasmodial stage. The wall, deposited as three layers, was also

mostly composed of galactosamine. The alkali-insoluble polymer was closely associated with a glucan and it appeared to be synthesized at different times during wall formation, first galactosamine followed by glucose.

Since encystment demanded the focus of cellular processes on wall synthesis and deposition, the remainder of this study was devoted to wall biogenesis. Essentially, two different approaches were used, each unique in its application to the Myxomycetes. The first study applied immunocytochemistry. Unexpected results suggested that the cell wall immunogen is at least partly composed of plasma and vacuolar membrane-associated proteins. While this data did not define the origin and pathway of cell wall components, it did indicate the importance of membrane cycling during cell wall biogenesis. It would be of interest to have antibodies against wall fraction 2 and repeat the study.

The second approach involved the use of radiolabeled monosaccharides. Incorporation of ^{3}H-galactose into the insoluble wall fraction did correlate with the amount of polysaccharide and the ultrastructural appearance of cell wall formation. Assimilation of each precursor into galactosamine suggested that it was synthesized via the UDP-N-acetylglucosamine epimerase pathway. This study demonstrated the movement of label from a cytoplasmic pool into extracellular material. Due to the limitations of resolution of electron microscope autoradiography (EM-ARG), particularly when dealing with single cells, this approach failed to define the synthetic pathway of wall biogenesis. These results and observations from freeze-fracture did not show evidence for wall synthesis occuring at the plasma membrane.

While not totally convincing, cytochemical and EM-ARG data suggested the involvement of cytoplasmic vesicles.

This study is the only comprehensive treatment of differentiation of the haploid, vegetative phase in this group of lower fungi. Information about cellular events associated with these processes, the biochemical composition of extracellular materials formed during differentiation, and insight into the cellular processes involved in the formation of this material are reported.

LITERATURE CITED

Akins, R. A., and Byers, T. J. (1979). Encystment enhancing activity produced by Acanthamoeba castellanii. J. Cell Biol. 83, 21a.

Aldrich, H. C. (1974). Spore cleavage and the development of wall ornamentation in two Myxomycetes. Proc. Iowa Acad. Sci. 81, 28-35.

Aldrich, H. C., and Blackwell, M. (1976). Resistant structures in Myxomycetes. In: "The Fungal Spore" (Weber, D. J., Hess, W. M., eds.), pp. 413-466. New York, J. Wiley.

Alexopoulos, C. J., and Mims, C. W. (1979). "Introductory Mycology." New York, J. Wiley.

Applegarth, D. A. (1967). The cell wall of Penicillium notatum. Arch. Biochem. Biophys. 120, 471-478.

Band, R. N. (1963). Extrinsic requirements for encystation by the soil amoeba, Hartmannella rhyodes. J. Protozool. 10, 101-106.

Bardalaye, P. C., and Nordin, J. H. (1976). Galactosaminogalactan from cell walls of Aspergillus niger. J. Bacteriol. 125, 655-669.

Bartnicki-Garcia, S. (1968). Cell wall chemistry, morphogenesis, and taxonomy of fungi. Annu. Rev. Microbiol. 22, 87-108.

Bartnicki-Garcia, S., Bracker, C. E., Reyes, E., and Ruiz-Herrera, J. (1978). Isolation of chitosomes from taxonomically diverse fungi and synthesis of chitin microfibrils in vitro. Exp. Mycol. 2, 173-192.

Bartnicki-Garcia, S., and Hemmes, D. E. (1976). Some aspects of the formation and function of oomycete spores. In: "The Fungal Spore" (Weber, D. J., Hess, W. M., eds.), pp. 593-641. New York, J. Wiley.

Bendayan, M., and Zollinger, M. (1982). Protein A-gold immunocytochemical labeling on osmicated tissues. J. Histochem. Cytochem. 30, 576.

Boer, P. (1979). Glycosylation of yeast and fungal cell wall components. Biochem. Soc. Trans. 7, 331-333.

Bowers, B. and Korn, E. D. (1969). The fine structure of Acanthamoeba castellanii (Neff strain). II. Encystment. J. Cell Biol. 41, 786-805.

Branton, D., Bullivant, S., Gilula, N. B., Karnovsky, M. J., Moor, H., Muhlethaler, K., Northcote, D. H., Packer, L., Satir, B., Satir, P., Speth, V., Staehelin, L. A., Steere, R. L., and Weinstein, R. S. (1975). Freeze-etching nomenclature. Science 190, 54-56.

Braun, K. L. (1971). Effect of aeration on the germination of Fuligo septica spores. Mycologia 63, 669-671.

Buck, K. W., Chain, E. B., and Darbyshire, J. E. (1969). High cell wall galactosamine content and virus particles in Penicillium stoloniferum. Nature (London) 223, 1273.

Cabib, E., and Roberts, R. (1982). Synthesis of the yeast cell wall and its regulation. Annu. Rev. Biochem. 51, 763-793.

Callow, M. E., and Evans, L. V. (1974). Studies on the ship-fouling alga Enteromorpha. III. Cytochemistry and autoradiography of adhesive production. Protoplasma 80, 15-27.

Caro, L. G., and Schnos, M. (1965). Tritium and P^{32} in high-resolution autoradiography. Science 149, 60.

Chen, P. S., Toribara, T. Y., and Warner, H. (1956). Microdetermination of phosphorus. Anal. Chem. 28, 1756-1758.

Chet, I. and Huttermann, A. (1970). RNA and protein synthesis during germination of sphrules of Physarum polycephalum. Biochim. Biophys. Acta 224, 620-622.

Chet, I., and Huttermann, A. (1977). Germination-inhibition in slime mold Physarum polycephalum. FEMS Microbiol. Lett. 1, 149-152.

Chet, I., and Rusch, H. P. (1969). Induction of spherule formation in Physarum polycephalum by polyols. J. Bacteriol. 100, 673-678.

Cheung, L., Henney, Jr., H. R., and Clark, W. H. (1974). Ultrastructure of pure cultures of Physarum flavicomum. 1. Conversion of plasmodia to microplasmodia and microsclerotia, and the process of slime secretion. Cytobios 9, 193-205.

Chrispeels, M. J. (1976). Biosynthesis, intracellular transport, and secretion of extracellular macromolecules. Annu. Rev. Plant Physiol. 27, 19-38.

Churms, S. C. (1982). Carbohydrates. In: "Handbook of Chromatography" (Zweig, G., Sherma, J., eds.), vol. 1. Boca Raton, Florida, CRC Press.

Collins, O. R. (1979). Myxomycete biosystematics: Some recent developments and future research opportunities. Bot. Rev. 45, 145-201.

Craig, G. D., Newsam, R. J., Gull, K., and Wood, D. A. (1979). An ultrastructural and autoradiographic study of stipe elongation in Agaricus bisporus. Protoplasma 98, 15-29.

Dahlberg, K. R., and Franke, R. G. (1977). Spore germination in the Myxomycete Fuligo septica: Evidence for the existence of a soluble autocatalytic factor. Mycologia 69, 96-108.

Davidson, E. (1966). UDP-N-acetyl-D-glucosamine epimerase from embryonic cartilage. Methods Enzymol. 8, 277-281.

Dische, Z. (1947). A new specific color reaction of hexuronic acids. J. Biol. Chem. 167, 189-198.

Dische, Z. (1962). General color reactions. Methods Carbohyd. Chem. 1, 477-512.

Distler, J. J., and Roseman, S. (1960). Galactosamine polymer produced by Aspergillus parasiticus. J. Biol. Chem. 235, 2538-2541.

Dodgson, K. S., and Price, R. G. (1962). A note on the determination of the ester sulphate content of sulphated polysaccharides. Biochem. J. 84, 106-110.

Dougherty, W. G. (1976). Freeze-fracture characterization of the plasmodial plasmalemma. M. S. Thesis, University of Florida.

Dow, J. M., Carreon, R. R., and Villa, V. D. (1981). Role of membranes of mycelial Mucor rouxii in synthesis and secretion of cell wall matrix polymers. J. Bacteriol. 145, 272-279.

Dowbewko, D. J., and Ennis, H. L. (1982). Developmental regulation of protein synthesis during Polysphondylium pallidum cyst germination: A two-dimensional gel electrophoresis study. Biochim. Biophys. Acta 696, 218-222.

Dubois, M., Gilles, K. A., Hamilton, J. K., Rebers, P. A., and Smith, F. (1956). Colorimetric method for determination of sugars and related substances. Anal. Chem. 28, 350-356.

Edson, C. M., and Brody, S. (1976). Biochemical and genetic studies on galactosamine metabolism in Neurospora crassa. J. Bacteriol. 126, 799-805.

Elliott, E. W. (1949). The swarm cells of Myxomycetes. Mycologia 41, 141-170.

Ennis, H. L., Pennica, D., and Hill, J. M. (1978). Synthesis of macromolecules during microcyst germination in the cellular slime mold Polysphondylium pallidum. Dev. Biol. 65, 251-259.

Erdos, G. W., and Hohl, H. R. (1980). Freeze-fracture examination of the plasma membrane of the cellular slime mold Polysphondylium pallidum during microcyst formation and germination. Cytobios 29, 7-16.

Farley, F. E., Crang, R. E., and Brent, M. M. (1975). Ultrastructure of germinating spores of Physarella oblonga F. alba. Trans. Am. Microscop. Soc. 94, 136-141.

Farkas, V. (1979). Biosynthesis of cell walls of fungi. Microbiol. Rev. 43, 117-144.

Farquhar, M. G., and Palade, G. E. (1981). The Golgi apparatus (complex)-(1954-1981)-from artifact to center stage. J. Cell Biol. 91, 77s-103s.

Farr, D. R., Amster, H., and Horisberger, M. (1972). Composition and partial structure of the extracellular polysaccharide of Physarum polycephalum. Carbohydr. Res. 24, 207-209.

Farr, D. R., Schuler-Hovanessian, A., and Horisberger, M. (1977). Structure of an α-D-galactosaminoglycan from Physarum polycephalum spherule walls. Carbohydr. Res. 59, 151-154.

Faulk, W. P., and Taylor, G. M. (1971). The immunocolloid method for the electron microscope. Immunochemistry 8, 1081.

Fevre, M., and Rougier, M. (1982). Autoradiographic study of hyphal cell wall synthesis of Saprolegnia. Arch. Microbiol. 131, 212-215.

Frens, G. (1973). Controlled nucleation for the regulation of the particle size in monodisperse gold suspensions. Nature Phys. Sci. 241, 20-22.

Gander, J. E. (1974). Fungal cell wall glycoproteins and peptido-polysaccharides. Annu. Rev. Microbiol. 28, 103-119.

Geesey, G. G. (1982). Microbial Exopolymers: Ecological and economic considerations. Am. Soc. Microbiol. News 48, 9-14.

Gemperle, A., Holan, Z., and Pokorny, V. (1982). The glucan-chitin complex in Saccharomyces cerevisiae. IV. The electron diffraction of crustacean and yeast cell wall chitin. Biopolymers 21, 1-16.

Geoghegan, W. D., and Ackerman, G. A. (1977). Adsorption of horseradish peroxidase, ovomucoid and anti-immunoglobulin to colloidal gold for the indirect detection of concanavalin A, wheat germ agglutinin and goat anti-human immunoglobulin G on cell surfaces at the electron microscopic level: A new method, theory and application. J. Histochem. Cytochem. 25, 1187-1200.

Githens, S., and Karnovsky, M. L. (1973). Biochemical changes during growth and encystment of the cellular slime mold Polysphondylium pallidum. J. Cell Biol. 58, 522-535.

Glaser, L. (1959). The biosynthesis of N-acetylgalactosamine. J. Biol. Chem. 234, 2801-2805.

Gooday, G. W. (1971). An autoradiographic study of hyphal growth of some fungi. J. Gen. Microbiol. 67, 125-133.

Gooday, G. W. (1979). Chitin synthesis and differentiation in Coprinus cinereus. In: "Fungal Walls and Hyphal Growth" (Burnett, J. H., Trinci, A. P., eds.), pp. 203-223. New York, Cambridge Univ. Press.

Gooday, G. W., and Trinci, A. P. (1980). Wall structure and biosynthesis in fungi. In: "The Eucaryotic Microbial Cell: 30th Symposium of the Society for General Microbiology" (Gooday, G. W., Lloyd, D., and Trinci, A. P., eds.), pp. 207-251. New York, Cambridge Univ. Press.

Goodman, E. M., and Rusch, H. P. (1970). Ultrastructural changes during spherule formation in Physarum polycephalum. J. Ultrastruct. Res. 30, 172-183.

Gorman, J. A., Dove, W. F., and Shaibe, E. (1977). Anisomycin sensitive mutants of Physarum polycephalum isolated by cyst selection. Molec. Gen. Genet. 151, 253-259.

Gorman, J. A., and Wilkins, A. S. (1980). Developmental phases in the life cycle of Physarum polycephalum and related Myxomycetes. In: "Growth and Differentiation in Physarum polycephalum" (Dove, W. F., Rusch, H. P., eds.), pp. 157-202. Princeton, New Jersey, Princeton University Press.

Gray, W. D., and Alexopoulos, C. J. (1968). "Biology of the Myxomycetes." New York, Ronald Press.

Griffiths, A. J. (1970). Encystment in amoebae. Adv. Microbial Physiol. 4, 105-128.

Grove, S. N., and Bracker, C. E. (1978). Protoplasmic changes during zoospore encystment and cyst germination in Pythium aphanidermatum. Exp. Mycol. 2, 51-98.

Gwynne, D. I., and O'Day, D. H. (1978). RNA and protein synthetic patterns during germination of Polysphondylium pallidum microcysts. Can. J. Microbiol. 24, 480-486.

Haars, A., Zaar, K., and Huttermann, A. (1979). Induction of synchronous differentiation (encystment) in Physarum polycephalum myxamoebae. Arch. Microbiol. 120, 105-112.

Hansen, S. A. (1975). Thin-layer chromatographic method for identification of oligosaccharides in starch hydrolysates. J. Chromatog. 105, 388-390.

Henney, Jr., H. R. (1982). General Metabolism. In: "Cell Biology of Physarum and Didymium" (Aldrich, H. C., Daniel, J. W., eds.), vol. II, pp. 131-181. New York, Academic Press.

Henney, Jr., H. R., and Chu, P. (1977a). Differentiation of Physarum flavicomum: Metabolic patterns and the role of amino acids in the control of encystment. Exp. Mycol. 1, 41-51.

Henney, Jr., H. R., and Chu, P. (1977b). Chemical analyses of cell walls from microcysts and microsclerotia of Physarum flavicomum; Comparison to slime coat of microplasmodia. Exp. Mycol. 1, 83-91.

Henney, Jr., H. R., and Tavana, G. (1982). Evidence for the involvement of proteinases in the differentiation of haploid cells of Physarum flavicomum. Exp. Mycol. 6, 153-160.

Hohl, H. R., Miura-Santo, L. Y., and Cotter, D. A. (1970). Ultrastructural changes during formation and germination of microcysts in Polysphondylium pallidum, a cellular slime mold. J. Cell Sci. 7, 285-305.

Horisberger, M., and Rosset, J. (1977). Colloidal gold, a useful marker for transmission and scanning electron microscopy. J. Histochem. Cytochem. 25, 295-305.

Horisberger, M., Rosset, J., and Bauer, H. (1975). Colloidal gold granules as markers for cell surface receptors in the scanning electron microscope. Experentia 31, 1147.

Horst, M. N., Basha, S. M., Baumbach, G. A., Mansfield, E. H., and Roberts, R. M. (1980). Alkaline solubilization, two-dimensional electrophoresis and lectin staining of mammalian cell plasma membrane and plant seed proteins. Anal. Biochem. 102, 399-408.

Howard, F. L. (1931). The life history of Physarum polycephalum. Am. J. Bot. 18, 116-133.

Huttermann, A. (1973). Biochemical events during spherule formation of Physarum polycephalum. Ber. Dtsch. Bot. Ges. 86, 55-76.

Huttermann, A. (1982). Enzyme and protein synthesis during differentiation of Physarum polycephalum. In: "Cell Biology of Physarum and Didymium" (Aldrich, H. C., Daniel, J. W., eds.), vol. II, pp. 77-99. New York, Academic Press.

Jamieson, J. D., and Palade, G. E. (1967). Intracellular transport of secretory proteins in the pancreatic exocrine cell. II. Transport to condensing vacuoles and zymogen granules. J. Cell Biol. 34, 597-615.

Jeffery, W. R. (1979). Translational regulation of polysome formation during dormancy of Physarum polycephalum. J. Bacteriol. 140, 490-497.

Jockusch, B. M., Sauer, H. W., Brown, D. F., Babcock, K. L., and Rusch, H. P. (1970). Differential protein synthesis during sporulation in the slime mold Physarum polycephalum. J. Bacteriol. 103, 356-363.

Johnson, A. R. (1971). Improved method of hexosamine determination. Anal. Biochem. 44, 628-635.

Jones, R. L. (1972). Fractionation of the enzymes of the barley aleurone layer: Evidence for a soluble mode of enzyme release. Planta 103, 95-109.

Kazama, F. Y., and Aldrich H. C. (1972). Digestion and the distribution of acid phosphatase in the myxamoebae of Physarum flavicomum. Mycologia 64, 529-538.

Koevenig, J. L. (1964). Studies on the life cycle of Physarum gyrosum and other Myxomycetes. Mycologia 65, 170-184.

Kosinova, A., Farkas, V., Machala, S., and Bauer, S. (1974). Site of mannan synthesis in yeast: An autoradiographic study. Arch. Microbiol. 99, 255-263.

Kuroiwa, T. (1982). Mitochondrial nuclei. Int. Rev. Cytol. 75, 1-59.

Laemmli, U. K. (1970). Cleavage of structural proteins during assembly of the head of bacteriophage T4. Nature 227, 680-685.

Lang, W. C. (1982). Glycoprotein biosynthesis in Chlamydomonas. I. In vitro incorporation of galactose from UDP-[^{14}C]galactose into membrane-bound protein. Plant. Physiol. 69, 678-681.

Larue, H., Masson, S., Lafontaine, J. G., Nadeau, P., and Pallotta, D. (in manuscript). Changes in protein and RNA during asexual differentiation of Physarum polycephalum.

Lewis, P. R., and Knight, D. P. (1977). Staining methods dfor sectioned material. In: "Practical Methods in Electron Microscopy" (Glauert, A. M., ed.). Amsterdam, North-Holland Pub.

Ling, H., and Moore, D. (1979). Multinucleate cysts of the Myxomycete Didymium iridis. Mycologia 71, 713-721.

Lonski, J., and Pesut, N. (1977). Induction of encystment of Polysphondylium pallidum amoebae. Can. J. Microbiol. 23, 518-521.

Lowry, O. H., Rosebrough, N. J., Farr, A. L., and Randall, R. J. (1951). Protein measurement with the Folin dphenol reagent. J. Biol. Chem. 193, 265-275.

Luft, J. H. (1961). Improvements in epoxy resin embedding methods. J. Biophys. Biochem. Cytol. 9, 409.

Mahadevan, P. R., and Tatum, E. L. (1965). Relationship of the major constituents of the Neurospora crassa cell wall to wild type and colonial morphology. J. Bacteriol. 90, 1073-1081.

Maley, F., and Maley, C. F. (1959). The enzymic conversion of glucosamine to galactosamine. Biochim. Biophys. Acta 31, 577-578.

Matsusaka, T. (1976). An ultrastructural study of encystment in the hypotrichous ciliate Pleurotricha sp. Kumamoto J. Sci. Biol. 13, 13-26.

Matsusaka, T. (1977). Induction of synchronous encystment in a hypotrichous ciliate, Histriculus sp. Exp. Cell Res. 110, 459-462.

Mattar, F. E., and Byers, T. J. (1971). Morphological change and requirements for macromolecule synthesis during excystment of Acanthamoeba castellanii. J. Cell Biol. 49, 507-519.

McCormick, J. J., Blomquist, J. C., and Rusch, H. P. (1970a). Isolation and characterization of an extracellular polysaccharide from Physarum polycephalum. J. Bacteriol. 104, 1110-1118.

McCormick, J. J., Blomquist, J. C., and Rusch, H. P. (1970b). Isolation and characterization of a galactosamine wall from the spores and spherules of Physarum polycephalum. J. Bacteriol. 104, 1119-1125.

Meyer, J. and Matile, P. H. (1975). Subcellular distribution of yeast invertase isoenzymes. Arch. Microbiol. 103, 51-55.

Mims, C. W. (1971). An ultrastructural study of spore germination in the Myxomycete Arcyria cinerea. Mycologia 63, 586-601.

Mims, C. W. (1972). Spore-wall formation in the Myxomycete Arcyria cinerea. Trans. Br. Mycol. Soc. 59, 477-481.

Mohberg, J., and Rusch, H. P. (1971). Isolation and DNA content of nuclei of Physarum polycephalum. Exp. Cell Res. 66, 305-316.

Morre, D. J., Kartenbeck, J., and Franke, W. W. (1979). Membrane flow and interconversions among endomembranes. Biochim. Biophys. Acta 559, 71-152.

Morre, D. J., and Ovtracht, L. (1977). Dynamics of the Golgi apparatus: Membrane differentiation and membrane flow. Int. Rev. Cytol. Suppl. 5, 61-188.

Muller, M., Meister, N., and Moor, H. (1980). Freezing in a propane jet and its application in freeze-fracturing. Mikroscopie 36, 129-140.

Muller, W. A., Steinman, R. M., and Cohn, Z. A. (1980). The membrane proteins of the vacuolar system. II. Bidirectional flow between secondary lysosome and plasma membrane. J. Cell Biol. 86, 304-314.

Neff, R. J., Ray, S. A., Benton, W. F., and Wilborn, M. (1964). Induction of synchronous encystment (differentiation) in Acanthamoeba sp. Methods Cell Physiol. 1, 55-83.

Newcomb, E. H. (1980). The general cell. In: "The Biochemistry of Plants" (Stumpf, P. K., Conn, E. E., eds.), vol. 1, pp. 1-54. New York, Academic Press.

Nichols, R. L., and McComb, D. E. (1962). Immunofluorescent studies with trachoma and related antigens. J. Immunol. 89, 545-554.

Nishi, A., Masumoto, K., Asamizu, T., Katoh, T., and Kinpara, H. (1981). Hexosamine metabolism during formation in Physarum polycephalum. Biochim. Biophys. Acta 673, 243-252.

Northcote, D. H. (1979). The involvement of the Golgi apparatus in the biosynthesis and secretion of glycoproteins and polysaccharides. In: "Biomembranes" (Manson, L. A., ed.), vol. 10, pp. 51-76. New York, Plenum Press.

Northcote, D. H., and Pickett-Heaps, J. D. (1966). A function of the Golgi apparatus in polysaccharide synthesis and transport in the root-cap cells of wheat. Biochem. J. 98, 159-167.

Novick, P., Ferro, S., and Schekman, R. (1981). Order of events in the yeast secretory pathway. Cell 25, 461-469.

Oades, J. M. (1967). Gas-liquid chromatography of alditol acetates and its application to the analysis of sugars in complex hydrolysates. J. Chromatog. 28, 246-252.

O'Day, D. H. (1974). Intracellular and extracellular enzyme patterns during microcyst germination in the cellular slime mold Polysphondylium pallidum. Dev. Biol. 36, 400-410.

O'Day, D. H., Gwynne, D. I., and Blakey, D. H. (1976). Microcyst germination in the cellular slime mold, Polysphondylium pallidum; Effects of actinomycin D and cycloheximide on macromolecular synthesis and enzyme accumulation. Exp. Cell Res. 97, 359-365.

Ottenstein, D. M., and Bartley, D. A. (1971). Improved gas chromatography separation of free acids C_2-C_5 in dilute solution. Anal. Chem. 43, 952-955.

Ouchterlony, O. (1949). Antigen-antibody reactions in gels. Acta Pathol. Microbiol. Scand. 26, 507-515.

Palade, G. E. (1975). Intracellular aspects of the process of protein synthesis. Science 189, 347-358.

Patterson, M. A., and Scheetz, R. W. (1977). Spherule wall formation in Physarum polycephalum. Protoplasma 92, 253-261.

Philippi, M. L., and Parish, R. W. (1981). Changes in glucan synthetase activity and plasma membrane proteins during encystment of the cellular slime mold Polysphondylium pallidum. Planta 152, 59-69.

Pickett-Heaps, J. D. (1967). The use of radioautography for investigating wall secretion in plant cells. Protoplasma 64, 49-66.

Porter, W. H. (1975). Application of nitrous acid deamination of hexosamines to the simultaneous GLC determination of neutral and amino sugars in glycoprotein. Anal. Biochem. 63, 27-43.

Rambourg, A. (1967). An improved silver methenamine technique for the detection of periodic acid-reactive complex carbohydrates with the electron microscope. J. Histochem. Cytochem. 15, 409-412.

Raub, T. J., and Aldrich, H. C. (1982). Sporangia, spherules, and microcysts. In: "Cell Biology of Physarum and Didymium" (Aldrich, H. C., Daniel, J. W., eds.), vol. II, pp. 21-75. New York, Academic Press.

Reynolds, E. S. (1963). The use of lead citrate at high pH as an opaque stain in electron microscopy. J. Cell Biol. 17, 208-212.

Rhea, R. P. (1966). Electron microscopic observations on the slime mold Physarum polycephalum with specific reference to fibrillar structures. J. Ultrastruct. Res. 15, 349-389.

Robb, J. (1972). Ultrastructure of Ustilago hordei. 1. Pregermination development of hydrating teliospores. Can. J. Bot. 50, 1253-1261.

Roth, J., and Binder, M. (1978). Colloidal gold, ferritin and peroxidase as markers for electron microscopic double labeling lectin techniques. J. Histochem. Cytochem. 26, 163-169.

Rothman, J. E. (1981). The Golgi apparatus: Two organelles in tandem. Science 213, 1212-1219.

Rothman, J. E., Fries, E., Dunphy, W. G., and Urbani, L. J. (1982). The Golgi apparatus, coated vesicles, and the sorting problem. Cold Spr. Harbor Symp. Quant. Biol. 46, 797-805.

Ruperz, P., and Leal, J. A. (1981). Extracellular galactosaminogalactan from Aspergillus parasiticus. Trans. Br. Mycol. Soc. 77, 621-625.

Schuster, F. L. (1965). Ultrastructure and morphogenesis of solitary stages of true slime molds. Protistologica 1, 49-62.

Sharon, N. (1975). "Complex Carbohydrates: Their Chemistry, Biosynthesis, and Functions." Massachusetts, Addison-Wesley Pub. Co.

Shipley, G. L., and Ross, I. K. (1978). The effects of proteases on plasmodium formation in Didymium iridis. Cell Differen. 7, 21-32.

Simon, H., and Henney, Jr., H. R. (1970). Chemical composition of slime from three species of Myxomycetes. FEBS Lett. 7, 80-82.

Smart, R. F. (1937). Influence of certain external factors on spore germination in the Myxomycetes. Am. J. Bot. 24, 145-159.

Smith, J. E., Gull, K., Anderson, J. G., and Deans, S. G. (1976). Organelle changes during fungal spore germination. In: "The Fungal Spore" (Weber, D. J., Hess, W. M., eds.), pp. 301-352. New York, J. Wiley.

Spurr, A. R. (1969). A low-viscosity epoxy resin embedding medium for electron microscopy. J. Ultrastruct. Res. 26, 31.

Stevens, A. R. (1966). High resolution autoradiography. Methods in Cell Physiol. 2, 255-310.

Taoma, M., and Raper, K. (1967). Microcysts of the cellular slime mold Polysphondylium pallidum. I. Factors influencing microcyst formation. J. Bacteriol. 94, 1143-1149.

Taylor, I. E., and Cameron, D. S. (1973). Preparation and quantitative analysis of fungal cell walls: Strategy and tactics. Annu. Rev. Microbiol. 27, 243-259.

Taylor, P., and Kahn, A. J. (1969). Initiation of encystment in the mycetozoan Protostelium mycophaga. J. Protozool. 16, 152-154.

Thompson, J. S., and Shockman, G. D. (1968). A modification of the Park and Johnson reducing sugar determination suitable for the assay of insoluble materials: Its application to bacterial cell walls. Anal. Biochem. 22, 260-268.

Towbin, H., Staehlin, T., and Gordon, J. (1979). Electrophoretic transfer of proteins from polyacrylamide gels to nitrocellulose sheets: Procedure and some applications. Proc. Natl. Acad. Sci. USA 76, 4350-4354.

Trotter, M. J., and Whistler, H. C. (1965). Chemical composition of the cell wall of Amoebidium parasiticum. Can. J. Bot. 43, 869-876.

Turner, H. M., and Johnson, J. (1975a). Transmission and scanning electron microscopy of changes associated with mirocyst formation in the Myxomycete Physarum polycephalum. Cytobios 12, 95-107.

Turner, H. M., and Johnson, J. (1975b). A biochemical analysis of induction of microcyst formation in Physarum polycephalum myxamoebae by mannitol. Cytobios 13, 229-239.

Turner, H. M., and Johnson, J. (1975c). Ultrastructural changes associated with induction of microcyst formation by mannitol in Physarum polycephalum amoebae. Cytobios 13, 241-250.

Yelton, D. E., and Sharff, M. D. (1981). Monoclonal antibodies: A powerful new tool in biology and medicine. Annu. Rev. Biochem. 50, 657-680.

Wardi, A. H., and Michos, G. A. (1972). Alcian blue staining of glycoproteins in acrylamide disc electrophoresis. Anal. Biochem. 49, 607-609.

Weisman, R. A. (1976). Differentiation in Acanthamoeba castellanii. Annu. Rev. Microbiol. 30, 189-219.

Whaley, W. G., and Dauwalder, M. (1977). The Golgi apparatus, the plasma membrane, and functional integration. Int. Rev. Cytology 58, 199-245.

Whitaker, D. (1982). The occurrence of discoidins I and II in the sexual life cycle of Dicytostelium discoideum. M. S. Thesis, University of Florida.

Wilkinson, M. J., and Northcote, D. H. (1980). Plasma membrane ultrastructure during plant protoplast plasmolysis, isolation and wall regeneration: A freeze-fracture study. J. Cell Sci. 42, 401-415.

Williams, M. A. (1977). Autoradiography and immunochemistry. In: "Practical Methods in Electron Microscopy" (Glauert, A. M., ed.), vol. 6, part I, pp. 77-155. Amsterdam, North-Holland Pub. Co.

Wischnitzer, S. (1973). Submicroscopic morphology of the interphase nucleus. Int. Rev. Cytol. 34, 1-48.

Wright, M., Moisand, A., and Mir, L. (1979). The structure of the flagellar apparatus of the swarm cells of Physarum polycephalum. Protoplasma 100, 231-250.

Zaar, K. (1978). Composition, secretion kinetics and radioactive labelling of the extracellular slime polysaccharide secreted during spherulation of Physarum polycephalum. Arch. Microbiol. 117, 303-308.

Zaar, K., Beyer, P., and Kleinig, H. (1979). The spherule wall of Physarum polycephalum. Chemical analyses and electron microscopy. Biochim. Biophys. Acta 582, 21-32.

Zaar, K., and Kleinig, H. (1974). Spherulation of Physarum polycephalum. I. Ultrastructure. Cytobiologie 10, 306-328.

Zacharius, R. M., Zell, T. E, Morrison, J. H., and Woodlock, J. J. (1969). Glycoprotein staining following electrophoresis on acrylamide gels. Anal. Biochem. 30, 148-152.

BIOGRAPHICAL SKETCH

Thomas Jeffrey Raub was the fourth child born October 21, 1956 to Verna Catherine and Stanley Ellis Raub in Phoenixville, Pennsylvania. Following several years in Denver, Colorado, and Seattle, Washington, the Raub family settled down in Hatboro, Pennsylvania. After graduating from Hatboro-Horsham High School in 1974, Tom began his undergraduate studies in biology at Slippery Rock State College, Pennsylvania. Here he received the Dean George Smith Achievement Award before graduating magna cum laude in 1978. Following marriage to Kathleen Ann Hollingsworth, they moved to Gainesville, Florida, for him to enter the Ph. D. program in the Department of Microbiology and Cell Science at the University of Florida.

Tom is a member of Sigma Xi, the American Society for Cell Biology, the American Society for Microbiology, the Mycological Society of America, and the American Association for the Advancement of Science.

I certify that I have read this study and that in my opinion it conforms to acceptable standards of scholarly presentation and is fully adequate, in scope and quality, as a dissertation for the degree of Doctor of Philosophy.

Henry C. Aldrich, Chairman
Professor of Microbiology and
Cell Science

I certify that I have read this study and that in my opinion it conforms to acceptable standards of scholarly presentation and is fully adequate, in scope and quality, as a dissertation for the degree of Doctor of Philosophy.

James F. Preston
Professor of Microbiology and
Cell Science

I certify that I have read this study and that in my opinion it conforms to acceptable standards of scholarly presentation and is fully adequate, in scope and quality, as a dissertation for the degree of Doctor of Philosophy.

Arnold S. Bleiweis
Professor of Microbiology and
Cell Science

I certify that I have read this study and that in my opinion it conforms to acceptable standards of scholarly presentation and is fully adequate, in scope and quality, as a dissertation for the degree of Doctor of Philosophy.

R. Michael Roberts
Professor of Biochemistry and
Molecular Biology

I certify that I have read this study and that in my opinion it conforms to acceptable standards of scholarly presentation and is fully adequate, in scope and quality, as a dissertation for the degree of Doctor of Philosophy.

Stephen G. Zam
Associate Professor of Microbiology
and Cell Science

This dissertation was submitted to the Graduate Faculty of the College of Agriculture and to the Graduate Council, and was accepted as partial fulfillment of the requirements for the degree of Doctor of Philosophy.

December 1982

Dean, College of Agriculture

Dean for Graduate Studies and
Research